Synthesis of 1,4-Diazacycles by Hydrogen-Borrowing

Anju Nalikezhathu, Adriane Tam, Valeriy Cherepakhin, Van K. Do, and Travis J. Williams*

Donald P. and Katherine B. Loker Hydrocarbon Institute and Department of Chemistry, University of Southern California, Los Angeles, California 90089-1661, United States

Supporting Information Placeholder

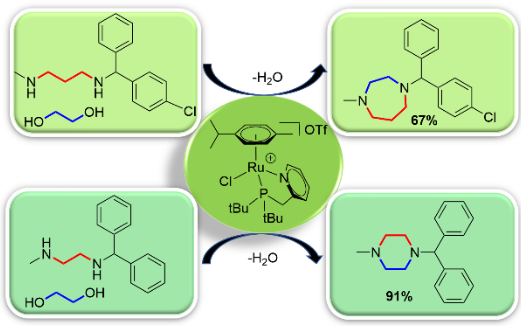

ABSTRACT: We report the syntheses of 1,4-diazacycles by diol-diamine coupling, uniquely made possible with a (pyridyl)phosphine-ligated ruthenium(II) catalyst (**1**). The reactions can exploit either two sequential *N*-alkylations or an intermediate tautomerization pathway to yield piperazines and diazepanes, the latter generally inaccessible by catalytic routes. Our conditions tolerate different amines and alcohols that are relevant to key medicinal platforms: we show the syntheses of the drugs cyclizine and homochlorcyclizine, respectively in 91% and 67% yields.

Diazacycles are privileged motifs of medicinal chemistry. For example, piperazine is the third most common nitrogen heterocycle and the fifth most common ring system in small-molecule drugs, including cyclizine, cetirizine, and sitagliptin.[1,2] Similarly, diazepanes, the corresponding seven-membered diazacycles, are found in numerous drugs including homochlorcyclizine and homofenazine.[3] Several useful piperazines syntheses are known,[4] but the same is not true for diazepanes, where cyclization is kinetically and energetically more challenging. Incumbent approaches to diazepanes span from classical methods such as amination of halides,[5] reaction of primary amines with vinyl cyanides,[6] reductive amination[7] to intermolecular cyclization,[8] intramolecular cyclization,[9] and Bode's new SnAP reagents.[10] We are particularly motivated to introduce hydrogen borrowing conditions to this toolkit[11] to deliver three key advantages: (1) these enable access to structures that are not easily accessed in other ways; (2) these generate water as the sole byproduct, making them atom- and cost-efficient and environmentally friendly; (3) these access products directly from amines and alcohols, which are inexpensive and readily available.

Our lab has developed a ruthenium catalyst (**1**) that enables hydrogen borrowing amination on substrates such as phenols, anilines, indoles, and halides, that are challenging or incompatible with other catalysts (Figure 1).[12] Complex **1** further facilitates a tandem alcohol amination/Pictet-Spengler reaction for the synthesis of tetrahydro-ß-carbolines, owing to its unique ability to operate independently of base, thus enabling an acid-catalyzed Pictet-Spengler reaction in situ.[13] Hypothesizing that chelation of starting diamines was the principle hurdle to a hydrogen borrowing route to diazacycles, we suspected that this same ruthenium catalyst might be tolerant of chelating diamines, thus avoiding this peril and cyclizing simple diamines and diols where other catalysts struggle. While **1** is not unique in the formation of piperazines,[14] we perceive a need to address low yield, high catalyst loading, long reaction time, or limited substrate scope (Figure 1) and fill the void for methods for the synthesis of 1,4-diazepanes from diamines and diols.[7b, 11, 15] Pharmaceutical producers have recently called out the hydrogen borrowing community for "high loading, poor turnover, and susceptibility to substrate inactivation of the catalysts" as key reasons that the method is not more widely adoped.[16] Here we confront these issues directly by exhibiting a hydrogen borrowing system that addresses vital, common diazacycle structures that pervade medicinal chemistry.

Ruthenium complex **1** efficiently cyclizes diamines and diols to yield piperazine and 1,4-diazepane products. Furthermore, we show how our strategy can be applied to drugs such as cyclizine and homochlorcyclizine. While excellent progress has been made by others (Figure 1), we know of no other method to synthesize these drugs from diamines/diols with a hydrogen borrowing approach. Particularly, we attribute slow prior progress to the chelating behavior of 1,2- and 1,3-diamines, which are known to poison many hydride transfer catalysts (vide infra). Therefore, by overcoming this poisoning problem, our synthetic strategy will enable the synthesis of otherwise challenging 1,4-diazacycles and related APIs (active pharmaceutical ingredients) from accessible starting materials that were not previously viable approaches for these heterocycles.

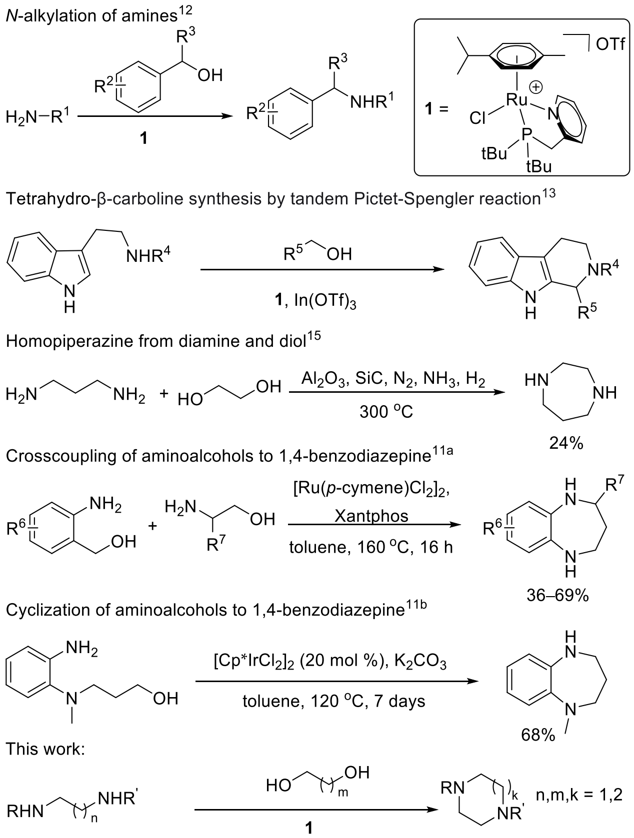

Figure 1. Previous work and proposed hydrogen borrowing strategy to access 1,4-diazacycles.

Whereas efficient routes to piperazines are known, we began by optimizing our reaction for a seven-membered compound **4a** (Table S1), using *N,N′*-dibenzylethylenediamine (**2a**) and 1,3-propanediol (**3a**). The best conditions supply the diol in gentle excess, with diminishing returns beyond 2 equivalents (compare entries 1/2 with 3, 4 and 5). Even though water is a side product, addition of molecular sieves decreased the yield (Table S1, entry 6), possibly because they impede stirring of the neat reaction. Reducing the catalyst loading (Table S1, entry 7) and reaction time (Table S1, entries 8 and 9) decreased conversion.

With high yielding conditions in hand, we proceeded to study the reaction's scope. While many useful methods exist for the formation of six-membered piperazine rings, we demonstrate here some representative examples of how catalyst **1** can contribute to this area (Table 1). These reactions proceed in high yield as expected (Table 1, entries 1-3). Compound **6a** has special value as a medicinal entity, whereas it has high affinity for sigma receptors and shows anticocaine activity.[17] Importantly, reaction of chiral diamines retained their configuration through the reaction, which is consistent with our mechanistic studies showing irreversibility of imine hydrogenation with catalyst **1**.[13] For example, coupling of (1*R*, 2*R*)-*N,N'*-dibenzylcyclohexane-1,2-diamine (**2b**) with ethylene glycol (**5a**) afforded **6b** with trans configuration and > 99% ee. Product **6b** belongs to the decahydroquinoxalines class of compounds, which are potent and selective κ-opioid receptor agonist with anti-inflammatory activity.[18] In addition to this, compound **6c**, generated from *N*-benzyl-*N′*-hydroxyethyl ethylenediamine (**2c**), is a structural motif found in APIs like opipramol and cetirizine. This example shows that our process works well in the presence of free hydroxyl groups, with minimal side reactivity.

Table 1. Substrate Scope for Piperazine Synthesis.

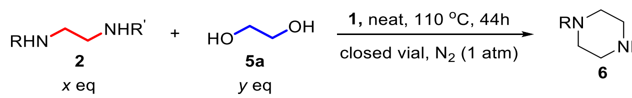

Entry	Diamine	x : y	Product	**1** loading Yield
1	 **2a**	1:2	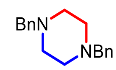 **6a**	2 mol % 86%
2	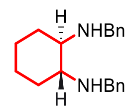 **2b**	1:4	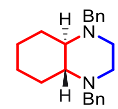 **6b**	5 mol % 84%
3	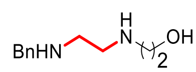 **2c**	1:3	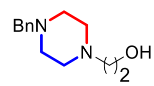 **6c**	1 mol % 78%

Unlike the corresponding piperazines, few catalytic syntheses are known for the analogous diazepanes. Table 2 show examples of diazepane synthesis featuring various substitution. While substituents on either the diamine or diol partner is tolerated, coupling between diamines and diols having substituent on both partners are less successful (see examples in Scheme S6). We further encountered an unanticipated advantage of utilizing glycols (as opposed to propanediols) as coupling partners: *N,N′*-dibenzylhomopiperazine (**4a**) is formed more efficiently from a three carbon diamine and a two carbon diol compared to the complementary reaction involving a three carbon diol (compare Table 2, entries 1 and 2 and other examples in Scheme S9). We attribute this to the availability of a tautomerization pathway in the former case, which is sketched in Scheme 1A. Here, the requisite second aldehyde (**9**) is generated from an intermediate iminium ion (**7**) through tautomerization of enamine **8**. By contrast, redox steps are needed to generate the second aldehyde (**12**) from iminium ion **10** in the case of reaction with propanediols (Scheme 1B). We infer that while both routes are accessible, the former is more efficient and leads to higher yielding reactions.

Scheme 1. Synthesis of 1,4-Diazepane A) from Three Carbon Diamine and Two Carbon Diol B) from Two Carbon Diamine and Three Carbon Diol.

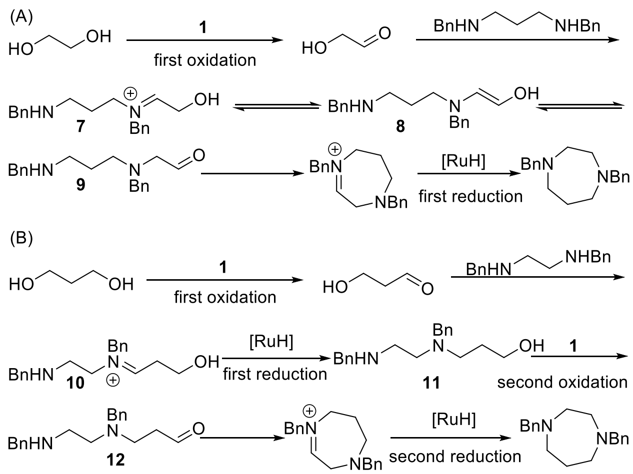

The scope of diazepane synthesis is further developed in Table 2. Alkyl groups are generally well tolerated either on the diamine or diol partner. For example, methyl substituted two- or three-carbon diols (Table 2, entries 3-5), and an ethyl-substituted diamine (Table 2, entry 6) afford the corresponding diazepanes in good yield. In the case of coupling diamine **2d** with chiral glycol **5c** (compare entries 3 and 4), a racemic cycloadduct (**4b**) results as expected, due to a planar intermediate aldehyde. These alkyl-substituted products are pharmaceutically valuable compounds, in fact **4c** has been employed as an intermediate in the preparation of suvorexant,[19, 20] an FDA-approved drug used to treat insomnia.

In addition to the benzyl group, we illustrate other substituents on nitrogen such as cyclohexylmethyl, methyl, isopropyl, and hydroxyethyl (Table 2, entries 7-11). These structures have special value, particularly whereas compounds **4f** and **4g** belong to a class of methyl-substituted diazepanes that are found in the APIs emedastine and homochlorcyclizine, and these structures are not easily prepared through other catalytic approaches. Further, *N,N'*-diisopropyl homopiperazine (**4h**) is used as a ligand for asymmetric deprotonation of *N*-Boc pyrrolidine.[21]

Although 1,4-diazepanes are observed as the major product in most cases, formation of materials such as hemiaminal and acyclic products are possible with some substrates. For example, we observed competition between intermolecular and intramolecular reactions in the case of *N*-benzyl-*N'*-hydroxyethyl ethylenediamine (**2c**) and diols (see Table S5 and Table S6). We successfully optimized the conditions to access our desired 1,4-diazepanes **4b** (Table 2, entry 3) and **4i** (Table 2, entry 11). Product **4i** represent structural motifs common in APIs such as dilazep and homofenazine.

Bicyclic compounds are attractive targets for our reaction scope (Table 1, entry 2; Table 2, entries 12-13). Sterically demanding cyclopropane dimethanol (**3c**) produced hemiaminal **4j** selectively instead of a simple amine alkylation compound (Table 2, entry 12). When we treated *N,N'*-dibenzyl-1,3-propanediamine (**2d**) with *cis*-cyclopentanediol (**5d**), we observed *cis*-fused product **4k** exclusively (Table 2, entry 13). Retention of configuration at the amine centers of **4k** was established in the crystal structure of its PF_6^- salt (Figure S85).

We have previously reported Pd/BaSO4 conditions for deprotecting the benzyl groups on nitrogen selectively in the presence of other hydrogenolysis-sensitive groups.[13] This facile debenzylation method can enable broad substrate scope including unprotected diazacycles using our methodology.

Whilst numerous catalysts are known to participate in hydrogen borrowing amination and none has yet been reported for cyclization of diamines to diazepanes, we screened other popular catalysts that we expected could be effective for this transformation. These include $[Cp^*IrCl_2]_2$,[22] [Ru(*p*-cymene)Cl_2]$_2$-xantphos,[11a] (phen)$NiBr_2$,[23] and the Shvo complex[24] (Table S8). None of these produced a 1,4-diazepane from either an unsubstituted or substituted diamine (see Table S8 for specific conditions). In each case, we observed starting materials in the NMR spectra of the reaction mixture. We attribute this observation to a unique property of **1** to minimize the impact of catalytic poisoning from diamine chelation in the case of substituted diamines, which we propose to inhibit the other systems to a greater extent than **1**.

Table 2. Substrate Scope for 1,4-Diazepane Synthesis.

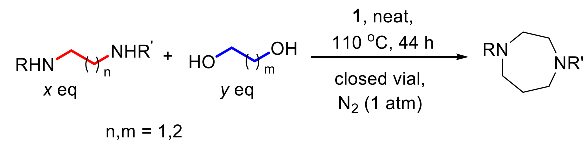

Entry	Diamine and Diol	x:y	Product	1 loading Yield
1	2a, 3a	1:2	4a	1 mol % 78%
2	5a, 2d	1:3	4a	2 mol % 86%
3	5b, 2d	1:3	4b	2 mol % 68%
4[a]	5c, 2d	1:3	4b	2 mol % 60%
5	2a, 3b	1:3	4c	2 mol % 71%
6	5a, 2e	1:5	4d	5 mol % 83%
7	2f, 3a	1:5	4e	1 mol % 70%

Table 2. Continued.

Entry	Diamine and Diol	x:y	Product	**1** loading Yield
8	 **2g**  **3a**	1:2	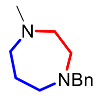 **4f**	1 mol % 71%
9	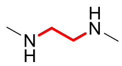 **2h**  **3a**	2:1	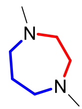 **4g**	1 mol % 88%[b]
10	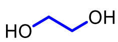 **5a**  **2i**	1:2	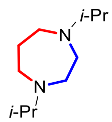 **4h**	1 mol % 80%[b]
11	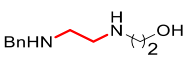 **2c** 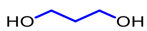 **3a**	1:2	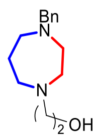 **4i**	1 mol % 68%
12	 **2a** 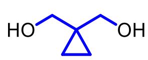 **3c**	1:4	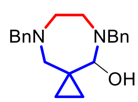 **4j**	1 mol % 50%[c]
13	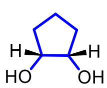 **5d**  **2d**	1:2	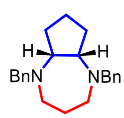 **4k**	2 mol % 58%

[a]Diol was (S)-(+)-1,2-propanediol. [b]The yield was determined by ^{1}H NMR with mesitylene as the internal standard due to product volatility. [c]The reaction yielded hemiaminal **4j** exclusively.

Orthophenylene diamine and ethylene diamine were inefficient in cyclizaton, likely due to catalytic poisoning by chelation. Details of these studies are reported in Scheme S10. In addition, reactions to yield eight membered diazo compounds were less successful (see Scheme S7 and S8).

Under the catalytic conditions, complex **1** reacts with diamines generating catalytically relevant species. For example, when **1** is reacted with ethylenediamine/ethylene glycol mixture (110 °C, 15 min) a new complex is formed [Ru(en)$_2$(PN)]Cl(OTf) (**13**). However, the reaction with *N,N'*-dibenzylethylenediamine (**2a**)/ethylene glycol mixture gives trans-[RuCl$_2$(PN)(BnNHCH$_2$CH$_2$NHBn)] (**13a**). The structures of complexes **13** and **13a** were established crystallographically (Figures S86 and S87). Catalytic tests showed that **13** is incompetent in the alcohol-amine coupling, while **13a** is active and enables full conversion of **2a** to **6a** (Table S7). It seems that the formation of diamine-chelated Ru(II) complexes is involved in the overall catalytic process, however in case of ethylenediamine this chelation happens irreversibly and poisons the catalyst. Interestingly, catalyst poisoning is not observed in the presence of 1,3-diamines (Scheme S11): here we observe a mixture of uncyclized and cyclized products. We attribute the reactivity difference to the greater stability of the ethylene- versus propane-diamine chelates. Importantly, this poisoning effect appears only to impact reactions involving diamines, whereas amino alcohols have been efficiently cyclized by others using hydrogen borrowing conditions.[11a]

Owing to the vital importance of piperazine and diazepane substructures in medicinal chemistry, we tested our method against two representative pharmaceutical applications (Scheme 2): cyclizine (**4l**),[2] an FDA approved essential drug used as anti-nausea, is produced in 91% yield from its corresponding diamine and diol. Similarly, a seven membered drug homochlorcyclizine (**4m**),[3] which is marketed in Japan as an antihistamine, was synthesized in 67% yield. Our synthetic strategy has significant importance in process chemistry department of drug discovery as it is a green, atom economic and cost-efficient approach.

Scheme 2. Pharmaceutical Application: Synthesis of Cyclizine and Homochlorcyclizine.

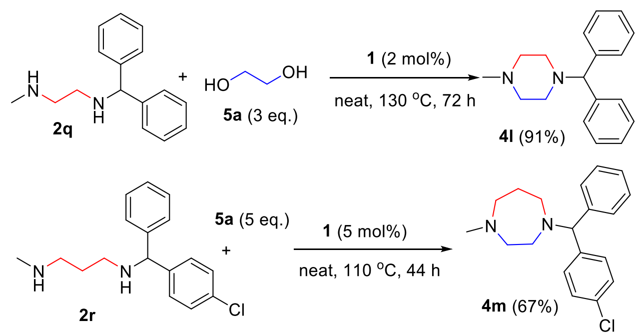

In sum, we report a catalytic synthesis of 1,4-diazacycles from diols and diamines that is uniquely enabled by our unusually reactive (pyridyl)phosphine ruthenium(II) complex **1**. The conditions tolerate a broad substrate scope including six- and seven-membered diazacycles with different substitution. The unique reactivity of our catalyst seems to include some resistance to diamine chelation: while **1** is susceptible to such chelation at high diamine loading, it maintains reactivity in the case of substituted diamines while other catalysts are not successful. In addition, we applied the hydrogen-borrowing strategy to the production of pharmaceutical compounds cyclizine and homochlorcyclizine, thus exhibiting the potential of the method in discovery or process medicinal chemistry.

ASSOCIATED CONTENT

Data Availability Statement

The data underlying this study are available in the published article and its Supporting Information and in the Cambridge Crystallographic Data Centre.

Supporting Information

The Supporting Information is available free of charge on the ACS Publications website.
Experimental procedures, graphical and tabular characterization information (PDF)
Crystallographic data for **4k** (#2217365, CIF)
Crystallographic data for **13** (#2217364, CIF)
Crystallographic data for **13a** (#2241666, CIF)

AUTHOR INFORMATION

Corresponding Author

*Email TJW: travisw@usc.edu

Funding Sources

This work was sponsored by the National Science Foundation, CHE-1856395. We thank the NSF (CHE-2018740, DBI-0821671, CHE-0840366, CHE-2018740), the NIH (S10 RR25432), and USC Research and Innovation Instrumentation Awards for analytical instrumentation. A.T. gratefully acknowledges USC Provost Fellowship funding.

Notes

While complex **1** is available from TCI America, the authors have no financial interest therein and no conflicting interests.

ACKNOWLEDGMENT

The authors thank Dr. Jeff Celaje (currently Provivi) for insightful discussions. We thank Dr. Thomas Saal, Jonas Schaab, Prof. Elias Picazo and Cesar Reyes (USC) for help with analytical instrumentation.

REFERENCES

1. (a) Vitaku, E.; Smith, D. T.; Njardarson, J. T. Analysis of the Structural Diversity, Substitution Patterns, and Frequency of Nitrogen Heterocycles among U.S. FDA Approved Pharmaceuticals. *Journal of Medicinal Chemistry* **2014**, *57* (24), 10257-10274.

2. (a) Cyclizine. https://en.wikipedia.org/wiki/Cyclizine (accessed May 1, 2022). (b) Cetirizine. https://pubchem.ncbi.nlm.nih.gov/compound/Cetirizine (accessed May 1, 2022). (c) Sitagliptin. https://en.wikipedia.org/wiki/Sitagliptin (accessed May 1, 2022).

3. (a) Homochlorcyclizine. https://en.wikipedia.org/wiki/Homochlorcyclizine (accessed May 1, 2022). (b) Homofenazine. https://pubchem.ncbi.nlm.nih.gov/compound/Homofenazine (accessed May 1, 2022).

4. For reviews, see: (a) Gettys, K. E.; Ye, Z.; Dai, M. Recent Advances in Piperazine Synthesis. *Synthesis* (Stuttgart) **2017**, *49* (12), 2589-2604. (b) Magriotis, P. A. Recent progress toward the asymmetric synthesis of carbon-substituted piperazine pharmacophores and oxidative related heterocycles. *RSC Medicinal Chemistry* **2020**, *11* (7), 745-759.

5. (a) Kono, S.; Watanabe, H. Homopiperazine from N,N'-dibenzylethylenediamine. JP43023629, 1968. (b) Sun, J.; Wu, X.; Zhang, F. A process for preparing homopiperazine. CN101891692, **2010**. (c) Liu, H. Process for the preparation of pharmaceutical intermediate homopiperazine using amino protection and cyclization reaction. CN103360330, **2013**.

6. (a) Lu, J.; Wang, S.; Lu, X.; Zou, Z. Process for preparation of N-monosubstituted homopiperazine. CN103121976, **2013**.

7. (a) (a) Gao, J.; Wang, X.; Li, Y.; Ye, D.; Xie, C. A process for preparing homopiperazine and its derivative. CN102120732, **2011**. (b) Periasamy, M.; Edukondalu, A.; Reddy, P. O. Synthesis of Chiral 2,3-Disubstituted 1,4-Diazabicyclo[2.2.2]octane Derivatives. *The Journal of Organic Chemistry* **2015**, *80* (7), 3651-3655.

8. (a) Crestey, F.; Witt, M.; Jaroszewski, J. W.; Franzyk, H. Expedite Protocol for Construction of Chiral Regioselectively N-Protected Monosubstituted Piperazine, 1,4-Diazepane, and 1,4-Diazocane Building Blocks. *The Journal of Organic Chemistry* **2009**, *74* (15), 5652-5655. (b) Montgomery, T. D.; Rawal, V. H. Palladium-Catalyzed Modular Synthesis of Substituted Piperazines and Related Nitrogen Heterocycles. *Organic Letters* **2016**, *18* (4), 740-743. (c) Ye, Z.; Adhikari, S.; Xia, Y.; Dai, M. Expedient syntheses of N-heterocycles via intermolecular amphoteric diamination of allenes. *Nature Communications* **2018**, *9* (1), 721.

9. (a) Lu, Z.; Stahl, S. S. Intramolecular Pd(II)-Catalyzed Aerobic Oxidative Amination of Alkenes: Synthesis of Six-Membered N-Heterocycles. *Organic Letters* **2012**, *14* (5), 1234-1237. (b) Ishiguro, T.; Matsumura, M. Synthesis of Piperazines. XII Synthesis of Homopiperazine. *Yakugaku Zasshi* **1959**, *79*, 153-156.

10. Vo, C.-V. T.; Luescher, M. U.; Bode, J. W. SnAP reagents for the one-step synthesis of medium-ring saturated N-heterocycles from aldehydes. *Nature Chemistry* **2014**, *6* (4), 310-314.

11. (a) Jumde, V. R.; Cini, E.; Porcheddu, A.; Taddei, M. A Metal-Catalyzed Tandem 1,4-Benzodiazepine Synthesis Based on Two Hydrogen-Transfer Reactions. *European Journal of Organic Chemistry* **2015**, *2015* (5), 1068-1074. (b) Todd Eary, C.; Clausen, D. Preparation of substituted 1,2,3,4-tetrahydroquinoxalines and 2,3,4,5-tetrahydro-1H-benzo[b][1,4]diazepines from catalytic Cp∗Ir hydrogen transfer N-heterocyclization of anilino alcohols. *Tetrahedron Letters* **2006**, *47* (38), 6899-6902. (c) Wu, Z.; Yang, F.; Wang, H.; Ma, J.; Chen, L.; Li, Y. A general process for the cyclization of aminoalcohols to the corresponding amines over Cu-Cr-La/γ-Al2O3. *React. Kinet., Mech. Catal.* **2012**, *106* (2), 485-493.

12. Celaje, J. J. A.; Zhang, X.; Zhang, F.; Kam, L.; Herron, J. R.; Williams, T. J. A Base and Solvent-Free Ruthenium-Catalyzed Alkylation of Amines. *ACS Catal.* **2017**, *7* (2), 1136-1142.

13. Nalikezhathu, A.; Cherepakhin, V.; Williams, T. J. Ruthenium Catalyzed Tandem Pictet–Spengler Reaction. *Organic Letters* **2020**, *22* (13), 4979-4984.

14. (a) Marichev, K. O.; Takacs, J. M. Ruthenium-Catalyzed Amination of Secondary Alcohols Using Borrowing Hydrogen Methodology. *ACS Catalysis* **2016**, *6* (4), 2205-2210. (b) Lorentz-Petersen, L. L. R.; Nordstrøm, L. U.; Madsen, R. Iridium-Catalyzed Condensation of Amines and Vicinal Diols to Substituted Piperazines. *European Journal of Organic Chemistry* **2012**, *2012* (34), 6752-6759. (c) Yang, P.; Zhang, C.; Gao, W.-C.; Ma, Y.; Wang, X.; Zhang, L.; Yue, J.; Tang, B. Nickel-catalyzed borrowing hydrogen annulations: access to diversified N-heterocycles. *Chemical Communications* **2019**, *55* (54), 7844-7847. (d) Crotti, C.; Farnetti, E.; Licen, S.; Barbieri, P.; Pitacco, G. Iridium-catalyzed N-alkylation of diamines with glycerol. *Journal of Molecular Catalysis A: Chemical* **2014**, *382*, 64-70.

15. Shimazu, H. Preparation of homopiperazine from 1,3-diaminopropane and ethylene glycol. JP2006306790, **2006**.

16. Leonard, J.; Blacker, A. J.; Marsden, S. P.; Jones, M. F.; Mulholland, K. R.; Newton, R. A Survey of the Borrowing Hydrogen Approach to the Synthesis of some Pharmaceutically Relevant Intermediates. *Org. Process. Res. Dev.* **2015**, *19*, 1400-1410.

17. Foster, A.; Wu, H.; Chen, W.; Williams, W.; Bowen, W. D.; Matsumoto, R. R.; Coop, A. 1,4-Dibenzylpiperazines possess anticocaine activity. *Bioorg. Med. Chem. Lett.* **2003**, *13* (4), 749-751.

18. Soeberdt, M.; Molenveld, P.; Storcken, R. P. M.; Bouzanne des Mazery, R.; Sterk, G. J.; Autar, R.; Bolster, M. G.; Wagner, C.; Aerts, S. N. H.; van Holst, F. R.; et al.. Design and Synthesis of Enantiomerically pure Decahydroquinoxalines as Potent and Selective κ-Opioid Receptor Agonists with Anti-Inflammatory Activity *in Vivo*. *J. Med. Chem*. **2017**, *60*, 2526-2551.

19. Barth, R.; Höferl-Prantz, K.; Richter, F.; Widschwenter, G. Novel routes of synthesis for the preparation of suvorexant. WO 2016020405 A1, February 11, 2016.

20. Jacobson, L.; Callander, G. E.; Hoyer, D. Suvorexant for the treatment of insomnia. *Expert Rev. Clin. Pharmacol.* **2014**, *7* (6), 711-730.

21. Blike, J. L.; O'Brien, P. On the Two-Ligand Catalytic Asymmetric Deprotonation of *N*-Boc Pyrrolidine: Probing the Effect of the Stoichiometric Ligand. *J. Org. Chem*. **2008**, *73*, 6452-6454.

22. Nordstrøm, L. U.; Madsen, R. Iridium Catalysed Synthesis of Piperazines from Diols. *Chemical Communications* **2007**, (47), 5034-5036.

23. Vellakkaran, M.; Singh, K.; Banerjee, D. An Efficient and Selective Nickel-Catalyzed Direct N-Alkylation of Anilines with Alcohols. *ACS Catal.* **2017**, *7*, 8152-8158.

24. Conley, B. L.; Pennington-Boggio, M. K.; Boz, E.; Williams, T. J. Discovery, Applications, and Catalytic Mechanisms of Shvo's Catalyst. *Chem. Rev*. **2010**, *110* (4), 2294-2312.

Supporting Information

Synthesis of 1,4-Diazacycles by Hydrogen-Borrowing

Anju Nalikezhathu, Adriane Tam, Valeriy Cherepakhin, Van K. Do, and Travis J. Williams*

Donald P. and Katherine B. Loker Hydrocarbon Institute and Department of Chemistry, University of Southern California, Los Angeles, California 90089-1661, United States

*travisw@usc.edu

Contents

I. General Procedure

All air and water sensitive procedures were carried out either in a Vacuum Atmospheres glove box under nitrogen (2-10 ppm O_2 for all manipulations) or using standard Schlenk techniques under nitrogen. Deuterated NMR solvents were purchased from Cambridge Isotopes Laboratories. Dichloromethane, methanol, ethyl acetate, and hexanes were purchased from VWR; toluene was dried using sodium benzophenone ketyl; dichloro(*p*-cymene)ruthenium(II) dimer was purchased from Strem. 2-((Di-tert-butylphosphino)methyl)pyridine[1] and ruthenium catalyst (**1**)[2] were synthesized using the published procedures. All other reagents were purchased and used as received if their syntheses are not described in SI.

A temperature-controlled oil bath was used as a heat source in all reactions where heating is required. NMR spectra were recorded on a Varian Mercury 400, Varian VNMRS 500, or VNMRS 600 spectrometer. All chemical shifts are reported in units of ppm and referenced to the residual ^{1}H or ^{13}C solvent peak. Spectra are line-listed according to (s) singlet, (bs) broad singlet, (d) doublet, (t) triplet, (dd) double doublet, etc. ^{13}C spectra are delimited by carbon peaks, not carbon count. Air sensitive NMR spectra were taken in 8" J-Young tubes (Wilmad or Norell) with Teflon valve plugs. IR spectra were recorded on Bruker OPUS FTIR spectrometer using type 61 polyethylene IR cards. Enantiomeric excess (ee) was determined by HPLC analysis on Agilent HPLC units, including the following instruments: pump, 1260 Infinity II G7104C Flexible Pump; detector, 1260 Infinity II Diode Array Detector WR (G7115A); column, Chiralpak IJ-3. X-ray crystallography data were obtained on a Rigaku XtaLAB Synergy, Dualflex, HyPiX diffractometer with Mo or Cu as the source as indicated in the CIF files. Optical rotations were recorded on a JASCO temperature-controlled digital polarimeter. High resolution mass spectrometry data were obtained from Agilent LC-QTOF instrument.

II. Optimization of the Homopiperazine Synthesis

Whereas efficient routes to piperazines are known, we began by optimizing our reaction for seven-membered ring synthesis (Table S1), using *N,N'*-dibenzylethylenediamine (**2a**) and 1,3-propanediol (**3a**). Beginning from our previous *N*-alkylation conditions with **1** (Table S1, entry 1), we went about finding conditions for a tandem cycloaddition reaction. The best conditions supply the diol in gentle excess, with diminishing returns beyond 2 equivalents (compare entries 1/2 with 3, 4 and 5). Even though water is a side product, addition of molecular sieves decreased the yield (Table S1, entry 6), possibly because they impede stirring of the neat reaction. Reducing the catalyst loading (Table S1, entry 7) and reaction time (Table S1, entries 8 and 9) decreased conversion. In the case of entry 5, LC-QTOF studies account for the material balance by showing imine and an oligomeric material along with the desired product (Figure S2).

General Procedure

In the drybox, a 1-dram vial was charged with 1,3-propanediol (1–4 equiv), *N,N'*-dibenzylethylenediamine, (1–2 equiv), and catalyst **1** (0.5–1.0 mol %). The vial was sealed, taken out of the glovebox, and heated to 110 °C. The solution turned to dark brown color. After the given time, the reaction mixture was allowed to cool to room temperature. Mesitylene was added to this reaction mixture as an internal standard, and an aliquot was taken for ^{1}H NMR analysis in $CDCl_3$. Results are summarized in Table S1.

Table S1. Optimization of the Homopiperazine Synthesis.

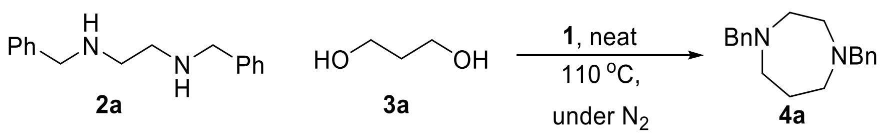

entry	diamine: diol	**1** loading	t (h)	yield[a]
1	1:1	1.0 mol %	44	71%
2	2:1	1.0 mol %	44	33%
3	1:2	1.0 mol %	44	84%
4	1:3	1.0 mol %	44	80%
5	1:4	1.0 mol %	44	80%
6[b]	1:2	1.0 mol %	44	66%
7	1:2	0.5 mol %	44	72%
8	1:2	1.0 mol %	10	60%
9	1:2	1.0 mol %	24	78%

[a]NMR yield with mesitylene as the internal standard. [b]With 4 Å molecular sieves.

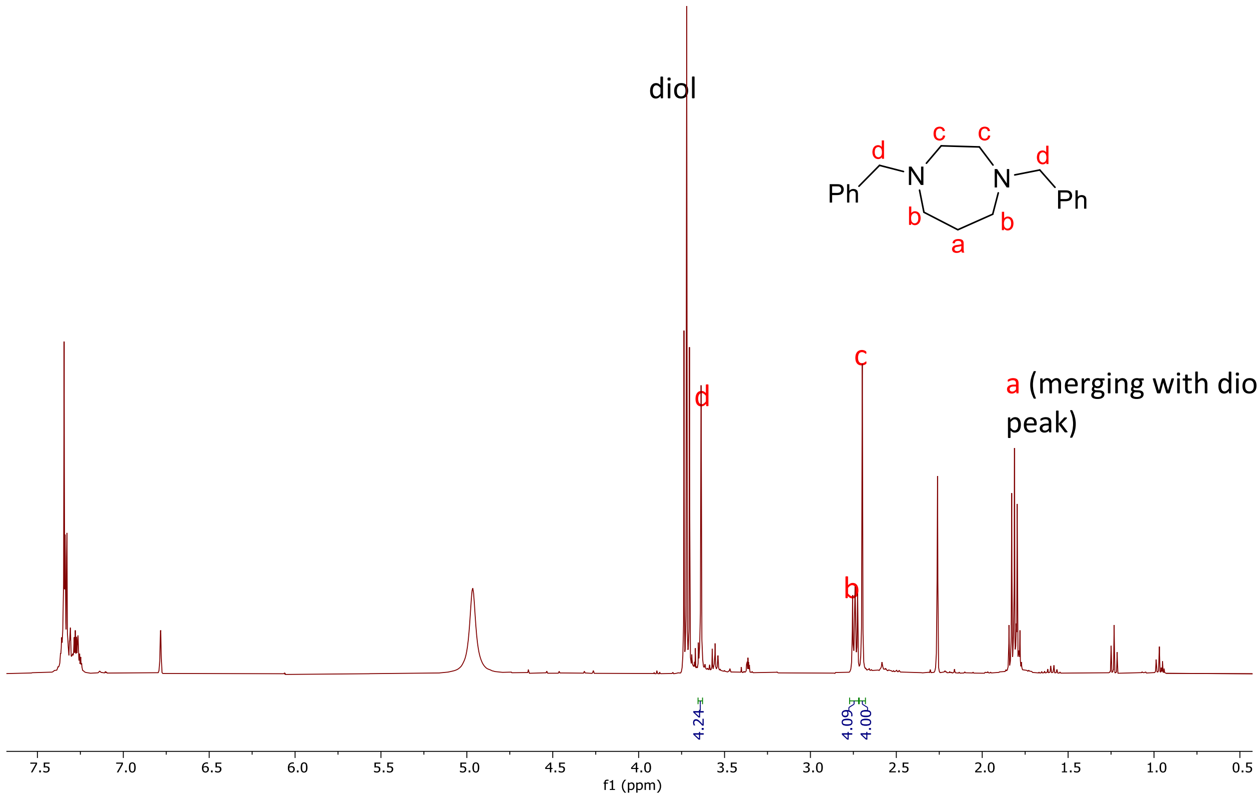

Figure S1. ^{1}H NMR spectrum of the crude reaction mixture for the coupling of *N,N'*-dibenzylethylenediamine (1equiv) and 1,3-propanediol (4 equiv) with 1 mol % **1** for 44 h.

Even though reactions with excess alcohol and 1 mol % **1** for 44 h achieved full conversion, crude NMR showed some peaks that do not correlate to the target compound (Figure S1). An LC-QTOF spectrum of the products of entry 5 (Table S1) with positive ionization method showed three major peaks (Figure S2), that may correspond to the desired product **I** (m/z calcd for $[C_{19}H_{25}N_2]^+$ 281.20122), an iminium ion intermediate **II** (m/z calcd for $[C_{19}H_{25}N_2O]^+$ 297.19614) and a dimerized side product **III** (m/z calcd for $[C_{38}H_{49}N_4O_2]^+$ 593.38500). This intermediate iminium ion supports the mechanism outlined in Scheme 1.

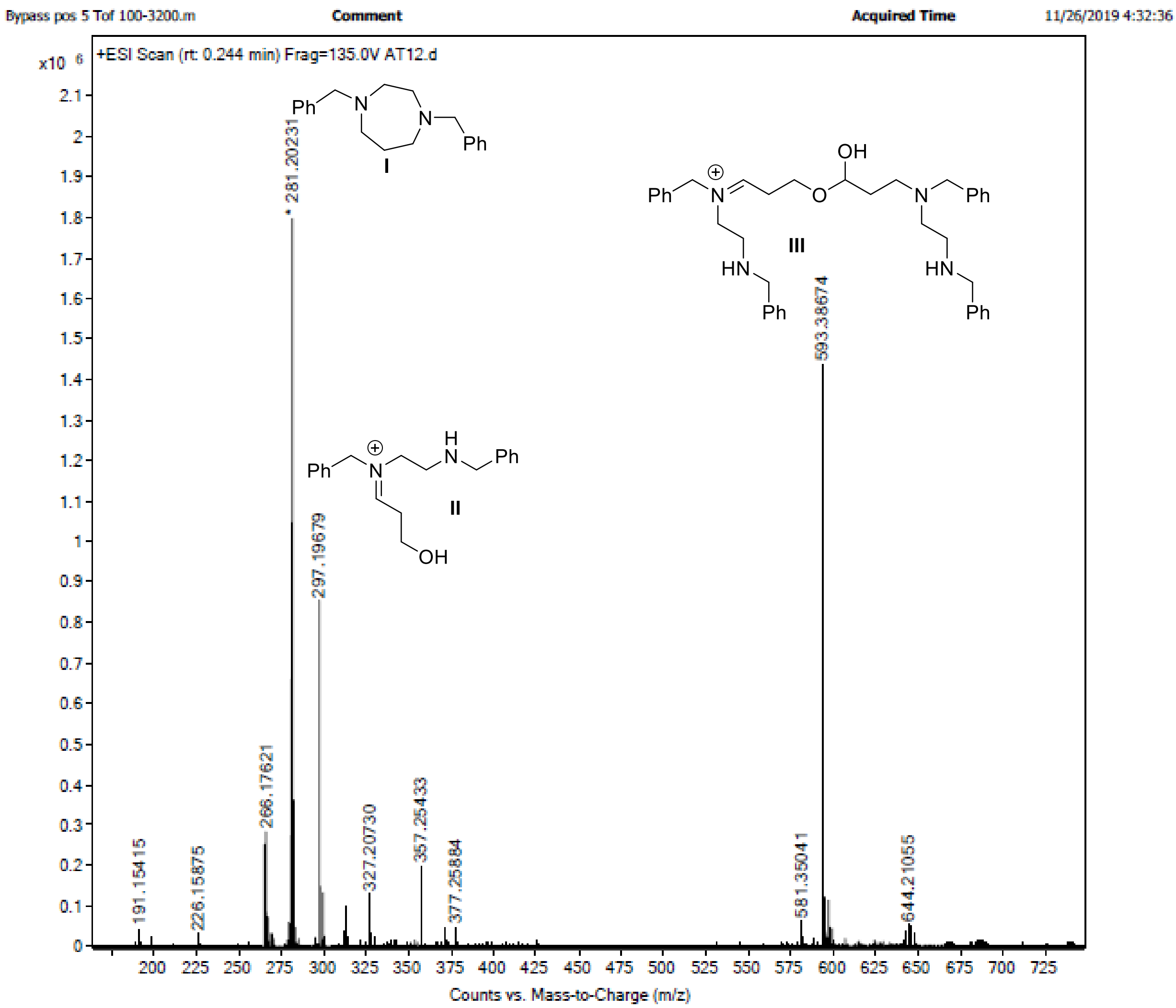

Figure S2. LC-QTOF spectrum of the crude reaction mixture for the coupling of *N,N'*-dibenzylethylenediamine (1equiv) and 1,3-propanediol (4 equiv) with 1 mol % **1** for 44 h.

III. Synthesis of Diamine Substrates

(1*R*,2*R*)-*N*[1],*N*[2]-dibenzylcyclohexane-1,2-diamine

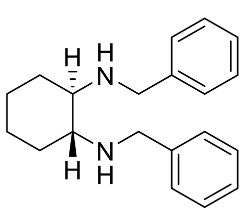

2b

In a 250 mL round bottom flask, the diamine (1*R*, 2*R*)-(–)-1,2-diaminocyclohexane (1 equiv, 13.13 mmol) and benzaldehyde (2 equiv, 26.26 mmol) were dissolved in methanol (80 mL) and stirred at room temperature. After 24 h, sodium borohydride (2.2 equiv, 28.89 mmol) was slowly added to the mixture at 0 °C and then stirred at room temperature for 24 hours. After this time, the solvent was removed under reduced pressure and DI water was added. The product was extracted into dichloromethane, dried over anhydrous Na_2SO_4; and the solvent was removed under reduced pressure.

The product **2b** was obtained in 88% yield (3.4 g) as an orange oil after silica flash chromatography (95:5 dichloromethane: methanol).

Data are consistent with the known compound.[3]

^{1}H NMR (600 MHz, $CDCl_3$) δ 7.34 – 7.28 (m, 8H), 7.26 – 7.22 (m, 2H), 3.91 (d, *J* = 13.1 Hz, 2H), 3.67 (d, *J* = 13.2 Hz, 2H), 2.33 – 2.25 (m, 2H), 2.20 – 2.13 (m, 2H), 1.78 – 1.68 (m, 2H), 1.29 – 1.18 (m, 2H), 1.11 – 1.00 (m, 2H).

^{13}C NMR (151 MHz, $CDCl_3$) δ 140.9, 128.5, 128.2, 127.0, 61.0, 50.9, 31.6, 25.1.

Optical Rotation: $[\alpha]_{\mathrm{WI}}^{20} = -55.4$ (c = 1.0, CH_2Cl_2).

Racemic compound (**2b'**) was synthesized for chiral HPLC from (±)-*trans*-1,2-diaminocyclohexane and benzaldehyde using the above procedure. The product was obtained in 87% yield as an orange oil after silica flash chromatography (50:50 hexanes: ethyl acetate).

^{1}H NMR (400 MHz, $CDCl_3$) δ 7.40 – 7.17 (m, 10H), 3.91 (d, *J* = 13.1 Hz, 2H), 3.67 (d, *J* = 13.2 Hz, 2H), 2.34 – 2.23 (m, 2H), 2.21 – 2.12 (m, 2H), 2.03 (bs, 2H), 1.79 – 1.67 (m, 2H), 1.31 – 1.16 (m, 2H), 1.13– 1.00 (m, 2H).

^{13}C NMR (151 MHz, $CDCl_3$) δ 141.2, 128.5, 128.2, 126.9, 61.0, 51.0, 31.7, 25.2.

Optical Rotation: $[\alpha]_{\mathrm{WI}}^{20} = 0.0$ (c = 0.8, CH_2Cl_2).

General Procedure A

In a 250 mL round bottom flask, diamine **14** and aldehyde **15** were dissolved in methanol at 0 °C then warm to room temperature while stirring. After 1 h, sodium borohydride was slowly added to the mixture at 0 °C, then stirred at room temperature for 40 hours. After the reaction, 1 M NaOH solution or saturated $NaHCO_3$ solution was added to the mixture until the pH is basic and stirred for 10 more minutes. The mixture was then concentrated to ca. half of its volume, partitioned with dichloromethane, and the organic extract was washed with brine. The collected organic layer was dried over anhydrous Na_2SO_4 and the solvent was removed under reduced pressure.

Table S2. Synthesis of simple diamine substrates.

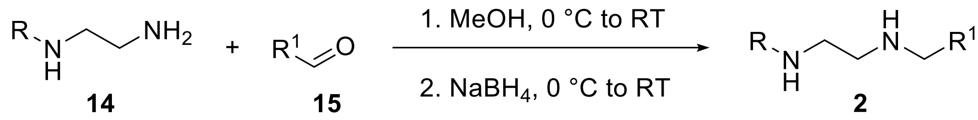

Entry	Diamine	R	Aldehyde	R^1	Product
1	**14a**	CH_2CH_2OH	**15a**	Ph	**2c**
2	**14b**	Bn	**15b**	Cy	**2f**
3	**14c**	Me	**15a**	Ph	**2g**
4	**14d**	Ph	**15a**	Ph	**2j**
5	**14b**	Bn	**15c**	4-OMePh	**2k**

2-((2-(Benzylamino)ethyl)amino)ethan-1-ol

Diamine **14a** (1 equiv, 39.9 mmol), aldehyde **15a** (1 equiv, 39.9 mmol) and sodium borohydride (2 equiv, 79.3 mmol) were subjected to general procedure A.

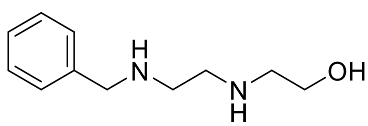

2c

The product **2c** was obtained in 81% yield (6.23 g) as a yellow oil. The diamine is used for the next step without further purification.

Data are consistent with the known compound.[4]

^{1}H NMR (600 MHz, $CDCl_3$) δ 7.34 – 7.22 (m, 5H), 3.79 (s, 2H), 3.63 (t, 2H), 2.76 – 2.72 (m, 6H), 2.41 (bs, 3H).

^{13}C NMR (151 MHz, $CDCl_3$) δ 140.2, 128.6, 128.3, 127.2, 61.0, 54.0, 51.2, 48.9, 48.8.

N^1-Benzyl-*N*^{2}-(cyclohexylmethyl)ethane-1,2-diamine

Diamine **14b** (1 equiv, 7.0 mmol), aldehyde **15b** (1 equiv, 7.0 mmol) and sodium borohydride (1 equiv, 7.0 mmol) were subjected to general procedure A.

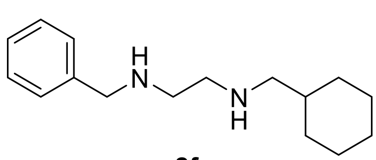

2f

The product **2f** was obtained in 93% yield (1.60 g) as a yellow oil after silica flash chromatography (75:25 dichloromethane: methanol).

^{1}H NMR (600 MHz, $CDCl_3$) δ 7.34 – 7.27 (m, 4H), 7.26 – 7.21 (m, 1H), 3.79 (s, 2H), 2.80 – 2.66 (m, 4H), 2.41 (d, J = 6.7 Hz, 2H), 1.87 – 1.58 (m, 7H), 1.49 – 1.38 (m, 1H), 1.28 – 1.08 (m, 3H), 0.95 – 0.83 (m, 2H).

^{13}C NMR (151 MHz, $CDCl_3$) δ 140.6, 128.5, 128.2, 127.0, 56.8, 54.1, 49.6, 48.8, 38.0, 31.6, 26.8, 26.2.

HRMS (LC-QTOF) m/z: $[M+H]^+$ Calcd for $C_{16}H_{27}N_2$ 247.2169; Found 247.2179.

FT-IR (thin film) cm^{-1}: 3385, 2920, 2850, 1647, 1577, 1452, 1406, 1265, 959, 809, 741, 698.

N^1-Benzyl-*N*^{2}-methylethane-1,2-diamine

Diamine **14c** (1 equiv, 9.31 mmol), aldehyde **15a** (1 equiv, 9.31 mmol) and sodium borohydride (2 equiv, 18.6 mmol) were subjected to general procedure A.

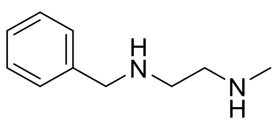

2g

The product **2g** was obtained in 56% yield (856 mg) as a yellow oil. The diamine is used without further purification.

Data are consistent with the known compound.[5]

^{1}H NMR (400 MHz, $CDCl_3$) δ 7.35 – 7.21 (m, 5H), 3.80 (s, 2H), 2.80 – 2.67 (m, 4H), 2.42 (s, 3H), 1.87 (bs, 2H).

N^1-Benzyl-*N*^{2}-phenylethane-1,2-diamine

Diamine **14d** (1 equiv, 16.0 mmol), aldehyde **15a** (1 equiv, 16.0 mmol) and sodium borohydride (1 equiv, 16.0 mmol) were subjected to general procedure A.

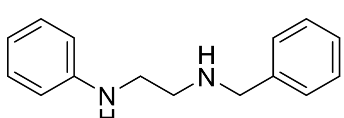

2j

The product **2j** was obtained in 88% yield (3.19 g) as a pale-yellow solid after silica flash chromatography (90:10 dichloromethane: methanol).

Data are consistent with the known compound.[6]

^{1}H NMR (500 MHz, $CDCl_3$) δ 7.37 – 7.23 (m, 5H), 7.22 – 7.15 (m, 2H), 6.72 (tt, J = 7.3, 1.1 Hz, 1H), 6.65 (dd, J = 8.6, 1.0 Hz, 2H), 3.83 (s, 2H), 3.24 (t, J = 5.7 Hz, 2H), 2.92 (t, 2H).

^{13}C NMR (126 MHz, $CDCl_3$) δ 148.6, 140.1, 129.4, 128.6, 128.3, 127.2, 117.5, 113.1, 53.7, 48.1, 43.6.

N^1-Benzyl-*N^2*-(4-methoxybenzyl)ethane-1,2-diamine

Diamine **14b** (1 equiv, 6.66 mmol), aldehyde **15c** (1 equiv, 6.66 mmol) and sodium borohydride (2 equiv, 13.0 mmol) were subjected to general procedure A.

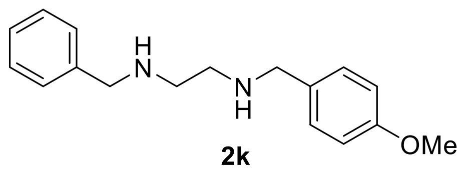

2k

The product **2k** was obtained in 85% yield (1.53 g) as a yellow oil after silica flash chromatography (90:10 dichloromethane: methanol).

^{1}H NMR (400 MHz, $CDCl_3$) δ 7.32 (d, J = 4.5 Hz, 4H), 7.28 – 7.22 (m, 3H), 6.89 – 6.83 (m, 2H), 3.79 (s, 3H), 3.78 (s, 2H), 3.74 (s, 2H), 2.78 (s, 4H).

^{13}C NMR (126 MHz, $CDCl_3$) δ 158.9, 140.0, 131.6, 129.7, 128.5, 128.3, 127.2, 113.9, 55.4, 53.8, 53.0, 48.2, 48.2.

HRMS (LC-QTOF) m/z: $[M+H]^+$ Calcd for $C_{17}H_{23}N_2O$ 271.1805; Found 271.1803.

FT-IR (thin film) cm^{-1}: 3275, 2918, 2848, 1675, 1610, 1512, 1457, 1252, 1177, 1032, 1839, 759, 697.

Table S3. Synthesis of substituted diamine substrates.

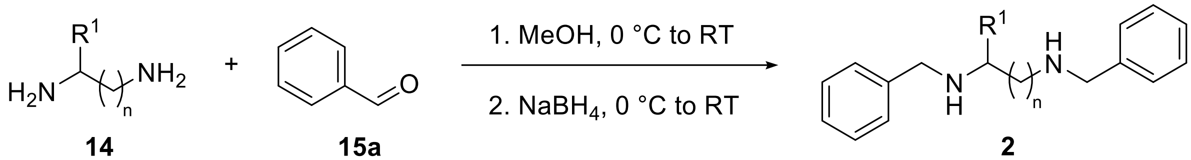

Entry	Diamine	n	R^1	Product
1	**14e**	2	Et	**2e**
2	**14f**	1	Me	**2l**
3	**14g**	3	H	**2m**

<u>N^1,N^3-Dibenzylpentane-1,3-diamine</u>

Diamine **14e** (1 equiv, 20.0 mmol), aldehyde **15a** (2 equiv, 40.0 mmol) and sodium borohydride (2 equiv, 40.0 mmol) were subjected to general procedure A.

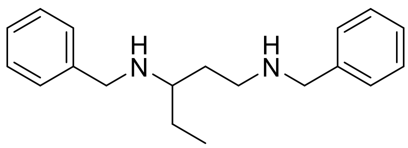

2e

The product **2e** was obtained in 73% yield (4.12 g) as a pale orange oil after silica flash chromatography (70:30 dichloromethane: methanol).

^{1}H NMR (500 MHz, $CDCl_3$) δ 7.49 – 7.16 (m, 10H), 3.88 – 3.73 (m, 4H), 2.91 – 2.60 (m, 3H), 2.27 (bs, 2H), 1.85 – 1.41 (m, 4H), 0.94 (t, J = 7.4 Hz, 3H).

^{13}C NMR (126 MHz, $CDCl_3$) δ 140.7, 140.0, 128.3, 128.3, 128.1, 126.9, 126.8, 57.4, 54.0, 50.9, 46.9, 33.1, 26.3, 9.8.

HRMS (LC-QTOF) m/z: $[M+H]^+$ Calcd for $C_{19}H_{27}N_2$ 283.2169; Found 283.2195.

FT-IR (thin film) cm^{-1}: 3295, 3030, 2934, 2913, 1494, 1455, 1364, 1121, 1028, 739, 698.

<u>N^1,N^2-Dibenzylpropane-1,2-diamine</u>

Diamine **14f** (1 equiv, 33.7 mmol), aldehyde **15a** (2 equiv, 67.4 mmol) and sodium borohydride (2 equiv, 67.4 mmol) were subjected to general procedure A.

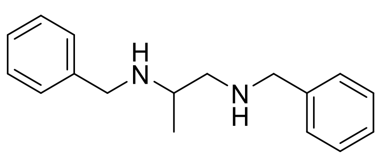

2l

The product **2l** was obtained as a yellow oil in 80% yield (6.86 g) after silica flash chromatography (80:20 dichloromethane: methanol).

Data are consistent with the known compound.[7]

^{1}H NMR (600 MHz, $CDCl_3$) δ 7.33 – 7.24 (m, 8H), 7.24 – 7.18 (m, 2H), 3.85 (d, J = 13.2 Hz, 1H), 3.71 (s, 2H), 3.66 (d, J = 13.1 Hz, 1H), 2.80 – 2.72 (m, 1H), 2.63 (dd, J = 11.8, 4.2 Hz, 1H), 2.49 (dd, J = 11.8, 8.4 Hz, 1H), 1.06 (d, J = 6.3 Hz, 3H).

^{13}C NMR (151 MHz, $CDCl_3$) δ 140.9, 140.7, 128.5, 128.4, 128.2, 128.1, 127.0, 126.9, 55.2, 54.0, 52.0, 51.4, 18.7.

N[1],N[4]-Dibenzylbutane-1,4-diamine

Diamine **14g** (1 equiv, 22.7 mmol), aldehyde **15a** (2 equiv, 45.5mmol) and sodium borohydride (2 equiv, 45.5mmol) were subjected to general procedure A.

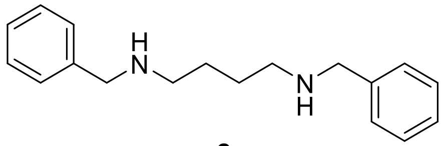

2m

The product **2m** was obtained in 99% yield (6.0 g) as a pale-yellow oil after silica flash chromatography (80:20 dichloromethane: methanol).

Data are consistent with the known compound.[8]

^{1}H NMR (500 MHz, $CDCl_3$) δ 7.43 – 7.20 (s, 10H), 3.81 (s, 4H), 2.72 – 2.60 (m, 4H), 1.67 – 1.47 (m, 6H).

^{13}C NMR (126 MHz, $CDCl_3$) δ 140.4, 128.3, 128.0, 126.8, 53.9, 49.2, 27.8.

N,N'-(Ethane-1,2-diyl)bis(2,2,2-trifluoroacetamide)

This compound was synthesized using published procedures.[9]

In a 25 mL round-bottom flask, ethylene diamine **14h** (1.0 equiv, 7.47 mmol) was dissolved in 5 mL diethyl ether at 0 °C. Then, trifluoroacetic anhydride **16** (2.2 equiv, 16.5 mmol) in diethyl ether (5 mL) was slowly added dropwise to the flask. After stirring for 1 hour, the white solid was concentrated *in vacuo* and then washed with water, filtered, and dried under reduced pressure.

Scheme S1. Synthesis of **2n**.

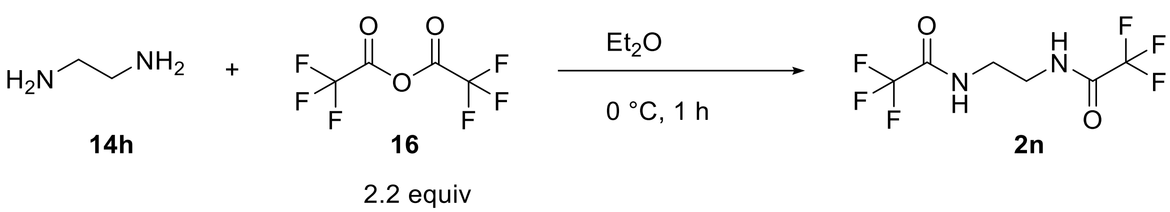

The product **2n** was obtained in 90% yield (1.70 g) as a white solid.

Data are consistent with the known compound.[9]

^{1}H NMR (600 MHz, CD_3OD) δ 3.46 (s, 4H).

^{13}C NMR (151 MHz, CD_3OD) δ 159.5 (q, J = 37.3 Hz), 117.4 (q, J = 286.7 Hz), 39.7.

Dibenzyl ethane-1,2-diyldicarbamate

This compound was synthesized using published procedures.[10]

In a 25 mL round-bottom flask, ethylene diamine **14h** (1 equiv, 4.48 mmol) was dissolved in 1 M NaOH solution (2 equiv, 8.96 mmol). This solution was cooled to 0 °C and benzyl chloroformate **17** (2 equiv, 8.94 mmol) was slowly added dropwise over the course of 45 minutes. The reaction was stirred for another 4 hours. The solid product was filtered, washed with water and hexane, and then left to airdry overnight.

Scheme S2. Synthesis of **2o**.

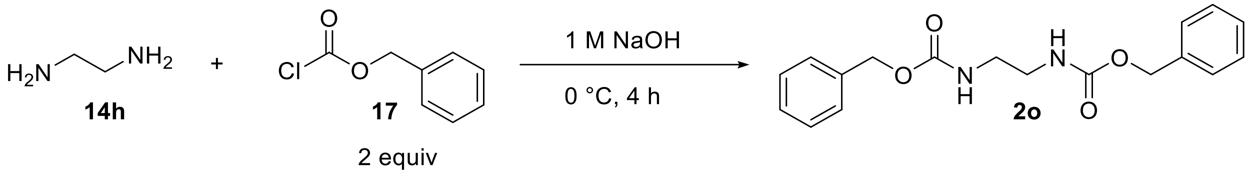

The product **2o** was obtained in 75% yield (1.10 g) as a white solid.

Data are consistent with the known compound.[10]

^{1}H NMR (600 MHz, $CDCl_3$) δ 7.39 – 7.28 (m, 10H), 5.19 (bs, 2H), 5.08 (s, 4H), 3.39 – 3.20 (m, 4H).

^{13}C NMR (151 MHz, $CDCl_3$) δ 157.0, 136.5, 128.8, 128.7, 128.3, 128.2, 67.0, 41.4.

Di-tert-butyl ethane-1,2-diyldicarbamate

This compound was synthesized using published procedures.[11]

In a 25 mL round-bottom flask, di-tert-butyl dicarbonate **18** (2 equiv, 14.94 mmol) and sulfamic acid (5 mol %, 0.374 mmol) were mixed. Then, ethylene diamine **14h** (1 equiv, 7.47 mmol) was added and the mixture was stirred for 3 minutes at room temperature. After the reaction, the white solid was filtered off and washed with cold water.

Scheme S3. Synthesis of **2p**.

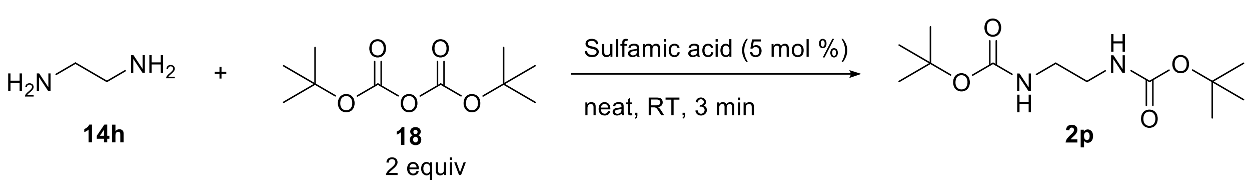

The product **2p** was obtained in 73% yield (1.42 g) as an off-white solid.

Data are consistent with the known compound.[12]

^{1}H NMR (600 MHz, $CDCl_3$) δ 4.86 (bs, 2H), 3.22 (s, 4H), 1.43 (s, 18H).

^{13}C NMR (151 MHz, $CDCl_3$) δ 156.5, 79.5, 40.9, 28.5.

General Procedure B

In a 100 mL round bottom flask, the diamine **14** and the aldehyde **19** were dissolved in toluene. *p*-TsOH•H_2O was then added, and the mixture was refluxed for 48 hours using a Dean Stark trap open to air. After the reaction, 40 mL of 1 M NaOH was added to the mixture until the pH is basic (according to pH paper). The solution was stirred for an additional 10 minutes. The organic layer was collected, and a fresh portion of toluene (15 mL) was added to the aqueous layer two more times to extract the product. The combined organic layer was dried over anhydrous Na_2SO_4 and the solvent was removed under reduced pressure.

The product from the first step (above) was dissolved in MeOH and sodium borohydride was added to the mixture at 0 °C. The mixture was brought to room temperature and stirred overnight. Thereafter, 40 mL of 1 M NaOH was added. The mixture was partitioned between dichloromethane and brine. The combined organic layers were collected, dried over anhydrous Na_2SO_4, and the solvent was removed under reduced pressure.

Table S4. Synthesis of substituted diimines and diamines.

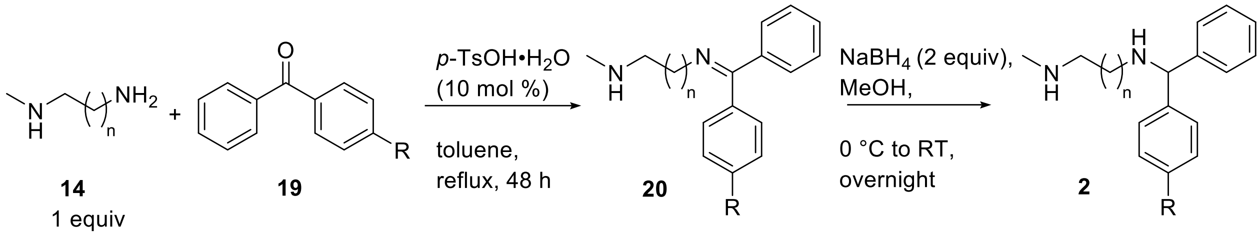

Entry	Diamine	n	Aldehyde	R	Product
1	**14c**	1	**19a**	H	**20a / 2q**
2	**14i**	2	**19i**	Cl	**20i / 2r**

N[1]-Benzhydryl-*N*[2]-methylethane-1,2-diamine

This was synthesized using General Procedure B. For the first step, the diamine **14c** (1 equiv, 13.5 mmol) and the aldehyde **19a** (1 equiv, 13.5 mmol) were dissolved in toluene (25 mL). Then, *p*-TsOH•H_2O (10 mol %, 1.35 mmol) was added.

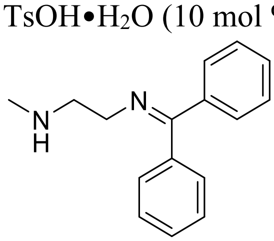

20a

^{1}H NMR (600 MHz, $CDCl_3$) δ 7.83 – 7.14 (m, 10H), 3.49 (t, J = 5.9 Hz, 2H), 2.89 (t, J = 6.3 Hz, 2H), 2.47 (s, 3H).

^{13}C NMR (151 MHz, $CDCl_3$) δ 169.3, 139.8, 137.7, 137.0, 132.5, 130.2, 130.1, 128.7, 128.5, 128.4, 128.4, 128.2, 127.8, 53.2, 52.8, 36.4.

For the second step, the resulting product from the first step **20a** was dissolved in 30 mL MeOH. Sodium borohydride (2 equiv, 27 mmol) was added at 0 °C.

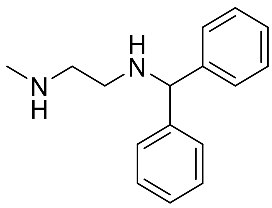

2q

The product **2q** was obtained in 58% yield (1.89 g) after silica flash chromatography (50:50 dichloromethane: methanol) as a colorless oil.

^{1}H NMR (600 MHz, $CDCl_3$) δ 7.44 (d, J = 6.7 Hz, 4H), 7.31 (t, J = 7.7 Hz, 4H), 7.22 (t, J = 7.3 Hz, 2H), 4.84 (s, 1H), 2.72 (s, 4H), 2.41 (s, 3H), 2.30 (bs, 2H).

^{13}C NMR (151 MHz, $CDCl_3$) δ 144.1, 128.3, 127.2, 126.8, 67.5, 51.4, 47.1, 36.0.

HRMS (LC-QTOF) m/z: $[M+H]^+$ Calcd for $C_{16}H_{21}N_2$ 241.1699; Found 241.1705.

FT-IR (thin film) cm^{-1}: 3301, 3027, 2918, 2849, 2798, 1600, 1493, 1383, 1262, 1105, 1028, 745, 703.

N^1-((4-Chlorophenyl)(phenyl)methyl)-*N*^{3}-methylpropane-1,3-diamine

This was synthesized using General Procedure B. For the first step, the diamine **14i** (1 equiv, 11.3 mmol) and the aldehyde **19i** (1 equiv, 11.3 mmol) were dissolved in toluene (25 mL). Then, *p*-TsOH•H_2O (10 mol %, 1.13 mmol) was added.

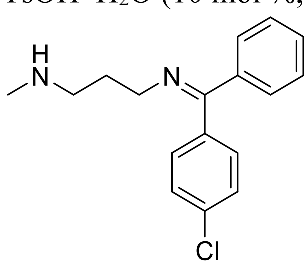

20i

^{1}H NMR (600 MHz, $CDCl_3$) δ 7.57 – 7.07 (m, 9H), 3.43 – 3.38 (m, 2H), 2.69 – 2.62 (m, 2H), 2.44 – 2.39 (m, 3H), 1.88 – 1.811 (m, 2H), 1.62 (bs, 1H).

For the second step, the resulting product from the first step **20i** was dissolved in 40 mL MeOH. Sodium borohydride (2 equiv, 21.9 mmol) was added at 0 °C.

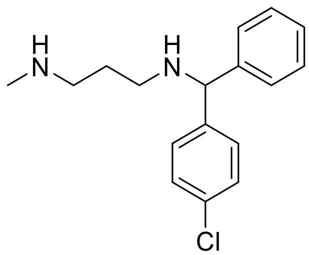

2r

The product **2r** was obtained in 73% yield as a pale-yellow oil (2.4 g) after silica flash chromatography (50:50 dichloromethane: methanol).

^{1}H NMR (600 MHz, $CDCl_3$) δ 7.37 – 7.15 (m, 9H), 4.76 (s, 1H), 2.68 – 2.55 (m, 4H), 2.40 (s, 3H), 1.83 (bs, 2H), 1.69 (p, J = 6.9 Hz, 2H).

^{13}C NMR (151 MHz, $CDCl_3$) δ 143.9, 142.8, 132.6, 128.6, 128.6, 127.2, 127.2, 67.1, 50.5, 46.6, 36.5, 30.2.

HRMS (LC-QTOF) m/z: $[M+H]^+$ Calcd for $C_{17}H_{22}N_2Cl$ 289.1466; Found 289.1467.

FT-IR (thin film) cm^{-1}: 3278, 3026, 2920, 2848, 2800, 1490, 1270, 1089, 1015, 809, 757, 717, 700.

IV. Substrate Scope

General Procedure

In the drybox, a 1-dram vial was charged with diamine (*x* equiv), diol (*y* equiv), and catalyst **1**. The vial was capped, taken out of the glovebox, and heated to 110 °C. The solution turned to a dark brown color. After the given time, the reaction mixture was allowed to cool to room temperature followed by a dichloromethane/water work up. Products were isolated either by a gravity column or flash column. Substrate concentrations are summarized in Table 1 and Table 2 (main text). Reactions are on 0.2 mmol scale unless otherwise noted. Structural assignments were made with additional information from gCOSY, gHSQC, and gHMBC experiments.

Scheme S4. Synthesis of 1,4-Diazacycles.

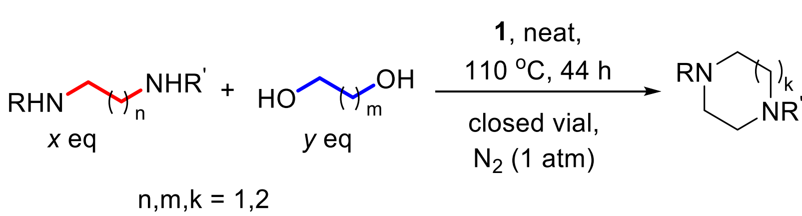

1,4-Dibenzylpiperazine

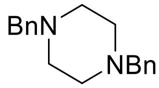

6a

The product was obtained in 86% yield (46 mg) as a white solid after silica flash column chromatography (90:10 hexanes: ethyl acetate).

Data are consistent with the known compound.[13]

^{1}H NMR (600 MHz, $CDCl_3$) δ 7.35 – 7.29 (m, 8H), 7.28 – 7.23 (m, 2H), 3.53 (s, 4H), 2.51 (s, 8H).

^{13}C NMR (151 MHz, $CDCl_3$) δ 138.3, 129.3, 128.3, 127.1, 63.2, 53.2.

(4a*R*, 8a*R*)-1,4-Dibenzyldecahydroquinoxaline

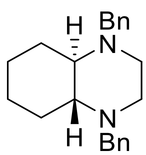

6b

The reaction was done on 0.6 mmol scale. The product was obtained in 84% yield (162 mg) as a colorless oil (which turned to off white solid upon standing) after silica flash column chromatography (80:20 hexanes: ethyl acetate).

^{1}H NMR (400 MHz, $CDCl_3$) δ 7.38 – 7.13 (m, 10H), 4.11 (d, J = 13.4 Hz, 2H), 3.17 (d, J = 13.4 Hz, 2H), 2.62 (d, J = 7.9 Hz, 2H), 2.33 – 2.25 (m, 2H), 2.21 (d, J = 7.8 Hz, 2H), 2.14 – 2.07 (m, 2H), 1.82 – 1.73 (m,2H), 1.44 – 1.12 (m, 4H).

^{13}C NMR (151 MHz, $CDCl_3$) δ 139.0, 129.3, 128.2, 126.8, 66.1, 57.6, 52.4, 29.7, 25.2.

FT-IR (thin film) cm^{-1}: 3030, 2969, 2941, 2919, 2855, 2799, 2750, 2713, 1494, 1455, 1378, 1253, 1155, 1087, 1029, 828,737, 696, 482.

HRMS (LC-QTOF) m/z: $[M+H]^+$ Calcd for $C_{22}H_{29}N_2$ 321.2331; Found 321.2344.

Optical Rotation: $[\alpha]_{\mathrm{WI}}^{20} = -118.2$ (c = 0.74, CH_2Cl_2). > 99% ee (HPLC condition: Chiralpak IJ-3 column, *n*-hexane/*i*-PrOH = 99:1, flowrate = 3mL/min, wavelength = 230 nm, t_R = 2.03 min for major isomer and t_R= 2.96 min for minor isomer).

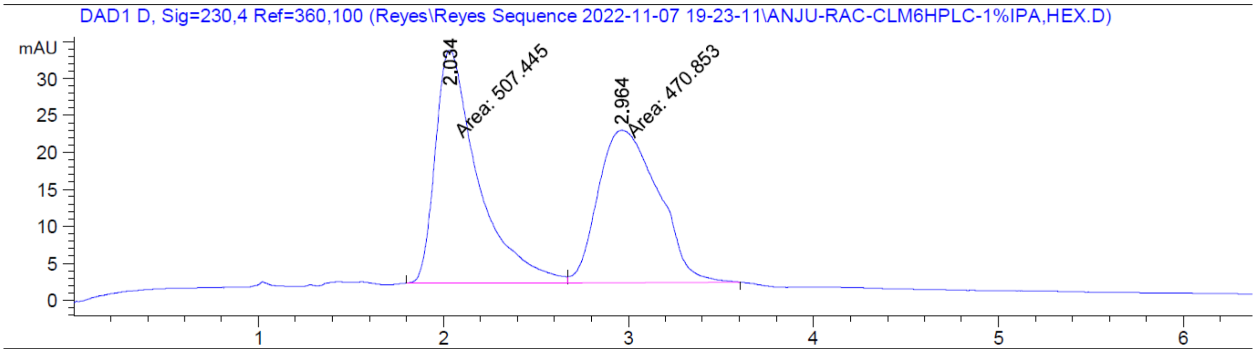

Peak #	RetTime [min]	Type	Width [min]	Area [mAU*s]	Height [mAU]	Area %
1	2.034	MF	0.2683	507.44473	31.52504	51.8702
2	2.964	FM	0.3801	470.85303	20.64745	48.1298

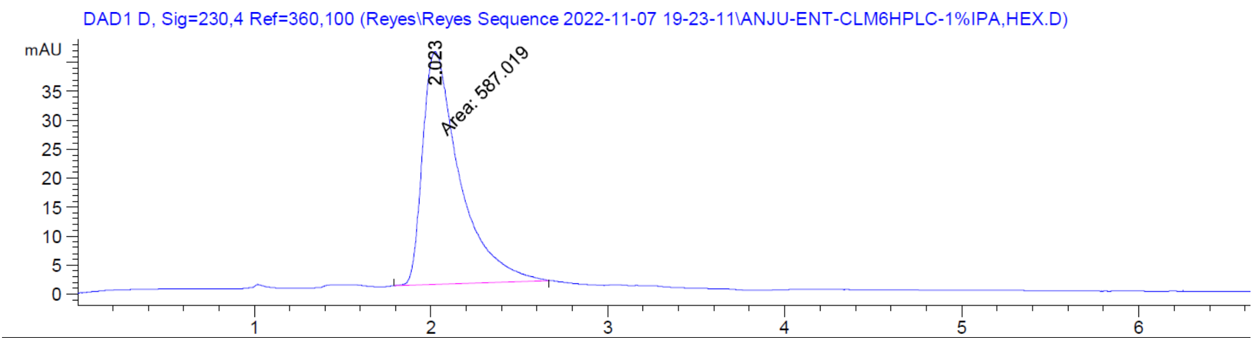

Peak #	RetTime [min]	Type	Width [min]	Area [mAU*s]	Height [mAU]	Area %
1	2.023	MM	0.2432	587.01874	40.22820	100.0000

Racemic compound was synthesized for chiral HPLC from **2b'** and ethylene glycol using the same procedure on 0.6 mmol scale. The product was obtained in 80% yield as colorless oil (which turned to off white solid upon standing) after silica flash chromatography (80:20 hexanes: ethyl acetate).

^{1}H NMR (400 MHz, $CDCl_3$) δ 7.42 – 7.13 (m, 10H), 4.11 (d, J = 13.4 Hz, 2H), 3.17 (d, J = 13.4 Hz, 2H), 2.63 (d, J = 7.9 Hz, 2H), 2.33 – 2.25 (m, 2H), 2.21 (d, J = 7.8 Hz, 2H), 2.14 – 2.05 (m, 2H), 1.84 – 1.75 (m, 2H), 1.44 – 1.13 (m, 4H).

^{13}C NMR (151 MHz, $CDCl_3$) δ 138.9, 129.4, 128.2, 126.9, 66.1, 57.6, 52.3, 29.6, 25.2.

HRMS (LC-QTOF) m/z: $[M+H]^+$ Calcd for $C_{22}H_{29}N_2$ 321.2331; Found 321.2341.

Optical Rotation: $[\alpha]_{\mathrm{WI}}^{20} = 0.0$ (c = 0.54, CH_2Cl_2).

2-(4-Benzylpiperazin-1-yl)ethan-1-ol

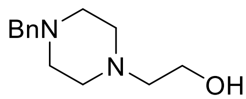

6c

The product was obtained in 78% yield (34.5 mg) as a yellow oil after silica gravity column chromatography (95:5 dichloromethane: methanol).

Data are consistent with the known compound.[14]

^{1}H NMR (500 MHz, $CDCl_3$) δ 7.32 (d, J = 4.4 Hz, 4H), 7.28 – 7.23 (m, 1H), 3.62 (t, J = 5.4 Hz, 2H), 3.52 (s, 2H), 3.18 (s, 1H), 2.75 – 2.31 (m, 10H).

^{13}C NMR (126 MHz, $CDCl_3$) δ 138.1, 129.3, 128.3, 127.2, 63.1, 59.4, 59.4, 57.8, 57.8, 53.1, 53.0.

1,4-Dibenzyl-1,4-diazepane

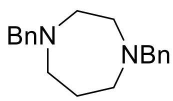

4a

The product was obtained in 78% yield (44 mg) from *N,N'*-dibenzylethylenediamine (**2a**) and 1,3-propanediol (**3a**); and in 86% yield (48 mg) from *N,N'*-dibenzylpropanediamine (**2d**) and ethylene glycol (**5a**) as a pale-yellow oil after silica flash column chromatography (50:50 hexanes: ethyl acetate).

Data are consistent with the known compound.[15]

^{1}H NMR (400 MHz, $CDCl_3$) δ 7.36 – 7.28 (m, 8H), 7.27 – 7.20 (m, 2H), 3.65 (s, 4H), 2.77 – 2.71 (m, 4H), 2.68 (s, 4H), 1.85 – 1.75 (m, 2H).

^{13}C NMR (151 MHz, $CDCl_3$) δ 139.8, 128.9, 128.2, 126.9, 62.8, 55.2, 54.4, 27.8.

1,4-Dibenzyl-2-methyl-1,4-diazepane

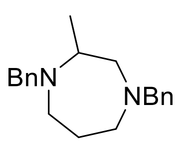

4b

The product was obtained in 68% yield (40 mg) as a colorless oil after silica flash column chromatography (90:10 hexanes: ethyl acetate).

^{1}H NMR (600 MHz, $CDCl_3$) δ 7.44 – 7.37 (m, 4H), 7.37– 7.30 (m, 4H), 7.29 – 7.22 (m, 2H), 3.86 (d, J = 13.9 Hz, 1H), 3.78 – 3.66 (m, 3H), 3.02 – 2.94 (m, 1H), 2.93 – 2.86 (m, 1H), 2.77 – 2.67 (m, 3H), 2.64 – 2.58 (m, 1H), 2.58 – 2.52 (m, 1H), 1.83– 1.75 (m, 1H), 1.70 – 1.61 (m, 1H), 1.04 (d, J = 6.5 Hz, 3H).

^{13}C NMR (151 MHz, $CDCl_3$) δ 141.1, 140.2, 128.9, 128.8, 128.3, 128.2, 126.9, 126.7, 63.1, 61.0, 57.4, 57.2, 55.9, 48.7, 28.0, 17.8.

FT-IR (thin film) cm^{-1}:2950, 2810, 1459, 1262, 1155, 1072, 756, 701, 638.

HRMS (LC-QTOF) m/z: $[M+H]^+$ Calcd for $C_{20}H_{27}N_2$ 295.2174; Found 295.2184.

The same compound was synthesized from the coupling of *N*,*N′*-dibenzyl-1,3-propanediamine (**2d**) and (*S*)-(+)-1,2-propanediol (**5c**). The product was obtained in 60% yield (350 mg) as a colorless oil after silica flash column chromatography (90:10 hexanes: ethyl acetate). Optical rotation of the compound was measured, which confirmed that it is a racemic mixture.

Optical Rotation: $[\alpha]_{\mathrm{WI}}^{25} = 0.0$ (c = 1.24, $CHCl_3$).

<u>1,4-Dibenzyl-5-methyl-1,4-diazepane</u>

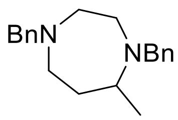

4c

The product was obtained in 71% yield (42 mg) as a colorless oil after silica flash column chromatography (95:5 dichloromethane: methanol with 1% Et_3N).

^1H NMR (600 MHz, $CDCl_3$) δ 7.37 – 7.20 (m, 10H), 3.79 (d, J = 13.8 Hz, 1H), 3.70 – 3.65 (m, 3H), 3.06 – 2.98 (m, 1H), 2.96 – 2.89 (m, 1H), 2.88 – 2.82 (m, 1H), 2.75 – 2.56 (m, 4H), 2.05 – 1.96 (m, 1H), 1.82 – 1.73 (m, 1H), 1.12 (d, J = 6.3 Hz, 3H).

^{13}C NMR (151 MHz, $CDCl_3$) δ 140.2, 129.5, 129.1, 128.9, 128.5, 128.4, 127.5, 127.0, 62.9, 58.1, 56.8, 56.2, 52.2, 48.2, 34.9, 18.6.

FT-IR (thin film) cm^{-1}: 2955, 2813, 1457, 1374, 1260, 1155, 1031, 738, 697, 639.

HRMS (LC-QTOF) m/z: $[M+H]^+$ Calcd for $C_{20}H_{27}N_2$ 295.2174; Found 295.2197.

<u>1,4-Dibenzyl-5-ethyl-1,4-diazepane</u>

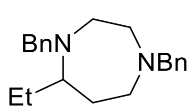

4d

The product was obtained in 83% yield (51 mg) as a colorless oil after silica flash column chromatography (80:20 hexanes: ethyl acetate).

^1H NMR (600 MHz, $CDCl_3$) δ 7.38 – 7.20 (m, 10H), 3.84 – 3.73 (m, 2H), 3.66 – 3.58 (m, 2H), 2.94 (dd, J = 16.4, 5.9 Hz, 1H), 2.85 – 2.79 (m, 1H), 2.77 – 2.67 (m, 2H), 2.63 – 2.51 (m, 3H), 1.98 – 1.87 (m, 1H), 1.84 – 1.75 (m, 1H), 1.68 – 1.56 (m, 1H), 1.52 – 1.42 (m, 1H), 0.91 (t, J = 7.4 Hz, 3H).

^{13}C NMR (151 MHz, $CDCl_3$) δ 140.9, 139.1, 129.2, 128.8, 128.3, 128.3, 127.1, 126.8, 64.2, 63.2, 57.1, 55.0, 53.4, 49.2, 32.4, 27.0, 11.2.

FT-IR (thin film) cm^{-1}: 2960, 2814, 1676, 1494, 1455, 1351, 1262, 1105, 1027, 734, 697.

HRMS (LC-QTOF) m/z: $[M+H]^+$ Calcd for $C_{21}H_{29}N_2$ 309.2325; Found 309.2349.

1-Benzyl-4-cyclohexyl-1,4-diazepane

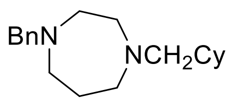

4e

The product was obtained in 70% yield (38 mg) as a colorless oil after silica flash column chromatography (50:50 hexanes: ethyl acetate).

^1H NMR (600 MHz, $CDCl_3$) δ 7.37 – 7.21 (m, 5H), 3.64 (s, 2H), 2.75 – 2.63 (m, 8H), 2.28 (d, J = 7.0 Hz, 2H), 1.82 – 1.74 (m, 4H), 1.73 – 1.62 (m, 3H), 1.46 – 1.36 (m, 1H), 1.27 – 1.10 (m, 3H), 0.90 – 0.80 (m, 2H).

^{13}C NMR (151 MHz, $CDCl_3$) δ 139.8, 129.0, 128.3, 126.9, 65.4, 62.7, 55.6, 55.0, 54.9, 54.6, 36.3, 32.0, 27.5, 27.0, 26.3.

FT-IR (thin film) cm^{-1}: 3028, 2920, 2848, 2811, 1680, 1449, 1356, 1124, 729, 697.

HRMS (LC-QTOF) m/z: $[M+H]^+$ Calcd for $C_{19}H_{31}N_2$ 287.2482; Found 287.2503.

1-Benzyl-4-methyl-1,4-diazepane

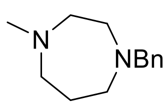

4f

The reaction was done on 0.4 mmol scale. The product was obtained in 71% yield (58 mg) as a pale-yellow oil after silica flash column chromatography (80:20 dichloromethane with 1 % Et_3N: methanol with 1% Et_3N).

^1H NMR (600 MHz, $CDCl_3$) δ 7.38 – 7.18 (m, 5H), 3.64 (s, 2H), 2.75 – 2.61 (m, 8H), 2.38 (s, 3H), 1.83 (p, J = 6.3 Hz, 2H).

^{13}C NMR (151 MHz, $CDCl_3$) δ 139.7, 129.0, 128.3, 127.1, 63.0, 58.3, 56.9, 54.4, 47.1, 27.4.

FT-IR (thin film) cm^{-1}: 3030, 2922, 2850, 1654, 1457, 1029, 742, 701.

HRMS (LC-QTOF) m/z: $[M+H]^+$ Calcd for $C_{13}H_{21}N_2$ 205.1699; Found 205.1702.

1,4-Dimethyl-1,4-diazepane

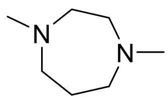

4g

Reaction was performed on 8.0 mmol scale in a Schlenk reactor. Volatility of the compound precluded its separation from the excess volatile diamine substrate. ^{1}H NMR spectra of the crude reaction mixture in $CDCl_3$ showed desired product in 88% NMR yield with mesitylene as the internal standard.

Data are consistent with the known compound.[16]

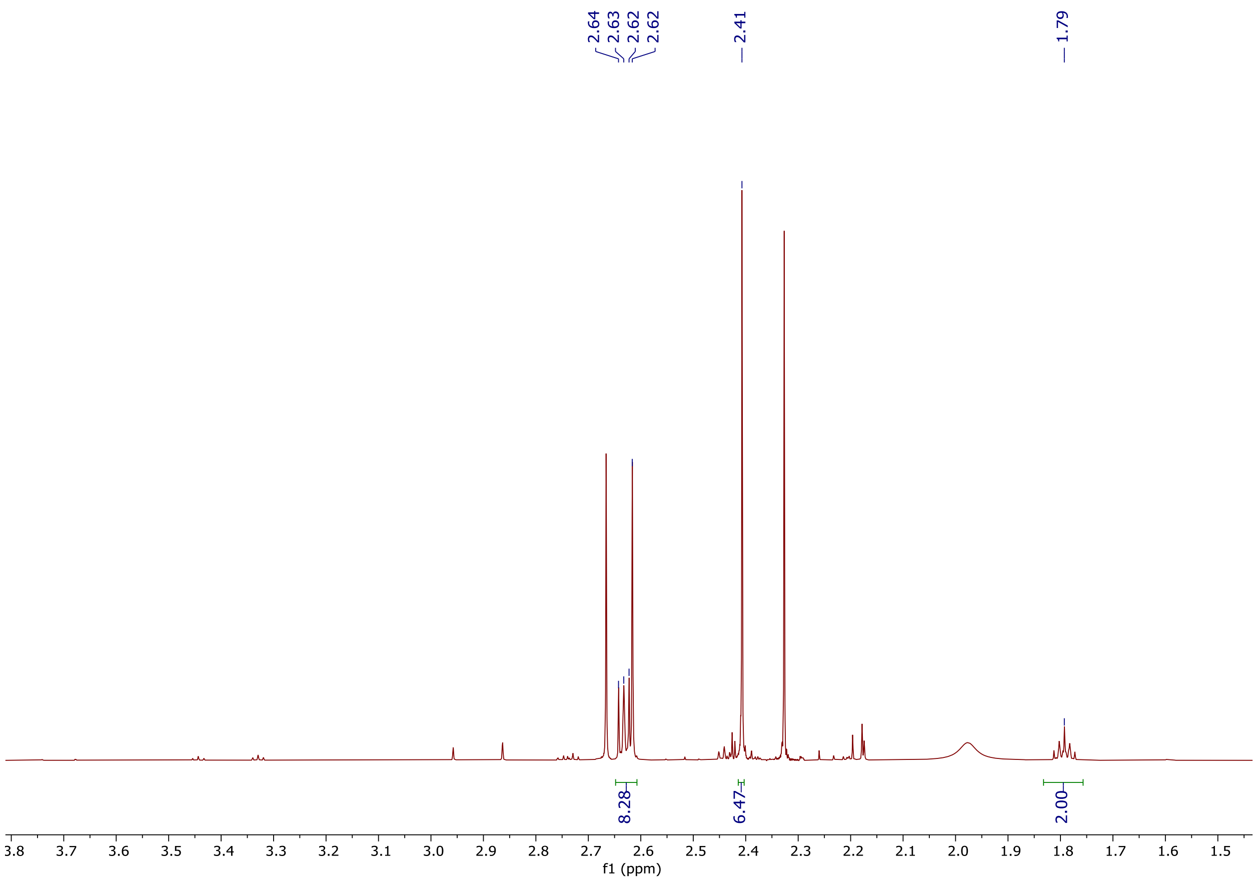

Figure S3. ^{1}H NMR spectrum of the crude reaction mixture for the coupling of *N,N'*-dimethylethylenediamine (2 equiv) and 1,3-propanediol (1 equiv) with 1 mol % **1** for 44 h. The peaks at 2.33 ppm and 2.67 ppm belongs to the excess starting diamine.

1,4-Diisopropyl-1,4-diazepane

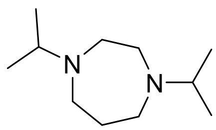

4h

Volatility of the compound precluded its separation from the excess volatile diamine substrate. [1]H NMR spectra of the crude reaction mixture in $CDCl_3$ showed desired product in 80% NMR yield with mesitylene as the internal standard.

Data are consistent with the known compound.[17]

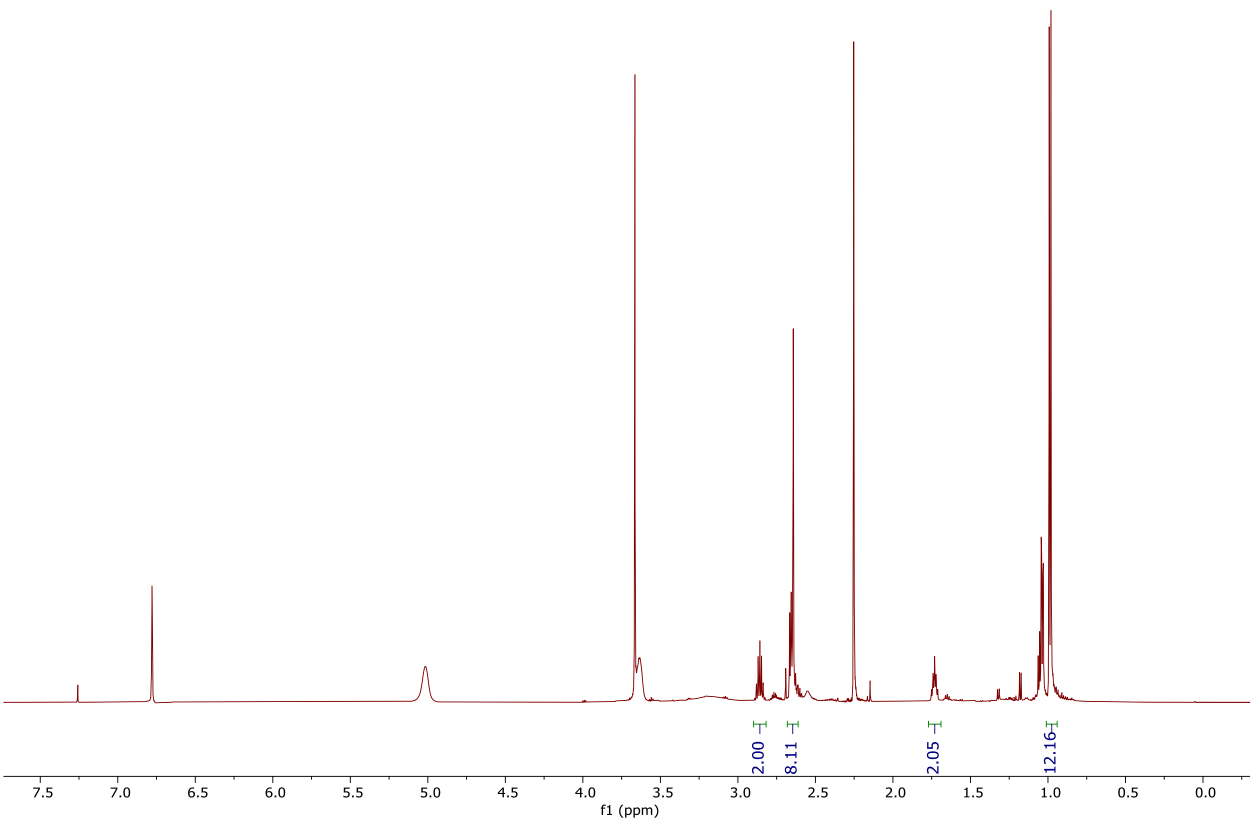

Figure S4. [1]H NMR spectrum of the crude reaction mixture for the coupling of *N,N'*-diisopropyl-1,3-propanediamine (1 equiv) and ethylene glycol (2 equiv) with 1 mol % **1** for 44 h.

2-(4-Benzyl-1,4-diazepan-1-yl)ethan-1-ol

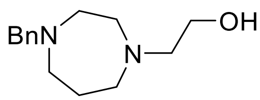

4i

The product was obtained in 68% yield (32 mg) as an orange oil after silica flash column chromatography (80:20 dichloromethane: methanol with 1% Et_3N).

^{1}H NMR (600 MHz, $CDCl_3$) δ 7.35 – 7.28 (m, 4H), 7.25 – 7.21 (m, 1H), 3.63 (s, 2H), 3.57 – 3.52 (m, 2H), 2.80 – 2.76 (m, 2H), 2.75 – 2.72 (m, 2H), 2.71 – 2.65 (m, 6H), 1.80 (tt, J = 7.1, 5.4 Hz, 2H).

^{13}C NMR (151 MHz, $CDCl_3$) δ 139.5, 128.9, 128.3, 127.0, 62.9, 59.2, 58.5, 55.5, 55.2, 54.3, 54.2, 28.0.

FT-IR (thin film) cm^{-1}: 3398, 2938, 2818, 1454, 1355, 1168, 1073, 1054, 740, 699.

HRMS (LC-QTOF) m/z: $[M+H]^+$ Calcd for $C_{14}H_{23}N_2O$ 235.1810; Found 235.1797.

5,8-Dibenzyl-5,8-diazaspiro[2.6]nonan-4-ol

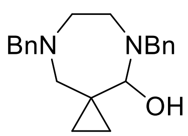

4j

The product was obtained in 50% yield (32 mg) as a colorless oil after amine modified silica flash column chromatography (95:5 hexanes: ethyl acetate).

^{1}H NMR (600 MHz, $CDCl_3$) δ 7.41 – 7.19 (m, 10H), 4.41 (d, J = 12.6 Hz, 2H), 3.75 (s, 2H), 3.22 (d, J = 12.7 Hz, 2H), 3.04 – 2.87 (m, 2H), 2.60 (s, 1H), 2.40 – 2.29 (m, 2H), 0.68 – 0.63 (m, 2H), 0.55 – 0.50 (m, 2H).

^{13}C NMR (151 MHz, $CDCl_3$) δ 138.9, 128.7, 128.6, 127.3, 91.6, 68.1, 58.4, 50.0, 20.4, 7.7.

FT-IR (thin film) cm^{-1}: 3298, 3029, 2834, 1495, 1453, 1028, 870, 742, 700.

HRMS (LC-QTOF) m/z: $[M+H]^+$ Calcd for $C_{21}H_{27}N_2O$ 323.2123; Found 323.2148.

cis-N, N'-Dibenzyl-2,6-diazabiyclo[5.3.0]decane

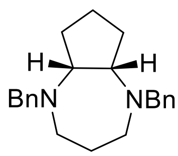

4k

The reaction was performed on 2.28 mmol scale using *N*,*N'*-dibenzyl 1,3-propanediamine (**2d**) and *cis*-1,2-cyclopentanediol (**3c**) as the starting materials. The product was obtained in 58% yield (421 mg) as a pale-orange oil after silica flash column chromatography (95:25 dichloromethane: methanol with 1% Et_3N).

^{1}H NMR (600 MHz, $CDCl_3$) δ 7.48 – 7.40 (m, 4H), 7.36 (t, J = 7.6 Hz, 4H), 7.30 – 7.24 (m, 2H), 4.16 (d, J = 13.7 Hz, 2H), 3.76 (d, J = 13.7 Hz, 2H), 3.27 – 3.20 (m, 2H), 2.92 – 2.83 (m, 2H), 2.55 (ddd, J = 14.3, 9.9, 3.1 Hz, 2H), 2.09 – 2.00 (m, 2H), 1.95 – 1.75 (m, 4H), 1.49 – 1.38 (m, 2H).

^{13}C NMR (151 MHz, $CDCl_3$) δ 141.0, 128.8, 128.3, 126.7, 68.1, 57.3, 51.7, 31.0, 28.4, 22.7.

FT-IR (thin film) cm^{-1}: 3026, 2950, 2868, 2833, 1493, 1451, 1348, 1028, 739, 698.

HRMS (LC-QTOF) m/z: $[M+H]^+$ Calcd for $C_{22}H_{29}N_2$ 321.2331; Found 321.2353.

Crystal structure of the compound with PF_6 showed retention of the *cis* configuration.

Scheme S5. Crystallization of Compound **4k** with KPF_6.

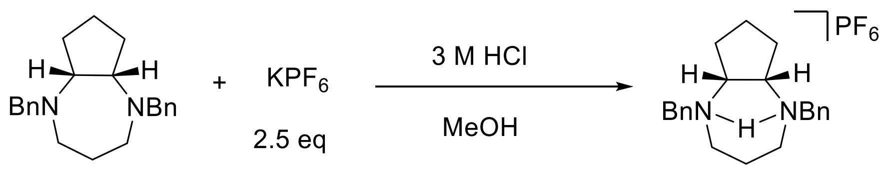

Cyclizine

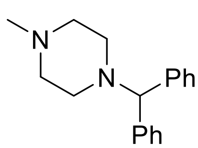

4l

The product was obtained in 91% yield (48 mg) as a white solid after silica gravity column chromatography (95:5 dichloromethane: methanol).

Data are consistent with the known compound.[18]

^{1}H NMR (500 MHz, $CDCl_3$) δ 7.45 (d, J = 6.6 Hz, 4H), 7.29 (t, J = 7.6 Hz, 4H), 7.19 (t, J = 7.3 Hz, 2H), 4.24 (s, 1H), 2.47 (bs, 8H), 2.31 (s, 3H).

^{13}C NMR (126 MHz, $CDCl_3$) δ 142.9, 128.6, 128.0, 127.0, 76.3, 55.4, 51.8, 45.9.

Homochlorcyclizine

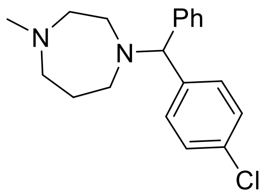

4m

The product was obtained in 67% yield (42 mg) as a pale-yellow oil after amine modified silica flash column chromatography (100% dichloromethane).

^{1}H NMR (500 MHz, $CDCl_3$) δ 7.41 – 7.16 (m, 9H), 4.57 (s, 1H), 2.80 – 2.57 (m, 8H), 2.40 (s, 3H), 1.81 (p, J = 6.3 Hz, 2H).

^{13}C NMR (126 MHz, $CDCl_3$) δ 143.1, 142.3, 132.5, 129.3, 128.7, 128.7, 127.9, 127.2, 74.9, 59.2, 56.4, 52.7, 52.7, 47.0, 27.7.

FT-IR (thin film) cm^{-1}: 2928, 2801, 1663, 1488, 1453, 1088, 1013, 805, 759, 701.

HRMS (LC-QTOF) m/z: $[M+H]^+$ Calcd for $C_{19}H_{24}ClN_2$ 315.1628; Found 315.1627.

Coupling between Substituted Diamine and Substituted Diol

Scheme S6. Coupling between Substituted Diamine and Substituted Diol.

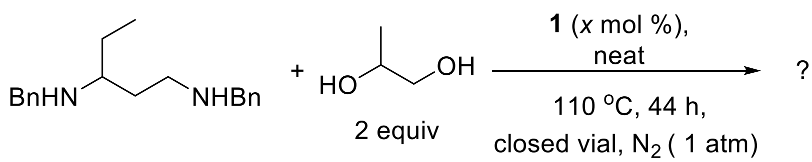

After executing the reaction as described in the general procedure, mesitylene was added to the mixture as an internal standard, and NMR were recorded in $CDCl_3$. While a reaction with 1 mol % catalyst loading gave back both starting materials, one with 5 mol % loading produced a complex mixture that was difficult to analyze.

V. Other Interesting Substrates through Diamine-Diol Coupling

Reactions to yield eight membered diazacycles produce side products. For example, coupling of *N*,*N'*-dibenzylethylenedimaine (**2a**) with 1,4-butanediol (**21**) showed both 1,4-diazocane (**22**) and an acyclic product **23** (Scheme S7). Moreover, a reaction between **2a** and 1,4-benzenedimethanol (**24**) favored a five membered compound imidazolidine **25** rather than an eight membered 1,4-diazocane (Scheme S8).

Reaction between N,N'-Dibenzylethylenediamine and 1,4-Butanediol

Scheme S7. Coupling between *N,N'*-Dibenzylethylenediamine and 1,4-Butanediol.

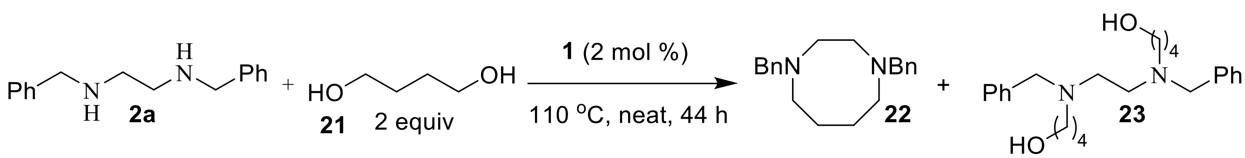

In the drybox, a 1-dram vial was charged with *N,N*'-dibenzylethylenediamine (1 equiv, 0.4 mmol), 1,4-butanediol (2 equiv, 0.8 mmol), and catalyst **1** (1.0 mol %, 0.004 mmol). The vial was capped, taken out of the glovebox, and heated to 110 °C. The solution turned to a brown color. After 44 h, the reaction mixture was allowed to cool to room temperature, mesitylene was added as an internal standard, and an aliquot was taken for ^{1}H NMR analysis in $CDCl_3$. Structure of the product was elucidated with the help of NMR spectroscopy and HRMS.

The ^{1}H NMR spectrum showed 1,4-diazocane in 30%, and LC-QTOF (positive ionization) showed both 1,4-diazocane and the acyclic product (**23**) from the coupling of diamine with two diols.

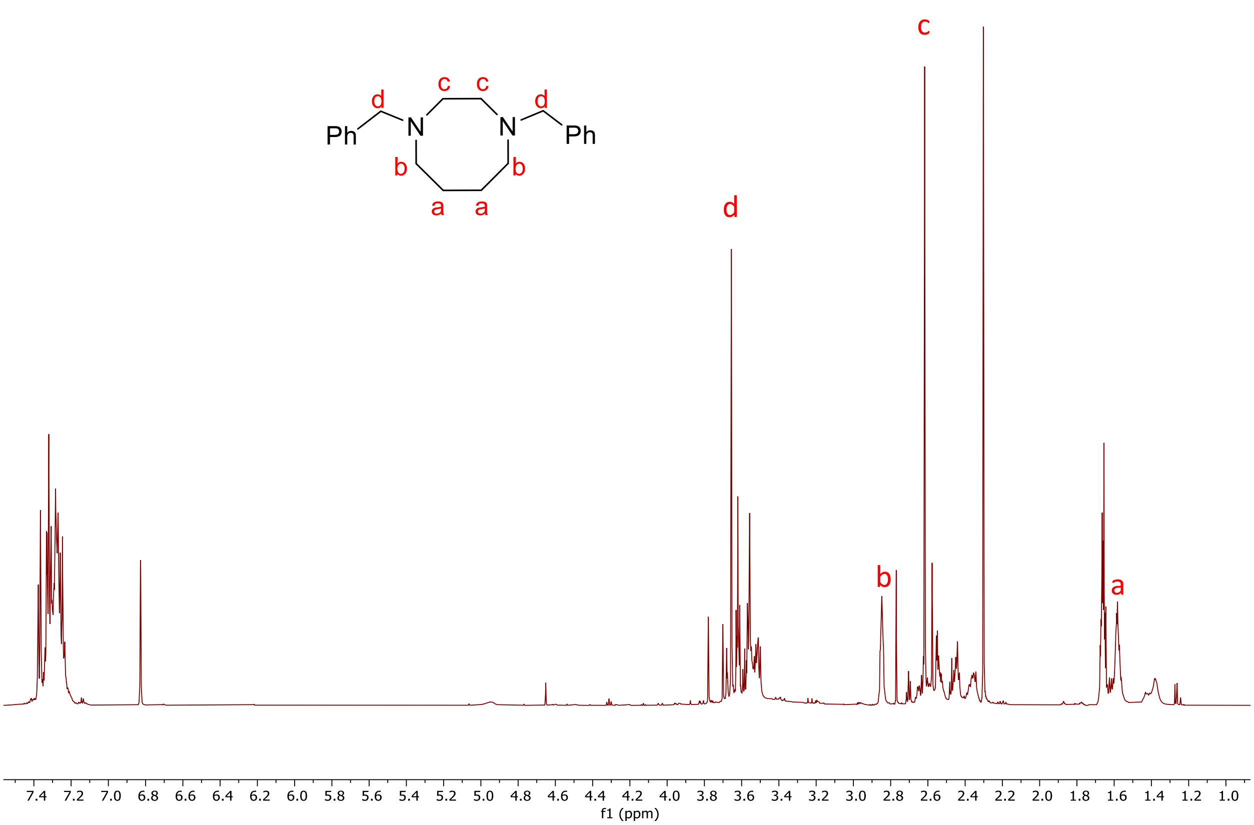

Figure S5. ^{1}H NMR spectrum of the crude reaction mixture for the coupling of *N,N'*-dibenzyl-ethylenediamine (1 equiv) and 1,4-butanediol (2 equiv) with 1 mol % **1** for 44 h.

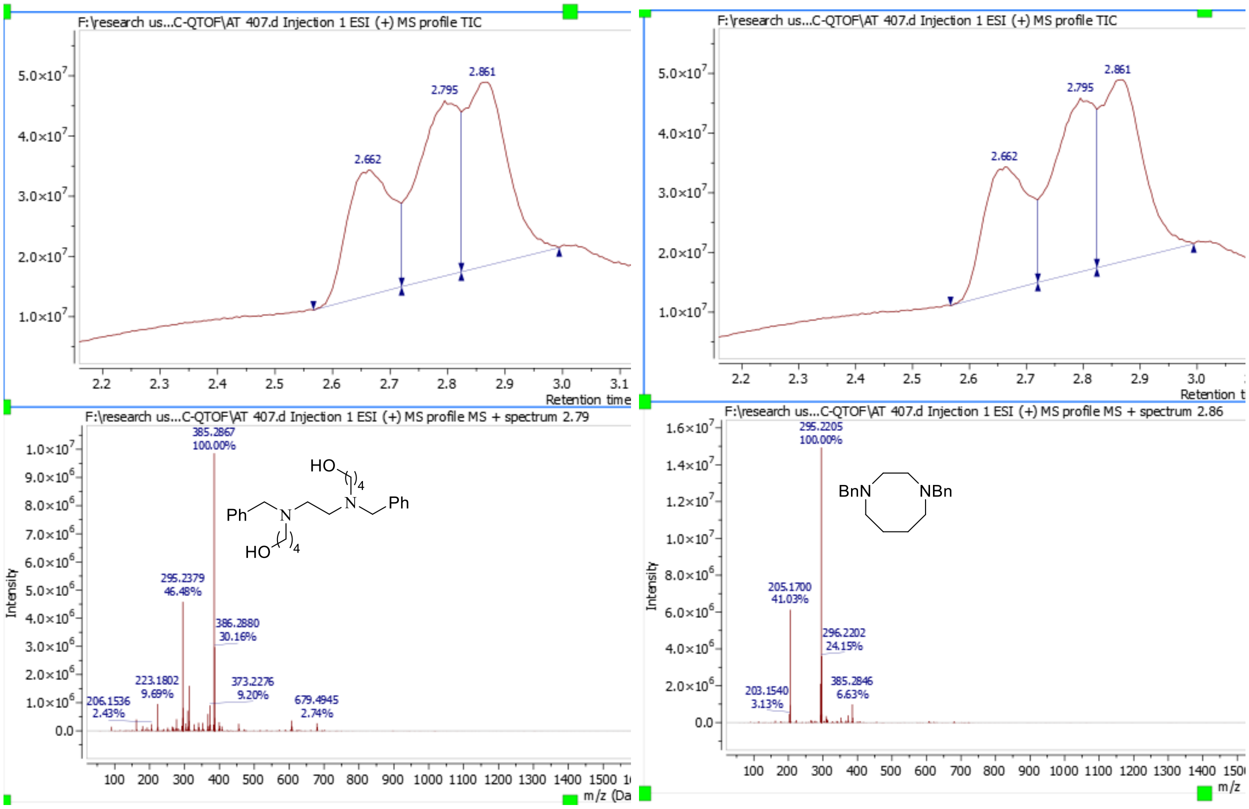

Figure S6. LC-QTOF spectra of the crude reaction mixture for the coupling of *N,N'*-dibenzyl-ethylenediamine (1 equiv) and 1,4-butanediol (2 equiv) with 1 mol % **1** for 44 h.

Reaction between N,N'-Dibenzylethylenediamine and 1,2-Benzenedimethanol

Scheme S8. Coupling between *N,N'*-Dibenzylethylenediamine and 1,2-Benzenedimethanol.

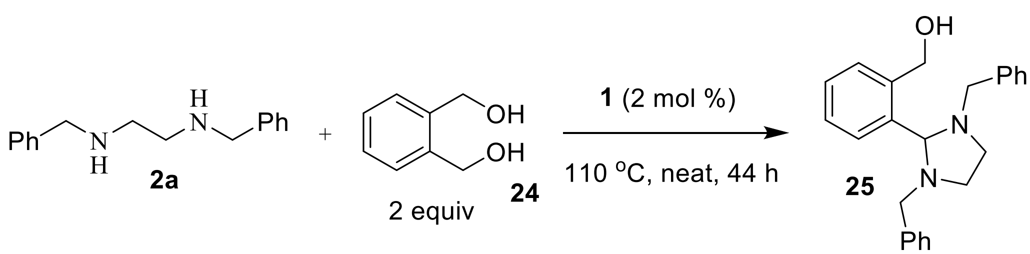

In the drybox, a 1-dram vial was charged with *N,N*'-dibenzylethylenediamine (1 equiv, 0.2 mmol), 1,2-benzenedimethanol (2 equiv, 0.4 mmol), and catalyst **1** (1.0 mol %, 0.002 mmol). The vial was capped, taken out of the glovebox, and heated to 110 °C. The solution turned to a yellow color. After 44 h, the reaction mixture was allowed to cool to room temperature, mesitylene was added as an internal standard, and an aliquot was taken for ^{1}H NMR analysis in $CDCl_3$. Structure of the product was elucidated with the help of 1-D and 2-D NMR spectroscopy and HRMS.

The ^{1}H NMR spectrum showed an imidazolidine compound **25** in 51%, starting diamine, and diol peaks.

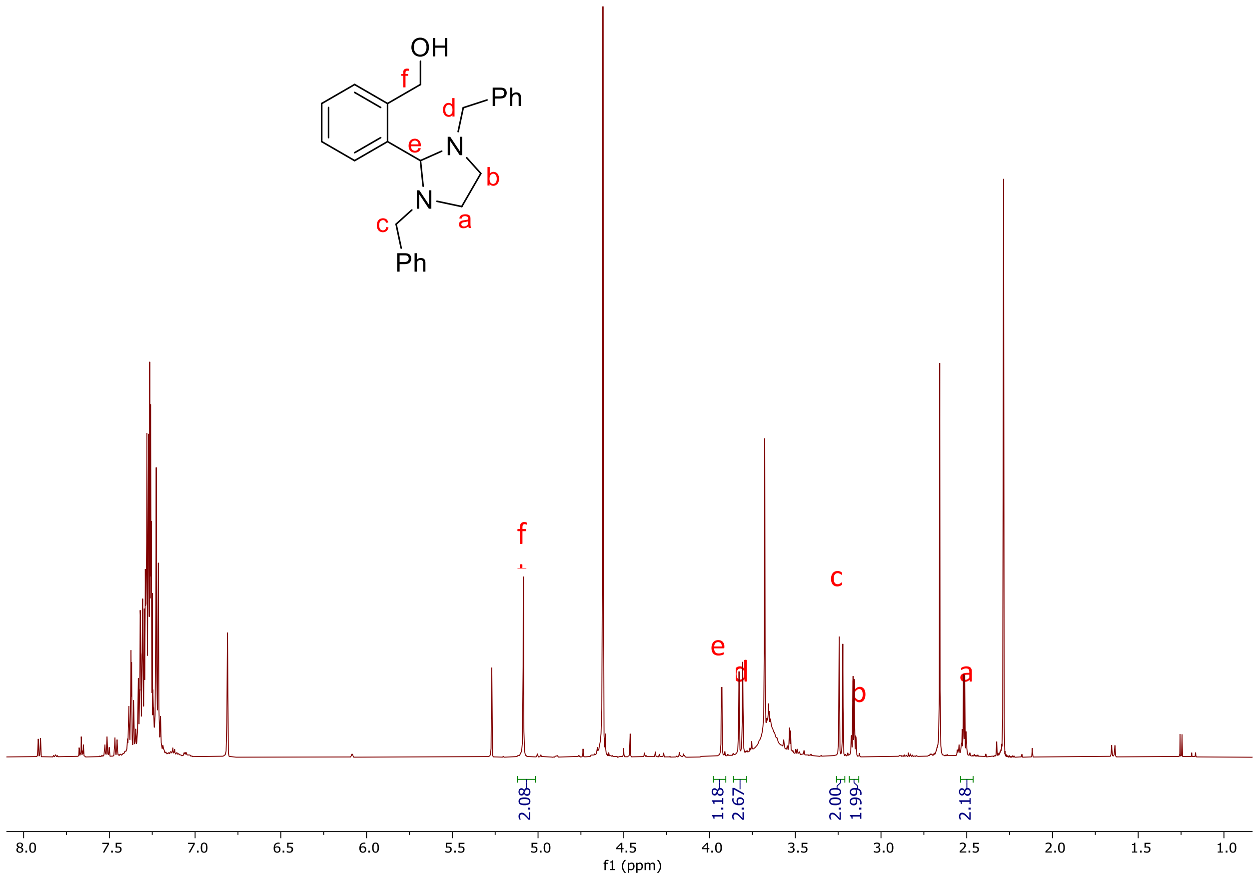

Figure S7. [1]H NMR spectrum of the crude reaction mixture for the coupling of *N,N'*-dibenzyl-ethylenediamine (1 equiv) and 1,2-benzenedimethanol (2 equiv) with 2 mol % **1** for 44 h.

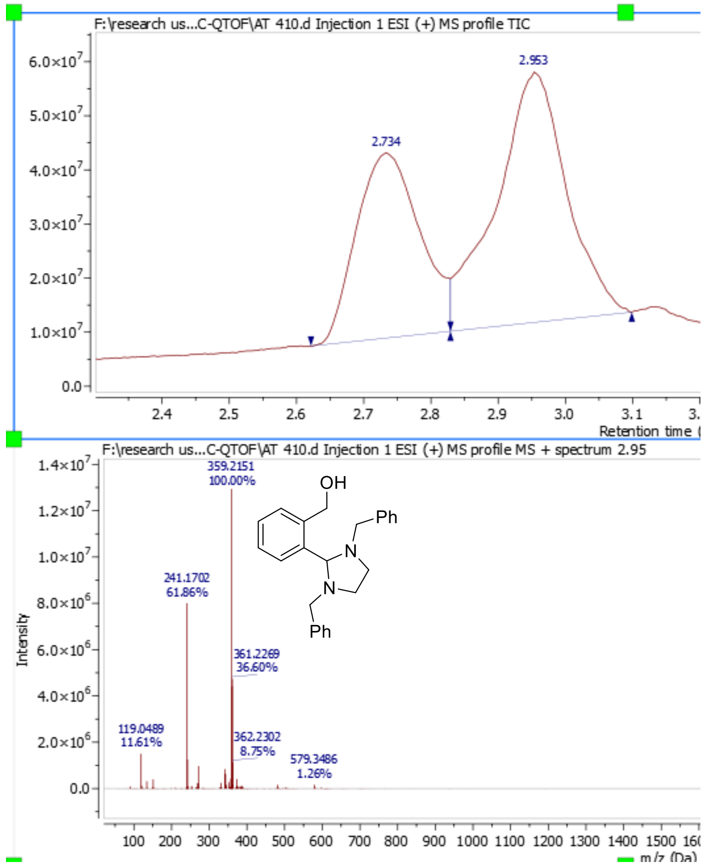

Figure S8. LC-QTOF spectrum of the crude reaction mixture for the coupling of *N,N'*-dibenzyl-ethylenediamine (1equiv) and 1,2-benzenedimethanol (2 equiv) with 2 mol % **1** for 44 h. Peak at 247.17 belongs to the starting diamine.

VI. Three Carbon Diamine/Two Carbon Diol Coupling Vs Two Carbon Diamine/Three Carbon Diol Coupling

1,4-Diazepanes can be synthesized either from three carbon diamines and two carbon diols or from two carbon diamines and three carbon diols. Reactions employing glycol adducts are favored compared to the three carbon diols as the first requires only one redox step to access diazacycles because of the two tautomerization steps involved (see main text scheme 1). This effect on yield of the number of redox is more evident in the synthesis of homochlorcyclizine and its dechlorinated analogue 1-benzhydryl-4-methyl-1,4-diazepane (Scheme S9).

Scheme S9. 1,4-Diazepane Synthesis from Two Carbon Diol Vs Three Carbon Diol.

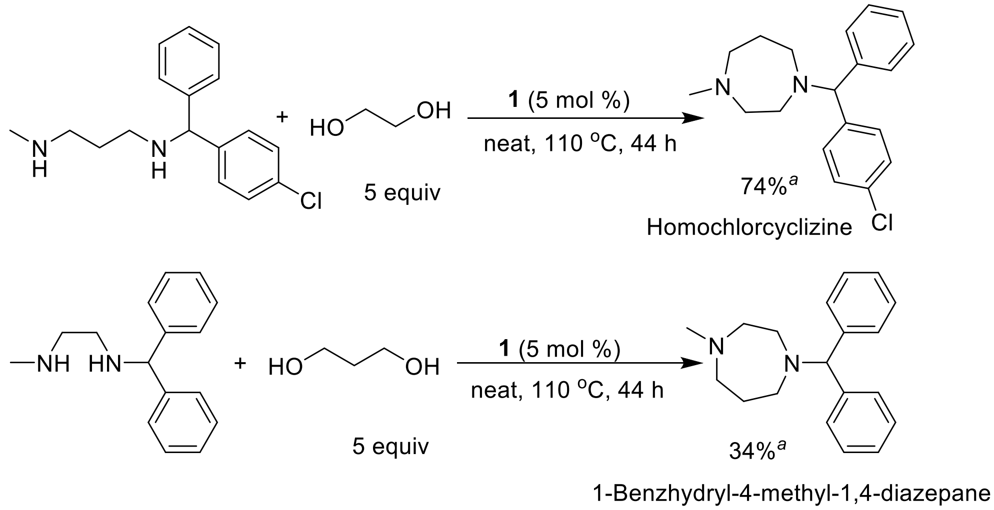

[a]NMR yield with mesitylene as the internal standard.

VII. Intramolecular vs Intermolecular Cyclization

We observed competition between intermolecular and intramolecular reactions in the case of *N*-benzyl-*N′*-hydroxyethyl ethylenediamine (**2c**) and diols (Table S5). While the reaction of **2c** with ethylene glycol (**5a**) can produce both intramolecular cyclization (**26**) and intermolecular cycloaddition (**6c**) products (Table S5); **6c** can be formed selectively with excess ethylene glycol. By contrast, treatment of **2c** with propanediol afforded seven membered intermolecular product **4i** selectively (Table S6).

Compound 26 is commercially available; CAS: 2759-28-6.

Table S5. Coupling between **2c** and ethylene glycol.

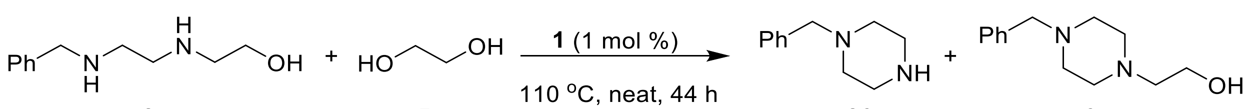

2c **5a** **26** **6c**

Entry	Diol (equiv)	Yield (%)[a]	
		26	**6c**
1	1	25	36
2	2	24	60
3	3	0	86

Table S6. Coupling between **2c** and 1,3-propanediol.

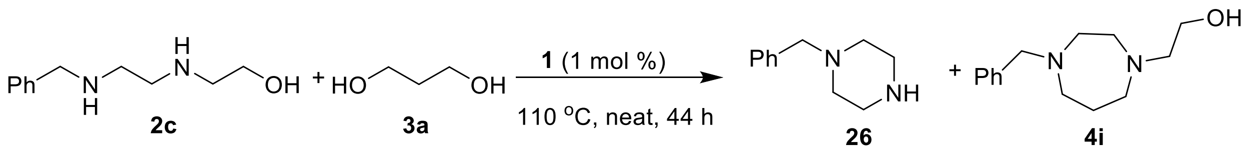

Entry	Diol (equiv)	Yield (%)[a]	
		26	**4i**
1	1	4	65
2	2	3	85

[a]NMR yield with mesitylene as an internal standard.

VIII. Scope Limitations

Diamines with electron deficient or bulky groups on nitrogen such as Boc, CBZ, TFA, *t*-butyl, or phenyl showed no hydrogen borrowing coupling in our reaction. In addition to this, two-carbon unsubstituted primary diamines are not coupling partners in diazacycle synthesis. Inactivity of the first group can be explained by the effects of electronic and steric factors on nitrogen nucleophilicity, while the second one is due to catalytic poisoning (Scheme S10). Diamines with highly electron withdrawing groups are not sufficiently nucleophilic to undergo high-yielding addition to intermediate aldehydes at the rate required bythe kinetics of the catalysis, so the reaction of Boc protected ethylenediamine showed no reactivity with benzaldehyde (**15a**, Scheme S10B). Similarly, coupling of ethylenediamine (**14h**) with benzyl alcohol (**27**) using our catalyst did not result in product, whereas reaction of **14h** with **15a** produced *N*,*N'*-dibenzylidine ethylenediamine (**28**). This shows the inability of the catalyst **1** to oxidize benzyl alcohol in the presence of an unsubstituted diamine. We further confirmed this catalytic inactivity by adding isopropanol to the reaction mixture **C** to check whether the catalyst could transfer hydrogen from isopropanol (**29**) to *N*,*N'*-dibenzylidine ethylenediamine. As expected, transfer hydrogenation was not observed.

Scheme S10. Reactions to Probe the Scope Limitation Factor.

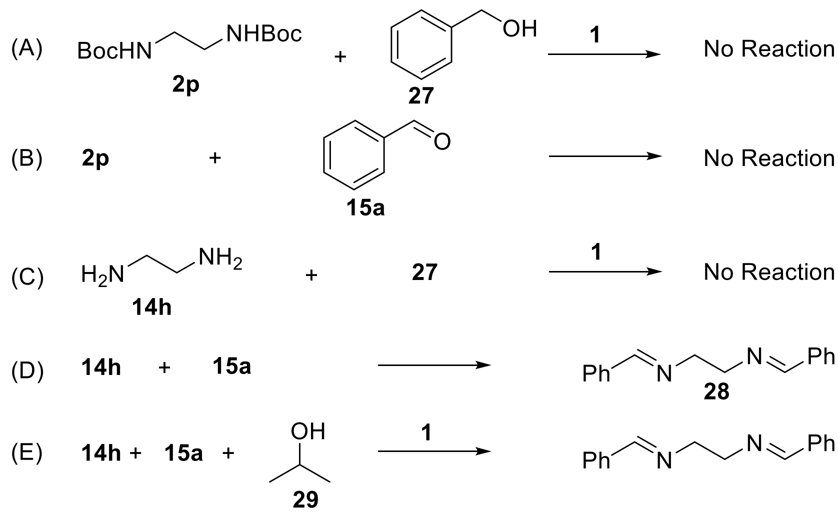

IX. Catalyst Poisoning Studies

*Synthesis and Characterization of Complex **13***

Experiment 1-3: Complex **1** (20 mg, 1 equiv) and freshly distilled ethylenediamine (22 mg, 12 equiv) were stirred at 110 ºC (oil bath) in a Schlenk reactor for 15 min (Exp. 1) or 21 h (Exp. 2) or 44 h (Exp. 3). Then, all volatile components were removed by heating at 75 ºC (oil bath) for 10 min, the residue was dissolved in dry deuterated methanol and analyzed by ^{1}H and ^{31}P NMR spectroscopy.

Experiment 4: Complex **1** (20 mg, 1 equiv) and ethylene glycol (19 mg, 10 equiv) were dissolved in freshly distilled ethylenediamine (0.8 mL), stirred at 110 ºC (oil bath) in a Schlenk reactor for 1h. Then, all volatile components were removed by heating at 90 ºC (oil bath) for 10 min, the residue was dissolved in dry deuterated methanol and analyzed by ^{1}H and ^{31}P NMR spectroscopy.

Stacked ^{1}H NMR spectra showed disappearance of cymene ligand within 15 min of stirring and formation of a new complex **13** with new phosphinopyridine ligands peak. Besides, ^{31}P spectrum showed a new peak corresponding to complex **13**.

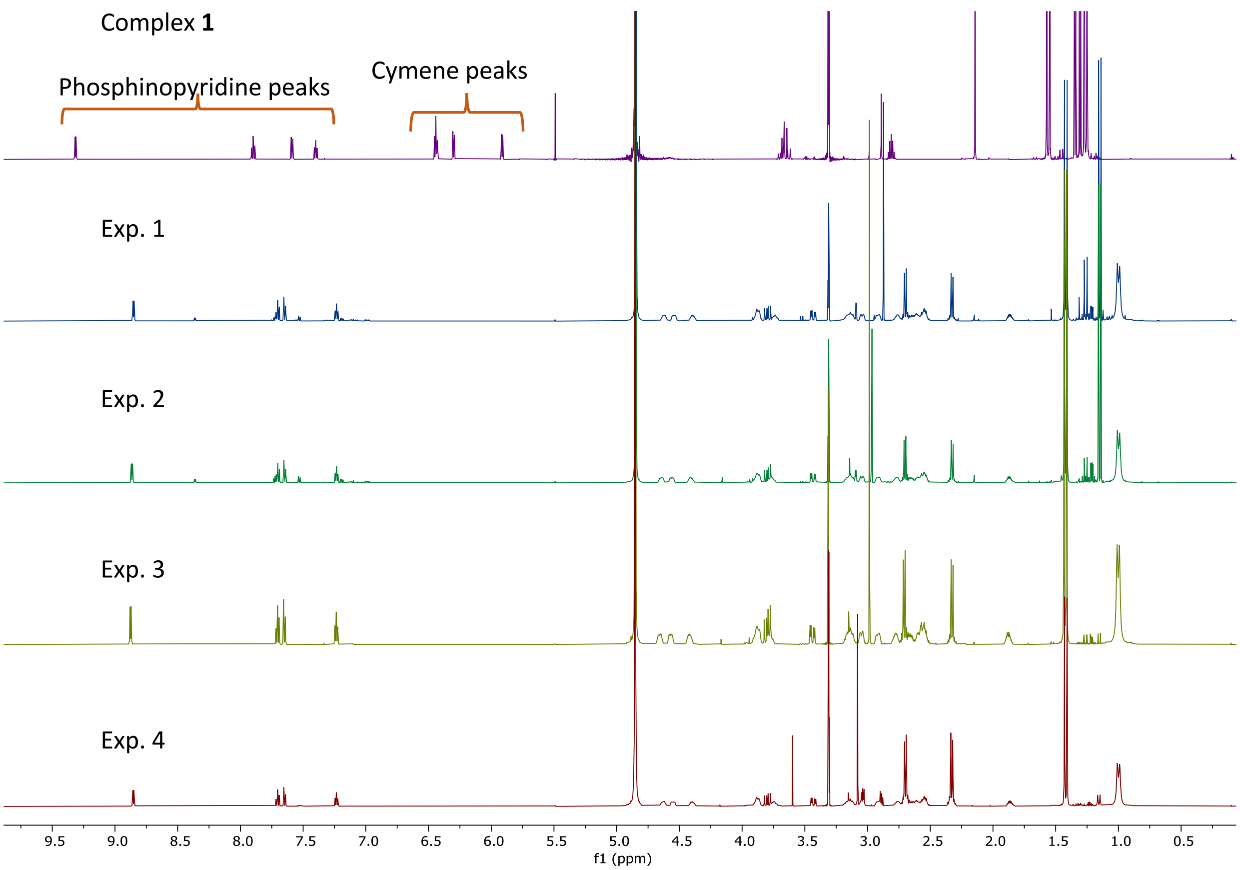

Figure S9. Stacked ^{1}H NMR spectrum of the crude reaction mixture for reaction between complex **1** and ethylenediamine.

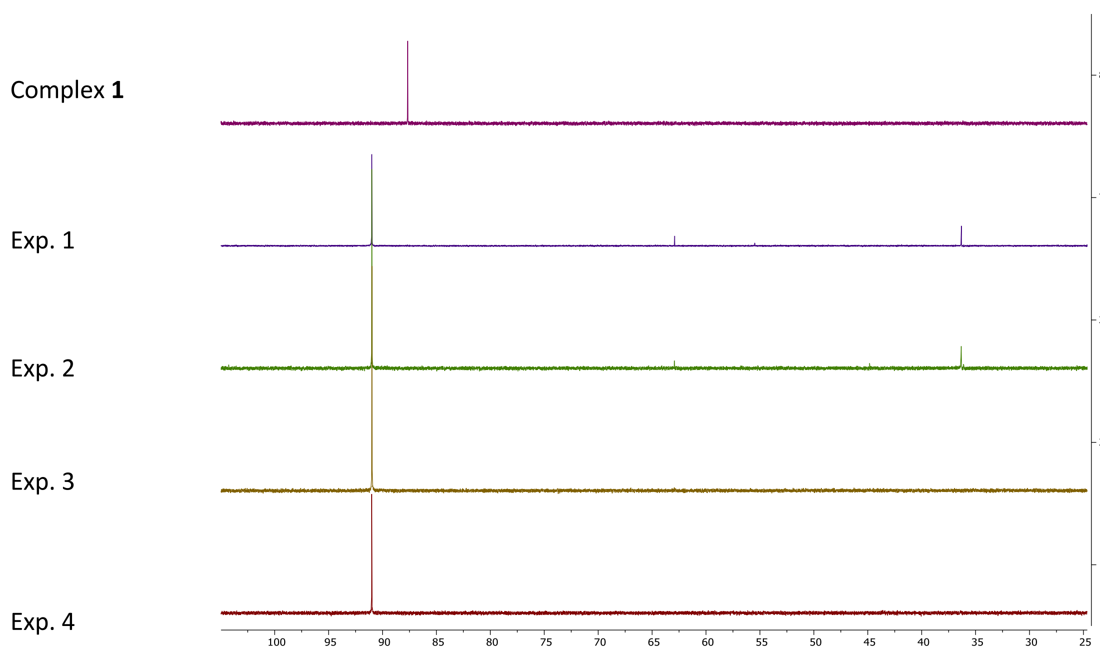

Figure S10. Stacked ^{31}P NMR spectrum of the crude reaction mixture for reaction between complex **1** and ethylenediamine.

Complex **13** was crystallized by adding dichloromethane and hexanes to the methanol solution of crude reaction mixture from experiment 4.

^{1}H NMR (600 MHz, MeOD) δ 8.84 – 8.80 (m, 1H), 7.74 – 7.68 (m, 1H), 7.67 – 7.63 (m, 1H), 7.26 – 7.20 (m, 1H), 4.62 – 4.48 (m, 2H, NH_2), 4.42 – 4.32 (m, 1H, NH_2), 3.91 – 3.85 (m, 2H, NH_2), 3.80 (dd, J = 17.4, 11.3 Hz, 1H), 3.72 – 3.65 (m, 1H, NH_2), 3.46 – 3.39 (m, 1H), 3.19 – 3.11 (m, 2H, NH_2), 3.09 – 3.00 (m, 1H), 2.95 – 2.88 (m, 1H), 2.78 – 2.69 (m, 1H), 2.66 – 2.50 (m, 4H), 1.89 – 1.80 (m, 1H), 1.42 (d, J = 12.4 Hz, 9H), 1.00 (d, J = 11.2 Hz, 9H).

^{13}C NMR (151 MHz, MeOD) δ 168.2 (d, J = 4.6 Hz), 154.8, 136.9, 125.5 (d, J = 8.1 Hz), 123.9, 122.9, 120.7, 47.3, 45.6, 43.7, 43.5, 38.1 (d, J = 11.6 Hz), 37.0 (d, J = 16.8 Hz), 36.9 (d, J = 18.5 Hz), 30.8 (d, J = 4.0 Hz), 30.1 (d, J = 3.5 Hz).

^{19}F NMR (564 MHz, MeOD) δ -76.17.

^{31}P NMR (243 MHz, MeOD) δ 94.96.

Anal. Calcd for $C_{19}H_{40}ClF_3N_5O_3PRuS$: C 35.49, H 6.27, N 10.89, S 4.99. Found: C 34.89, H 6.20, N 11.28, S 4.65

*Synthesis and Characterization of Complex **13a***

Complex **1** (20 mg, 1 eq.), *N*,*N*'-dibenzylethylenediamine (37 mg, 5 eq.), and ethylene glycol (40 mg, 20 eq.) were heated at 110 °C (oil bath) in a closed vial for 1 hour. The resulting mixture was dissolved in CD_3OD (1 mL) causing precipitation of orange complex **13a** [$RuCl_2$(PN)($BnNHCH_2CH_2NHBn$)]. It was separated by decantation, then washed with methanol and dried in vacuum. The solid was recrystallized from CH_2Cl_2/ether to give dark-red crystals suitable for X-ray analysis. The complex was also characterized by ^{1}H, ^{13}C, ^{31}P, COSY, and HSQC NMR spectroscopy.

^{1}H NMR (600 MHz, CD_2Cl_2): δ 9.03 (d, J = 5.4 Hz, 1H, Py), 7.48 (t, J = 7.4 Hz, 1H, Py), 7.45–7.25 (m, 11H, 2Ph, Py), 7.06 (t, J = 6.3 Hz, 1H, Py), 4.72 (d, J = 14.2 Hz, 1H, CH_2), 4.61 (br t, 1H, NH), 4.27 (br t, 1H, NH), 4.22–4.05 (m, 2H, $2CH_2$), 4.01 (dd, J = 15.3, 7.8 Hz, 1H, CH_2), 3.93–3.81 (m, 1H, CH_2), 3.56 (dd, J = 14.7, 11.5 Hz, 1H, CH_2), 2.91 (d, J = 11.0 Hz, 1H, $C\underline{H}_2Ph$), 2.82–2.65 (m, 2H, $C\underline{H}_2Ph$), 2.55 (d, J = 10.7 Hz, 1H, $C\underline{H}_2Ph$), 1.63 (d, J = 11.2 Hz, 9H, *t*-Bu), 1.04 (br s, 9H, *t*-Bu).

^{13}C{^{1}H} NMR (126 MHz, CD_2Cl_2): δ 168.92 (d, J = 4.4 Hz), 155.68 (Py), 138.23 (d, J = 2.1 Hz), 137.49, 133.60 (Py), 128.96, 128.81, 128.76, 128.73, 127.85, 127.57, 121.40 (d, J = 7.5 Hz, Py), 120.71 (Py), 62.21 (CH_2), 53.37 (CH_2), 50.17 ($\underline{C}H_2Ph$), 49.75 ($\underline{C}H_2Ph$), 38.68 (d, J = 9.9 Hz), 38.36 (d, J = 17.1 Hz, PCH_2), 36.21 (d, J = 12.7 Hz), 31.87 (d, J = 2.9 Hz, *t*-Bu), 28.41 (br s, *t*-Bu).

^{31}P{^{1}H} NMR (202 MHz, CD_2Cl_2): δ 87.15 (s).

Table S7. Catalytic Activity Screening of the Ru Complexes.[a]

Entry	Conditions	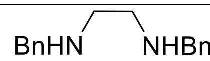 **2a**, %	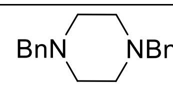 **6a**,%
1	**1** (1 eq.), **2a** (5 eq.) **5a** (20 eq.) 110 °C, 1 hour	0	100
2	**13** (20 mg), **2a** (183 mg) **5a** (189 mg) 110 °C, 1 hour	100	0
3	**13a** (5 mg), **2a** (183 mg) **5a** (189 mg) 110 °C, **1 hour**	74	26
4	**13a** (5 mg), **2a** (183 mg) **5a** (189 mg) 110 °C, **3 days**	0	100

[a]The yields of **6a** were derived from ^{1}H NMR spectra of the crude reaction mixture in CD_3OD. A characteristic signal of **6a** (3.5 ppm) was used for the quantification.

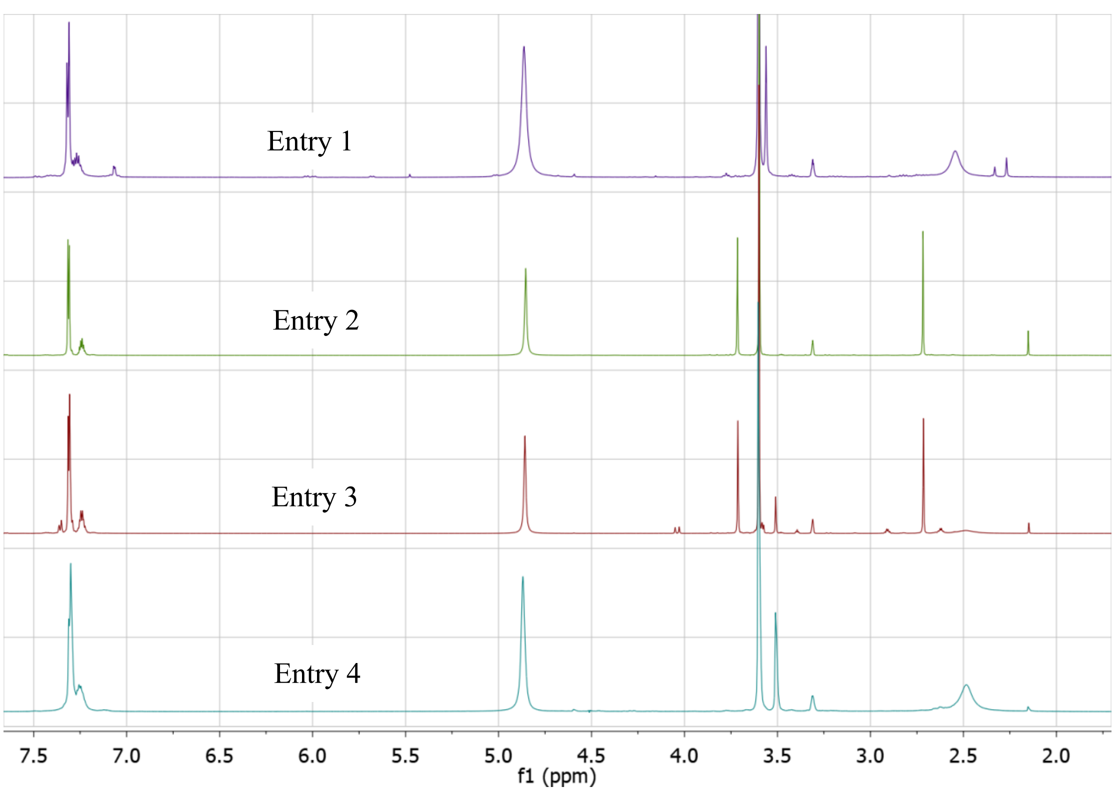

Figure S11. ^{1}H NMR spectra showing formation of **6a** (CD_3OD, 25 °C).

X. Reaction of Three Carbon Diamine with Diols

In the drybox, a 1-dram vial was charged with *N*-methylethylenediamine (1 equiv, 0.2 mmol), ethylene glycol (2 equiv, 0.4 mmol), and catalyst **1**. The vial was sealed, taken out of the glovebox, and heated to 110 °C. The solution turned to yellow color. After 44 h, the reaction mixture was allowed to cool to room temperature and analyzed by LC-QTOF.

Scheme S11. Coupling between *N*-Methylethylenediamine (**14c**) and Ethylene Glycol (**5a**).

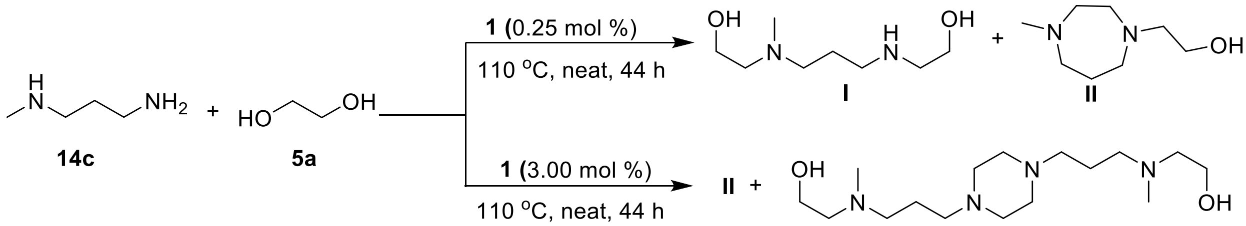

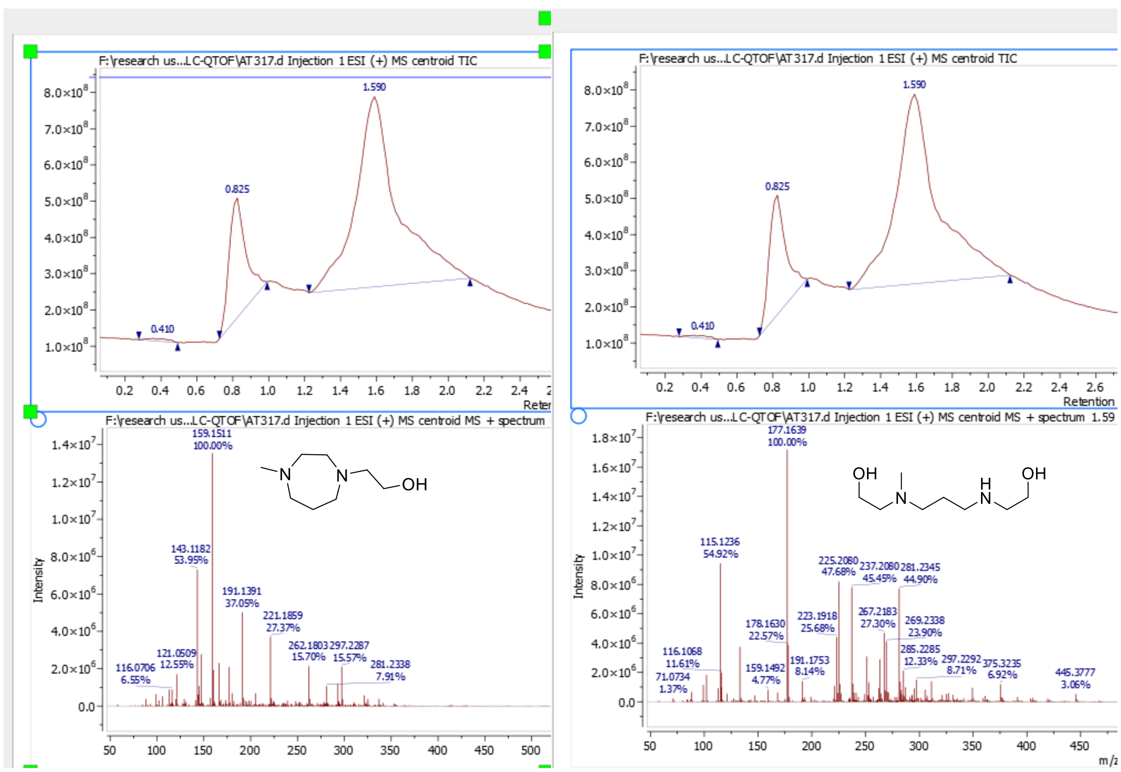

Figure S12: Mass spectra of reaction of *N*-methylethylenediamine (**14c**) with ethylene glycol (**5a**) at 0.25% **1**.

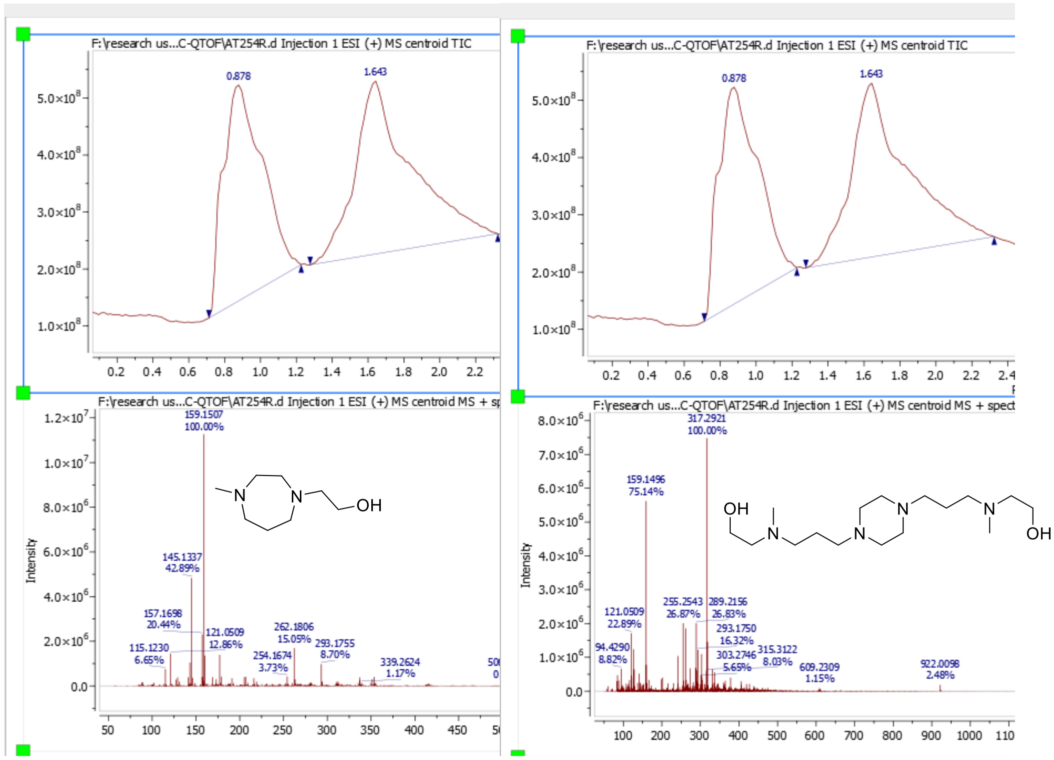

Figure S13: Mass spectra of reaction of **14c** with **5a** at 3.0 mol % **1**.

XI. Catalyst Screening

Different catalysts were screened under the condition specific to the catalyst that is reported in the literature for hydrogen-borrowing piperazine[19] or benzodiazepine[20] synthesis, or *N*-alkylation.[21] Unfortunately, none of the catalysts that were examined, except complex **1**, showed activity for the 1,4-diazepane synthesis.

Table S8: Screening of different hydrogen-borrowing catalysts for 1,4-diazepane synthesis.

Entry	Diamine	Diol	Catalyst	Condition	Result
1	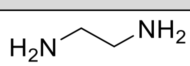 **14h**	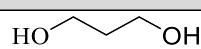 **3a**	**1** (1 mol %)	neat, 110 °C, 44 h, sealed vial	no reaction[a]
2	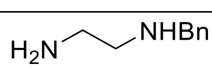 **14b**	**3a**	**1** (1 mol %)	"	no reaction
3	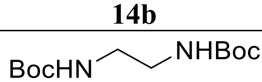 **2p**	**3a**	**1** (1 mol %)	"	no reaction
4	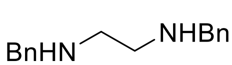 **2a**	**3a**	**1** (1 mol %)	"	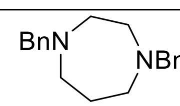 78%

5	**14h**	**3a**	Shvo catalyst (1 mol %)	KOH (5 mol %), neat, 110 ºC, 44 h, sealed vial	no reaction
6	**2a**	**3a**	Shvo catalyst (1 mol %)	"	no reaction
7	**14h**	**3a**	$[Cp^*IrCl_2]_2$ (0.5 mol %)	$NaHCO_3$ (5 mol %), toluene (0.5 mL)/neat, 110 ºC, 24 h, sealed vial	no reaction
8	**14b**	**3a**	$[Cp^*IrCl_2]_2$ (0.5 mol %)	"	no reaction
9	**2p**	**3a**	$[Cp^*IrCl_2]_2$ (0.5 mol %)	"	no reaction
10	**2a**	**3a**	$[Cp^*IrCl_2]_2$ (0.5 mol %)	"	no reaction
11	**14b**	**3a**	[Ru(*p*-cymene)$Cl_2]_2$ (5 mol %)	Xantphose (5 mol %), toluene (1 mL)/neat, 160 ºC, 24 h, Schlenk reactor	no desired product[b]
12	**2a**	**3a**	[Ru(*p*-cymene)$Cl_2]_2$ (5 mol %)	"	no desired product
13	**14b**	**3a**	$NiBr_2$ (10 mol %)	Phen (20 mol %), *t*-BuOK (1 equiv), toluene, 130 ºC, 48 h, Schlenk reactor	no reaction
14	**2a**	**3a**	$NiBr_2$ (10 mol %)	"	no reaction

[a]No reaction means that we observed only both starting materials in the ^{1}H NMR spectra. [b]No desired product means that we observed some other compounds along with starting materials; but we were not able to elucidate the structure of the compounds present in the mixture.

XII. NMR Spectra

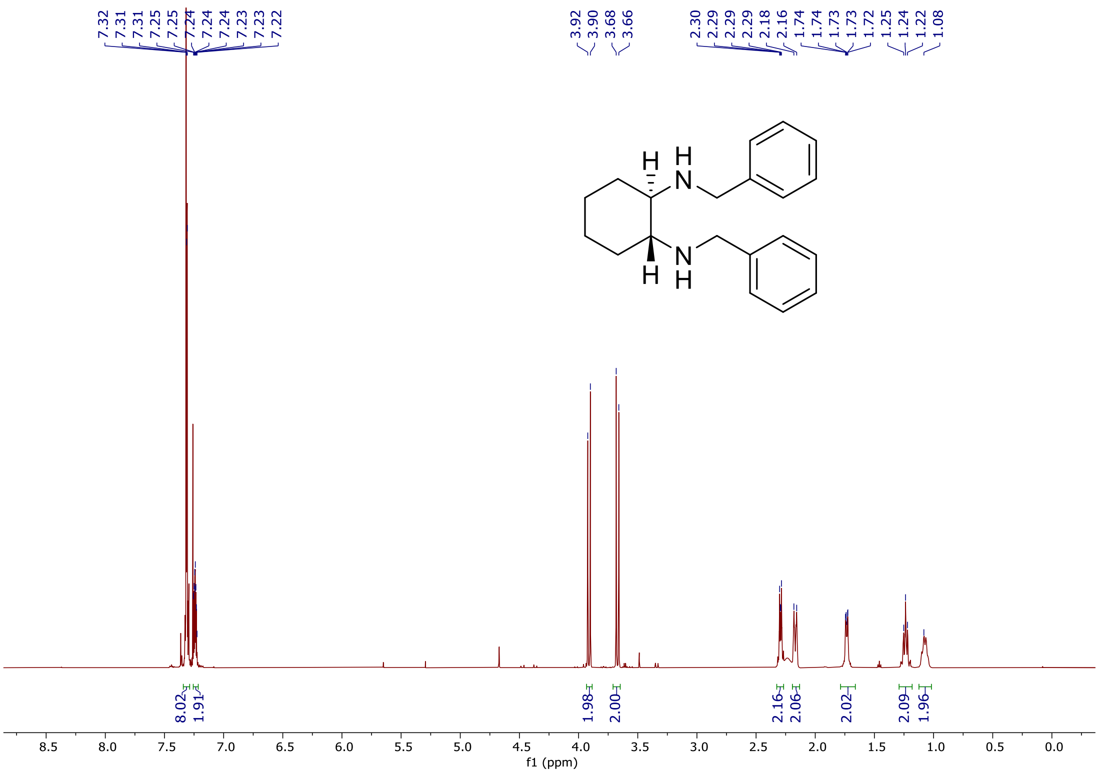

Figure S14. ^{1}H NMR (500 MHz) spectrum of **2b** at 25 °C in $CDCl_3$.

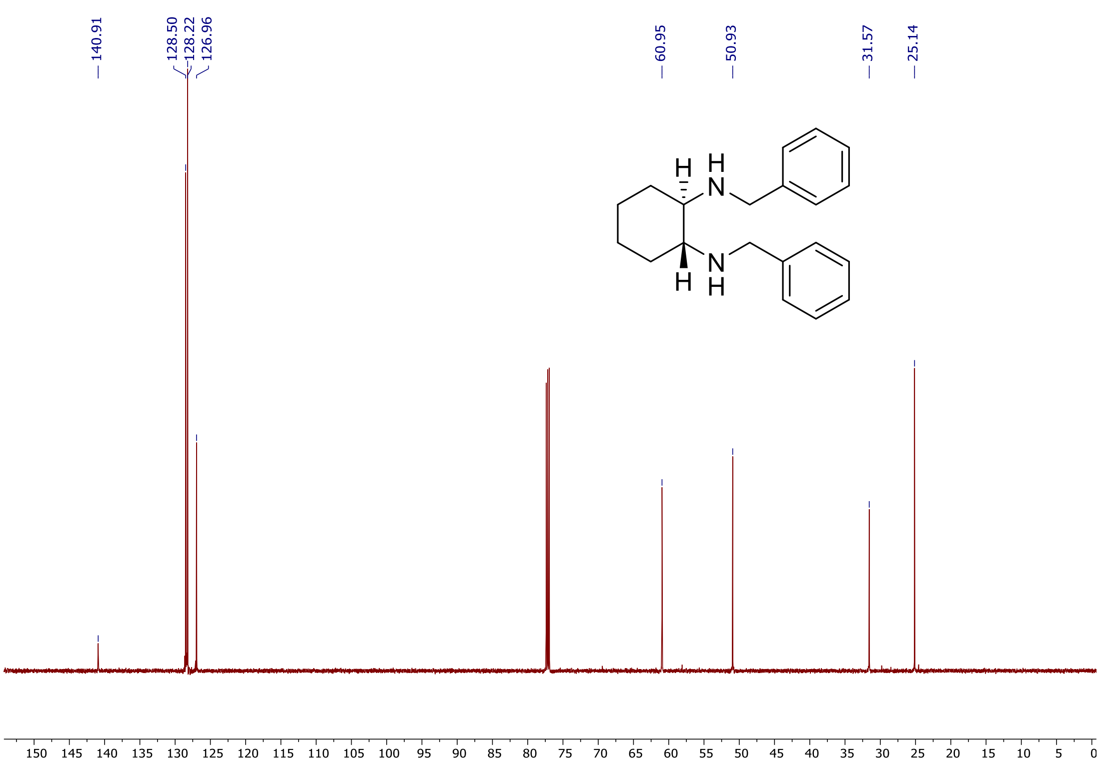

Figure S15. ^{13}C NMR (151 MHz) spectrum of **2b** at 25 °C in $CDCl_3$.

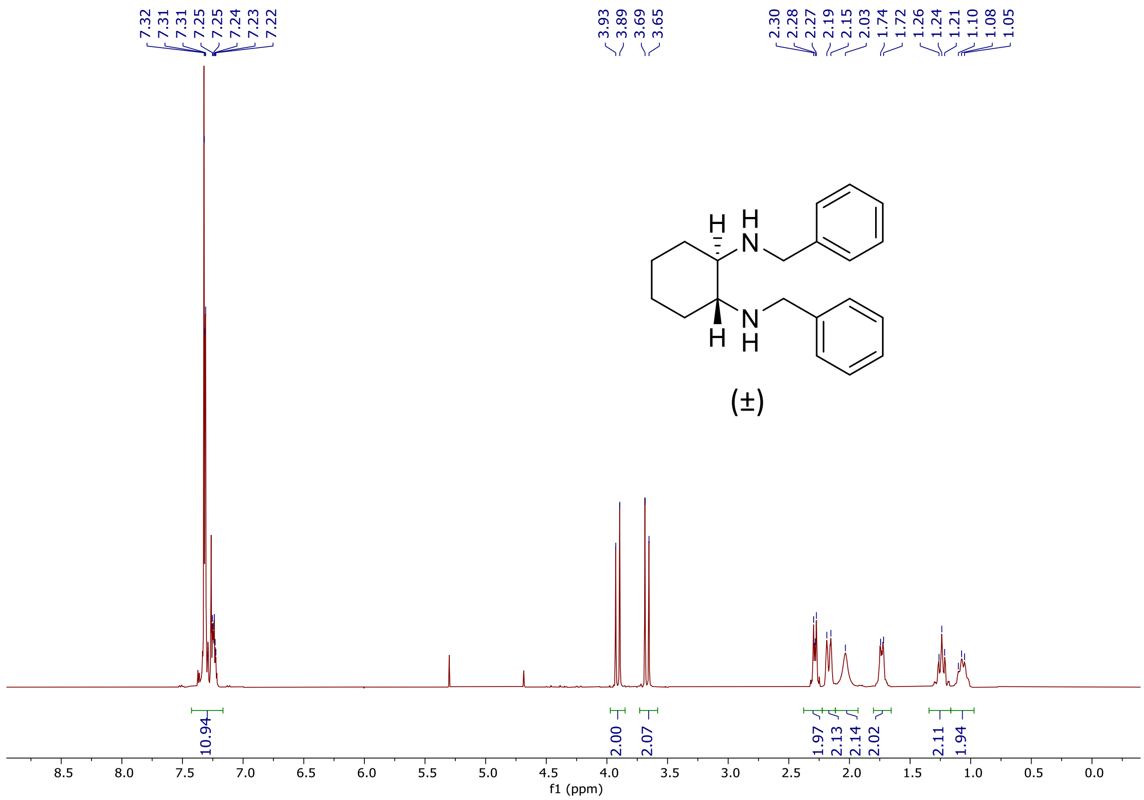

Figure S16. [1]H NMR (600 MHz) spectrum of **2b'** at 25 °C in $CDCl_3$.

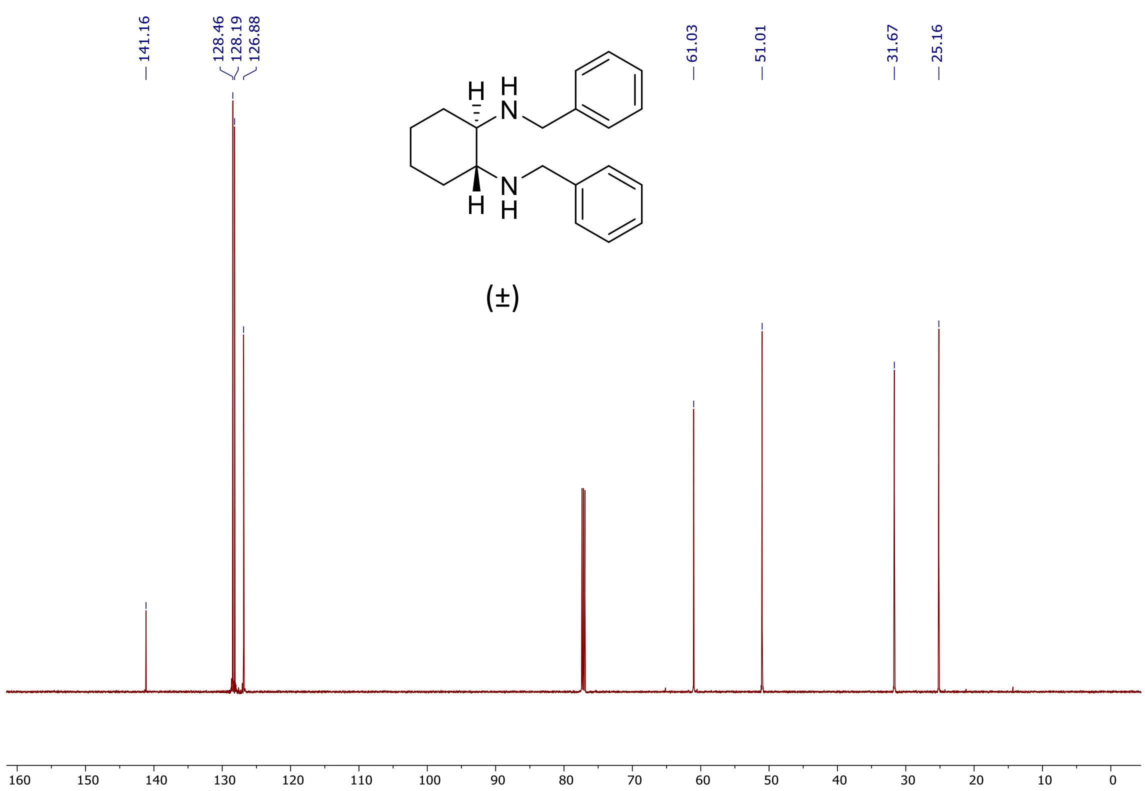

Figure S17. [13]C NMR (151 MHz) spectrum of **2b'** at 25 °C in $CDCl_3$.

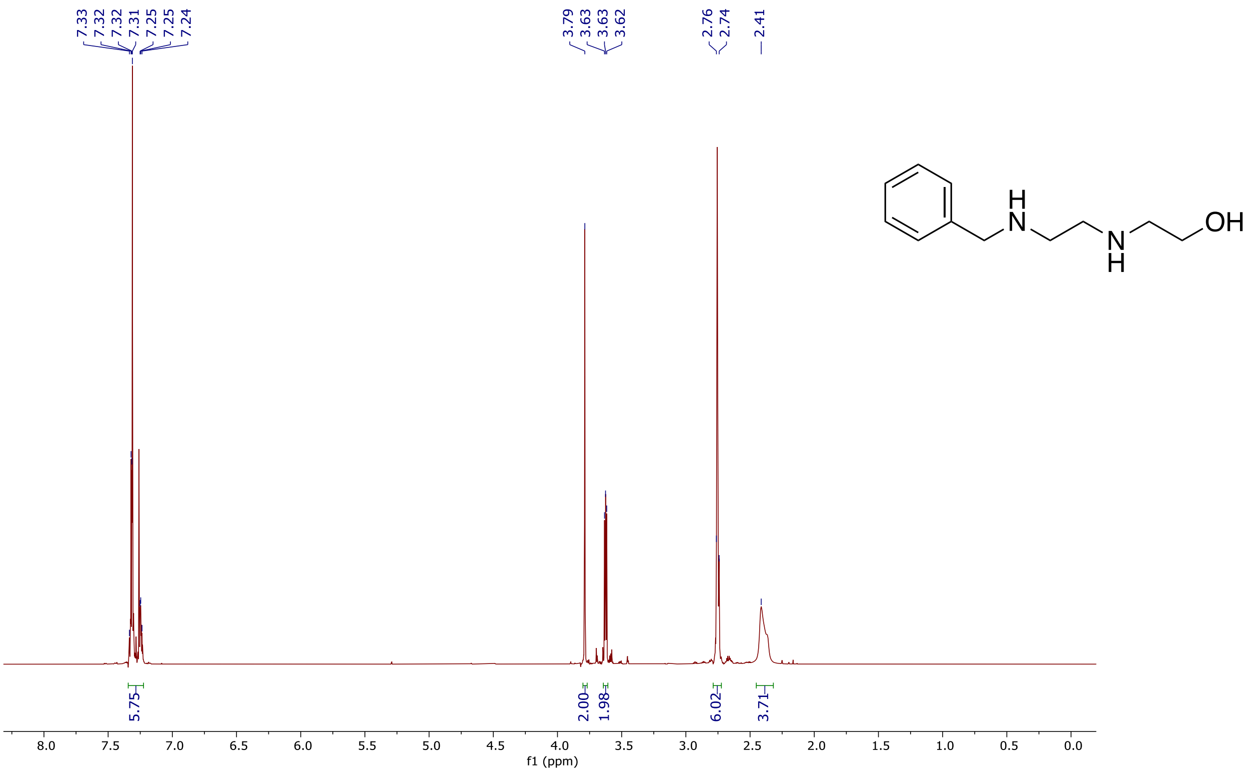

Figure S18. ^{1}H NMR (600 MHz) spectrum of **2c** at 25 °C in $CDCl_3$.

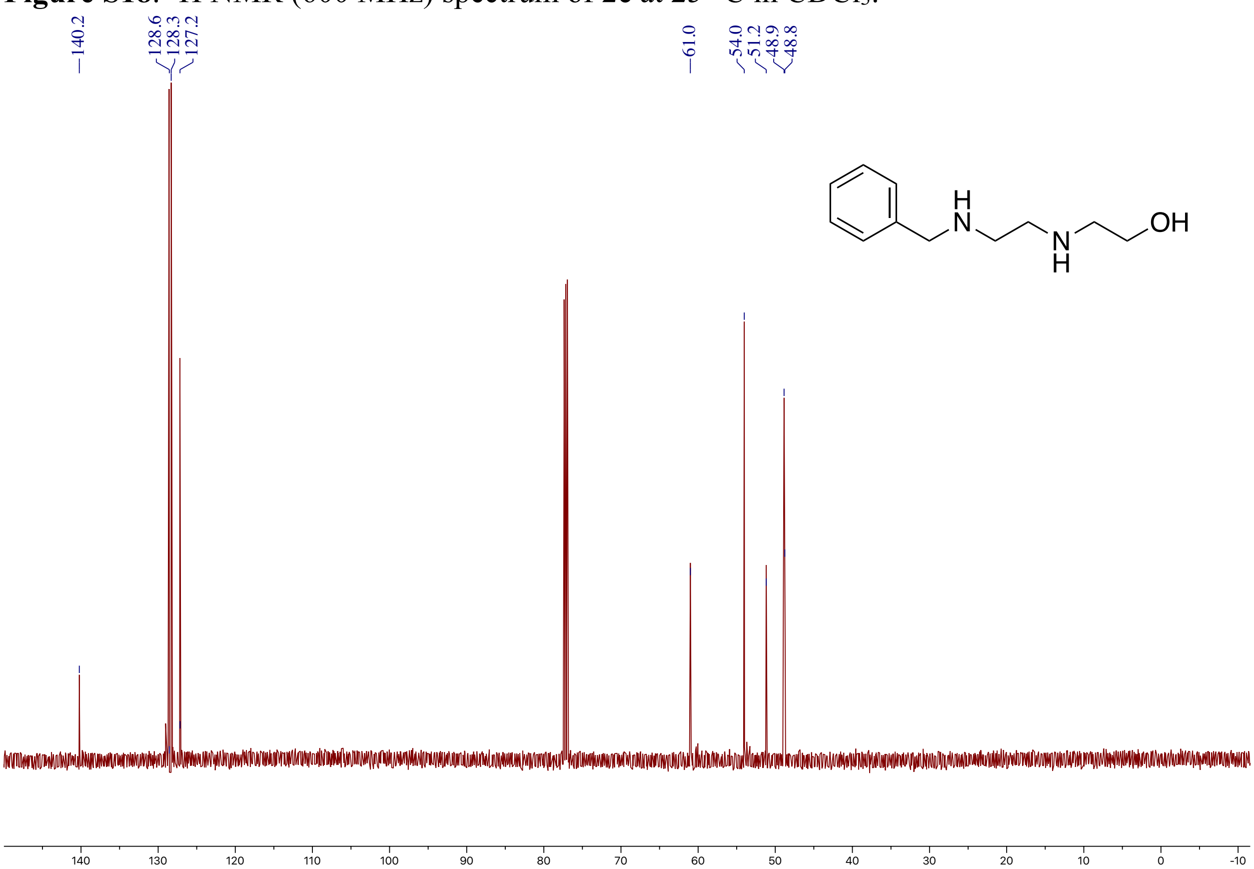

Figure S19. ^{13}C NMR (151 MHz) spectrum of **2c** at 25 °C in $CDCl_3$.

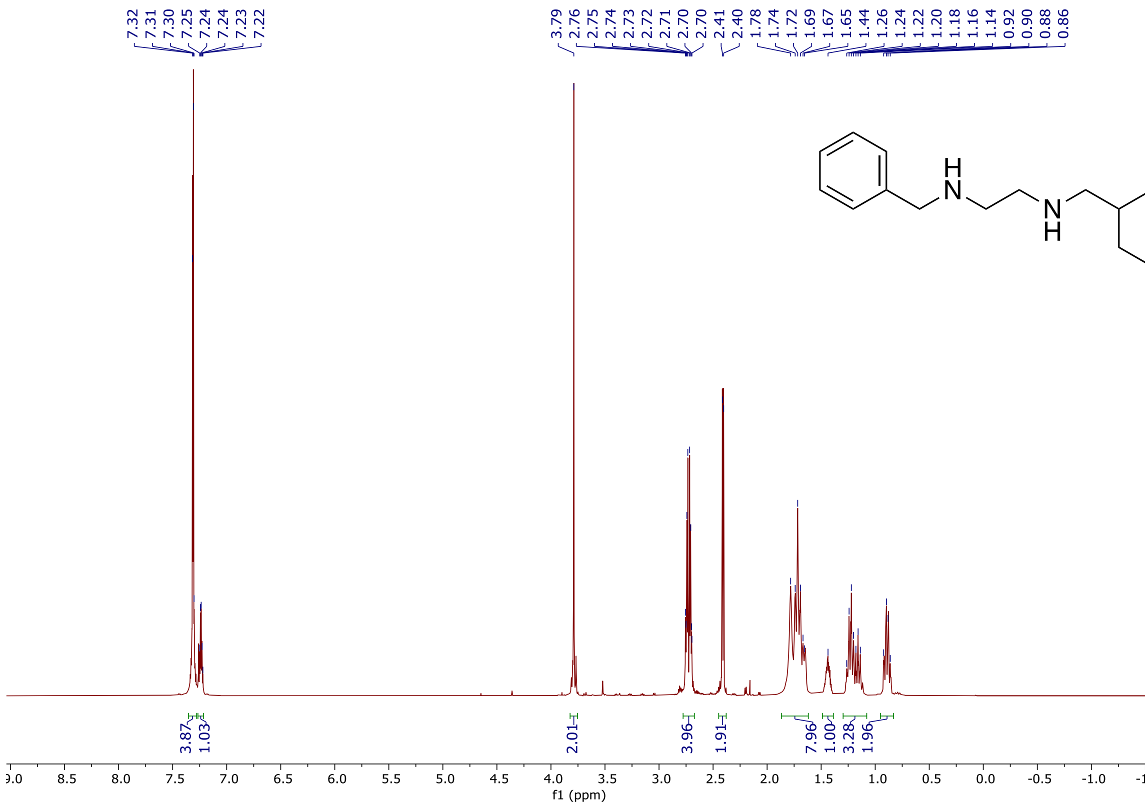

Figure S20. [1]H NMR (600 MHz) spectrum of **2f** at 25 °C in $CDCl_3$.

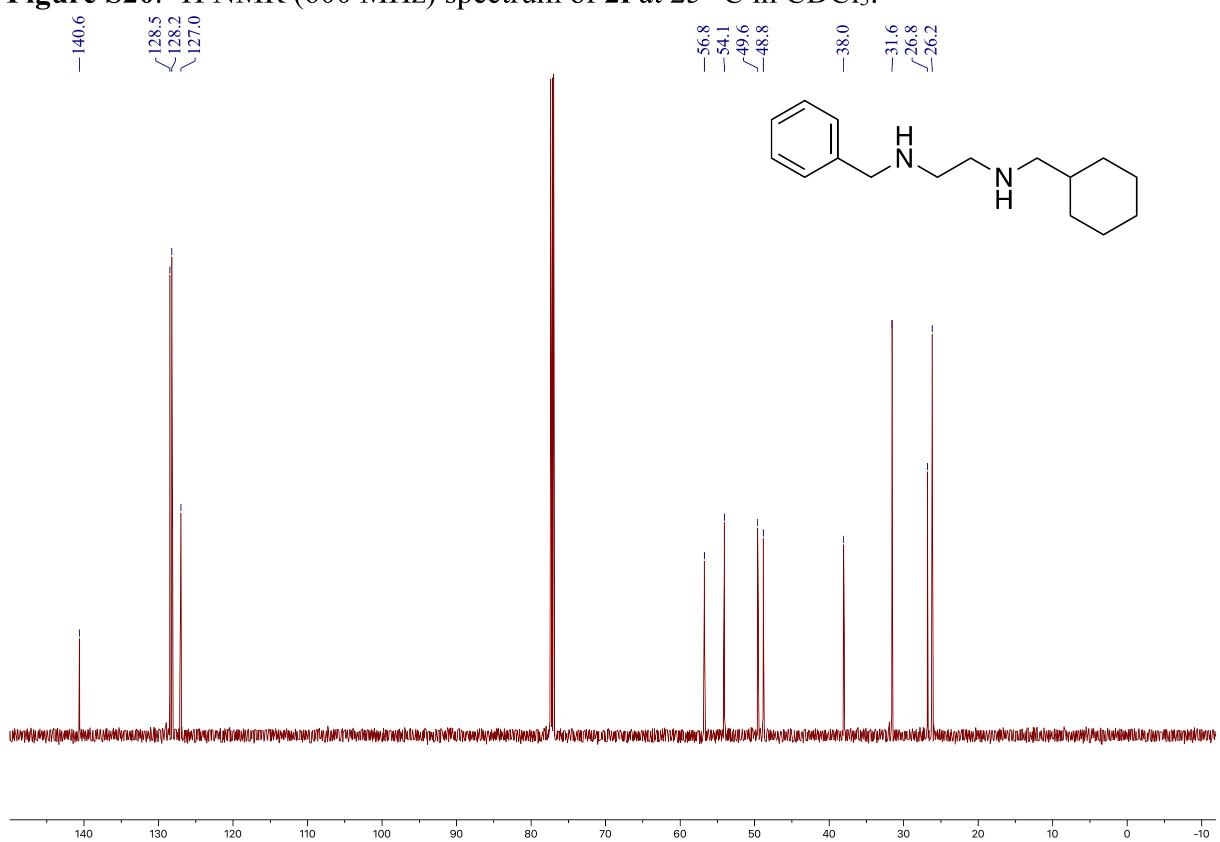

Figure S21. [13]C NMR (151 MHz) spectrum of **2f** at 25 °C in $CDCl_3$.

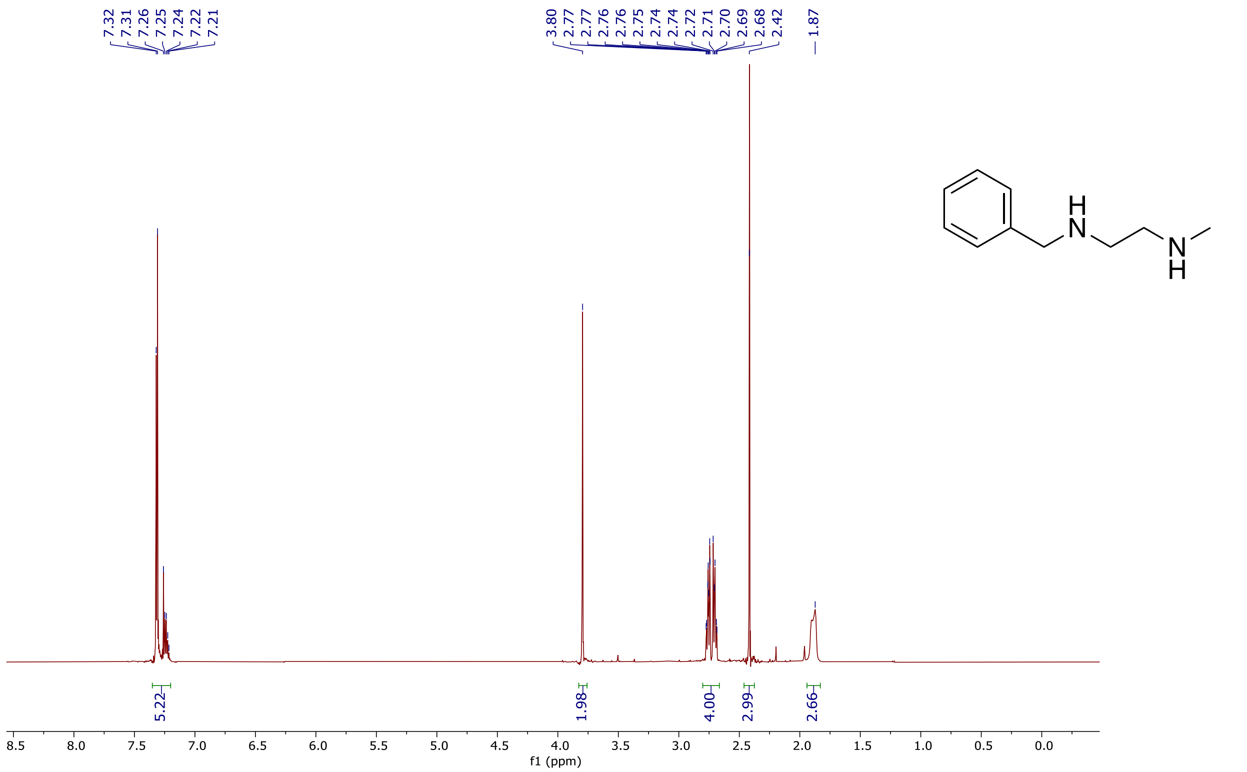

Figure S22. [1]H NMR (400 MHz) spectrum of **2g** at 25 °C in $CDCl_3$.

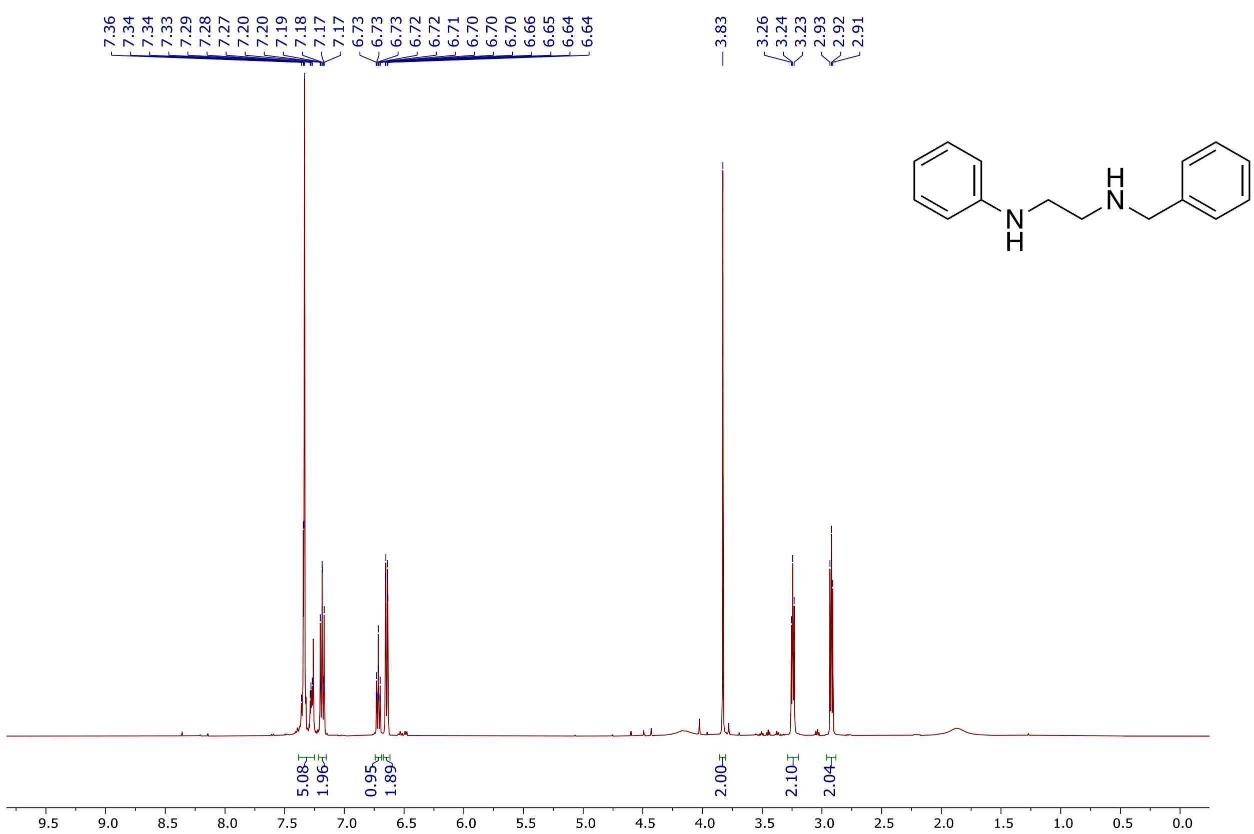

Figure S23. [1]H NMR (500 MHz) spectrum of **2j** at 25 °C in $CDCl_3$.

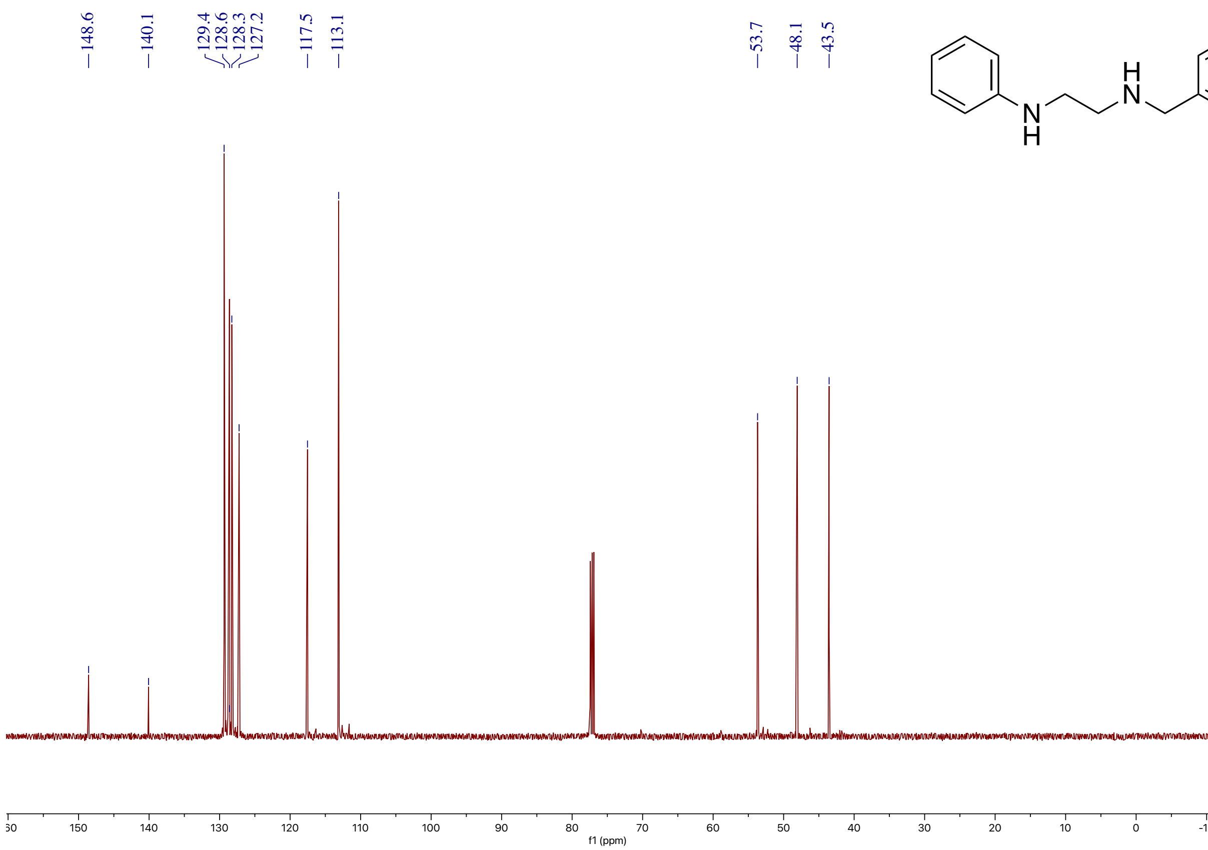

Figure S24. ^{13}C NMR (126 MHz) spectrum of **2j** at 25 °C in $CDCl_3$.

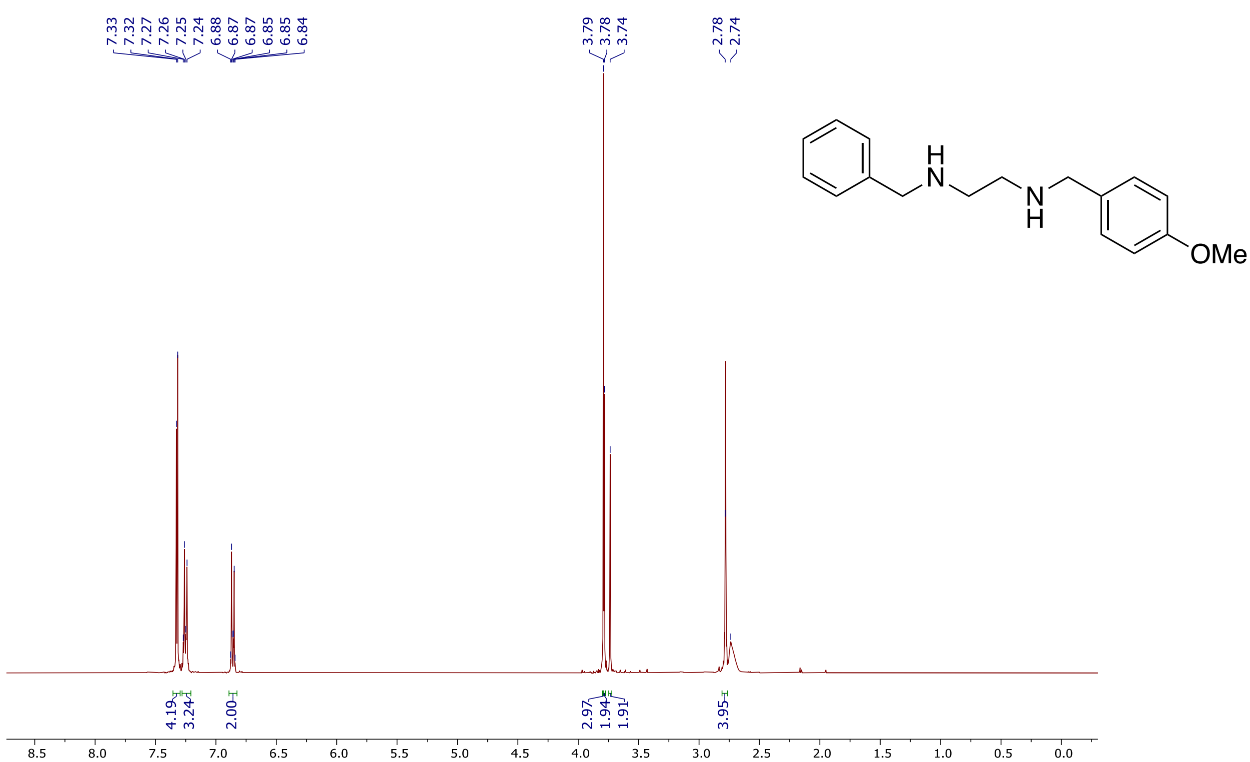

Figure S25. ^{1}H NMR (400 MHz) spectrum of **2k** at 25 °C in $CDCl_3$.

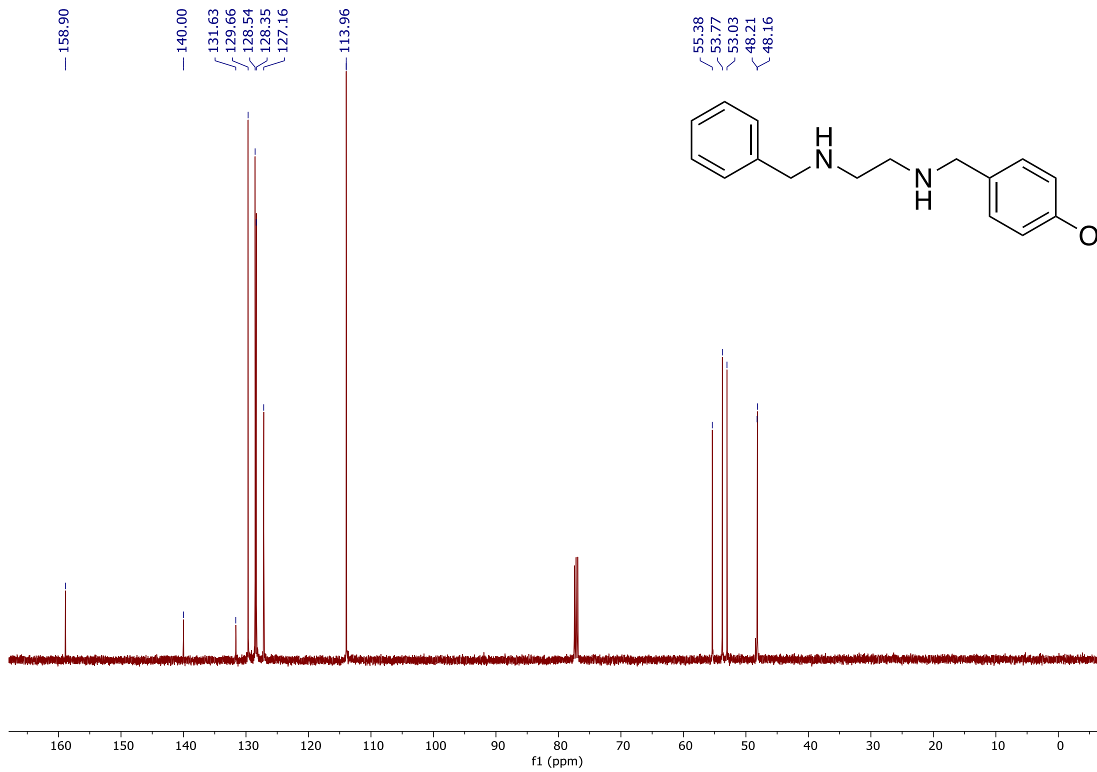

Figure S26. ^{13}C NMR (126 MHz) spectrum of **2k** at 25 °C in $CDCl_3$.

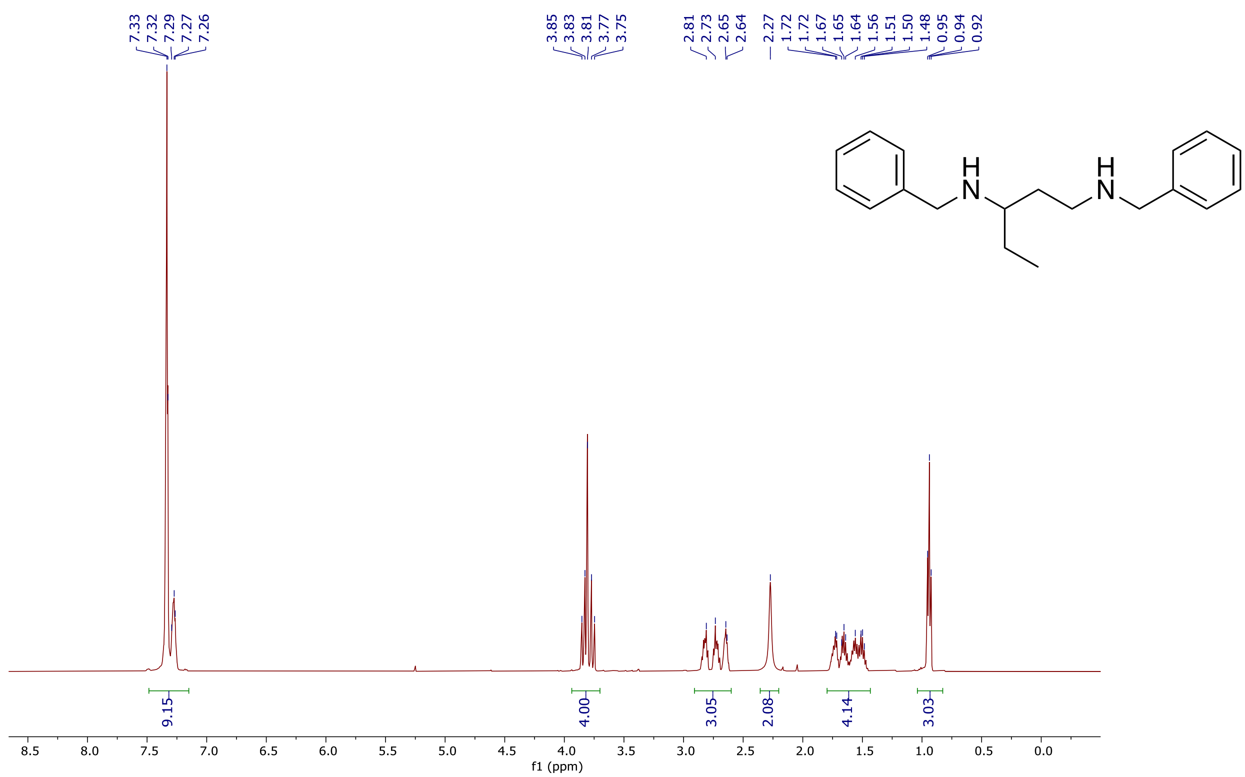

Figure S27. ^{1}H NMR (500 MHz) spectrum of **2e** at 25 °C in $CDCl_3$.

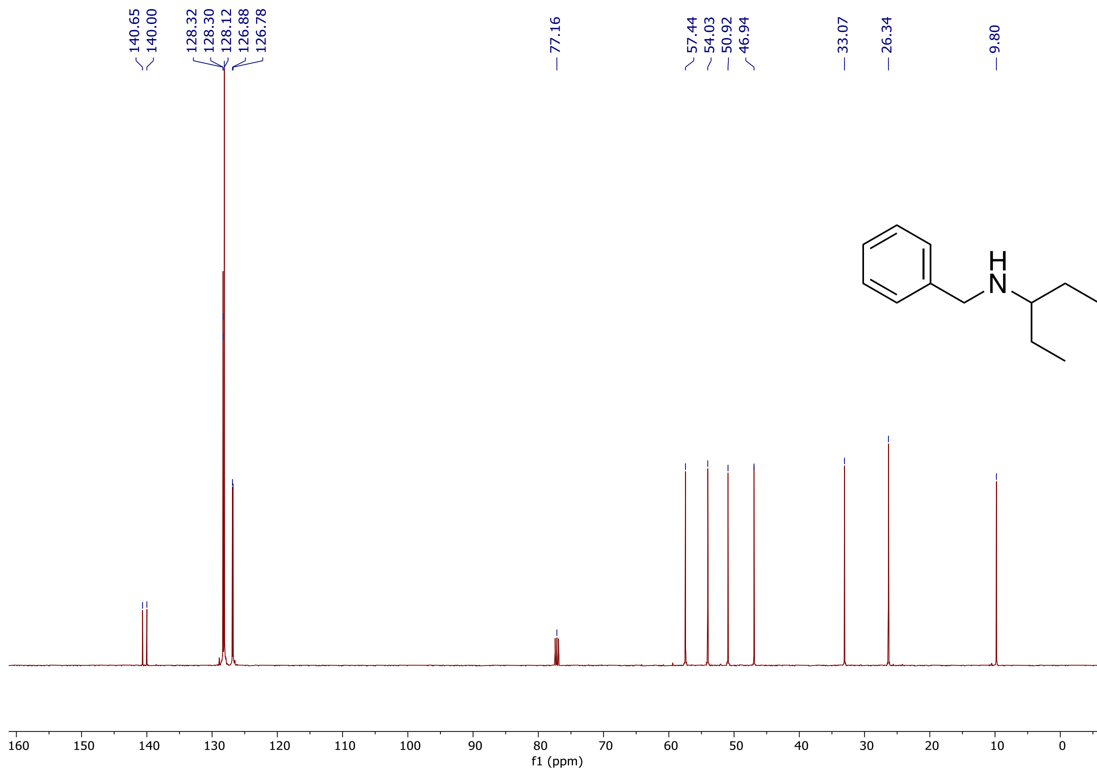

Figure S28. ^{13}C NMR (151 MHz) spectrum of **2e** at 25 °C in $CDCl_3$.

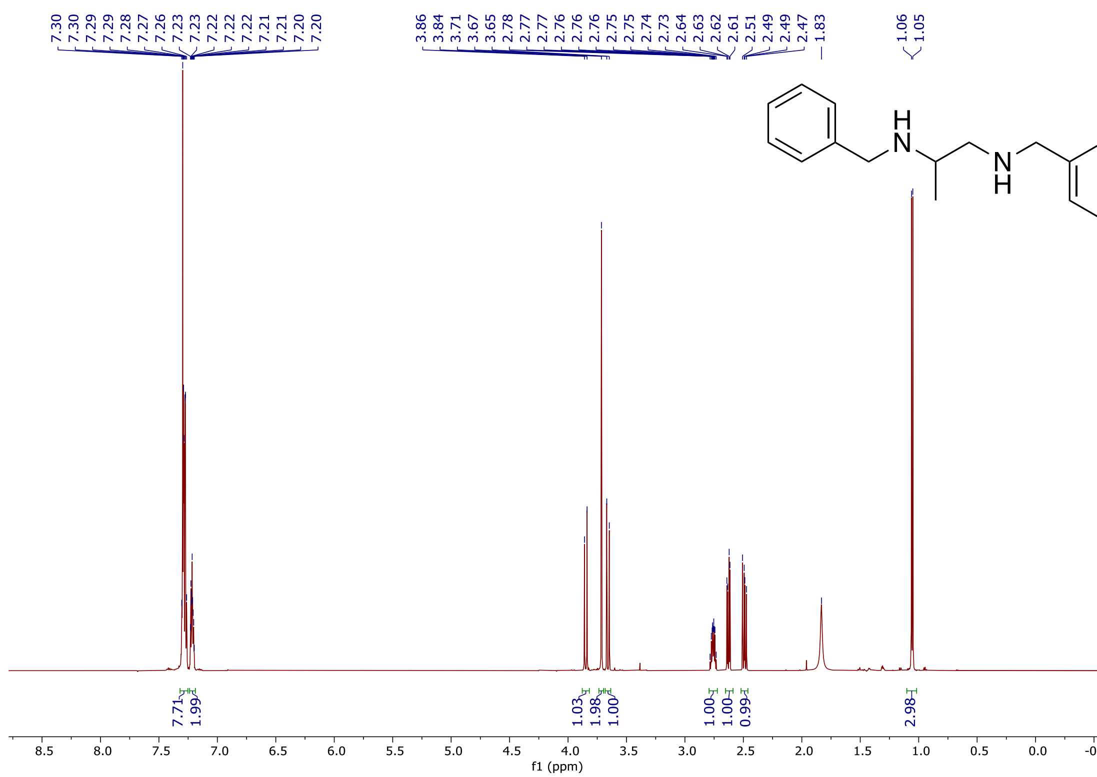

Figure S29. ^{1}H NMR (600 MHz) spectrum of **2l** at 25 °C in $CDCl_3$.

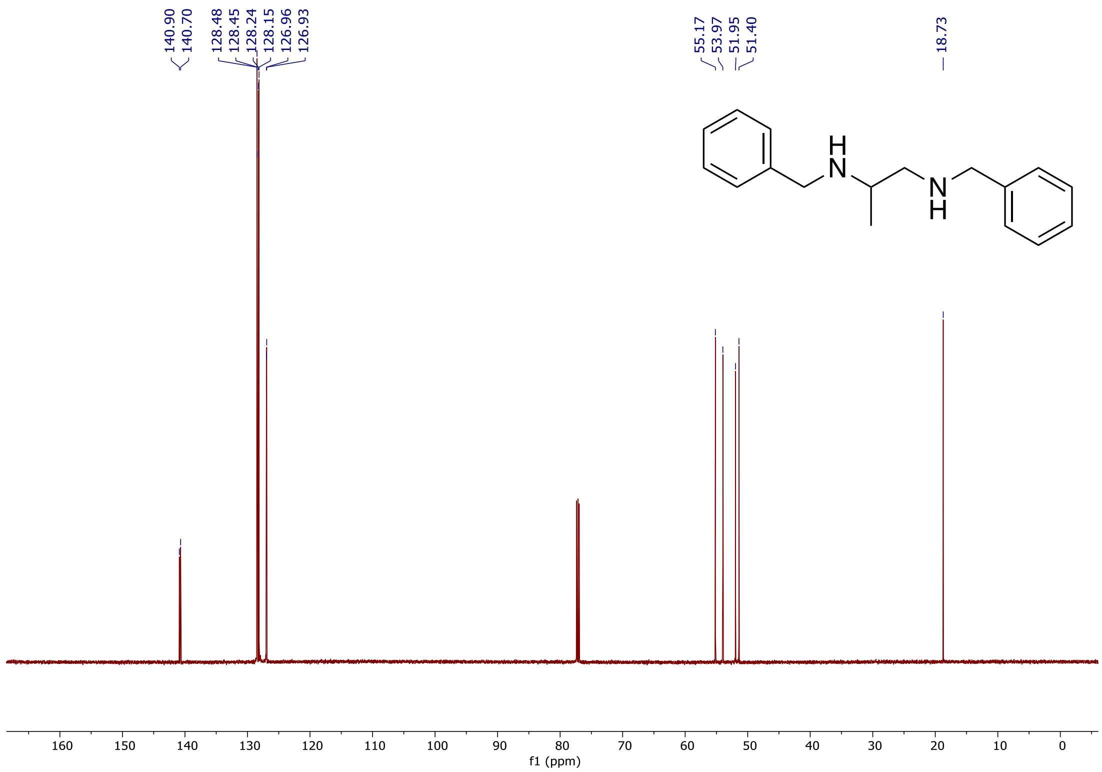

Figure S30. ^{13}C NMR (151 MHz) spectrum of **2l** at 25 °C in $CDCl_3$.

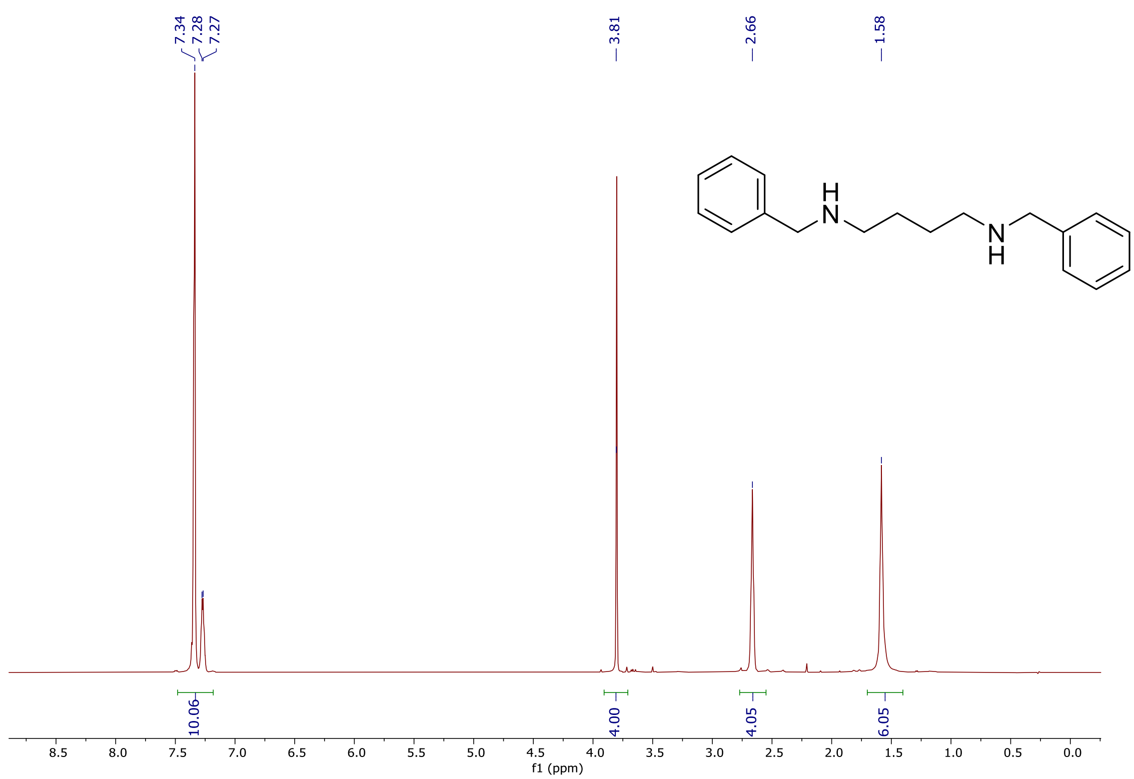

Figure S31. ^{1}H NMR (500 MHz) spectrum of **2m** at 25 °C in $CDCl_3$.

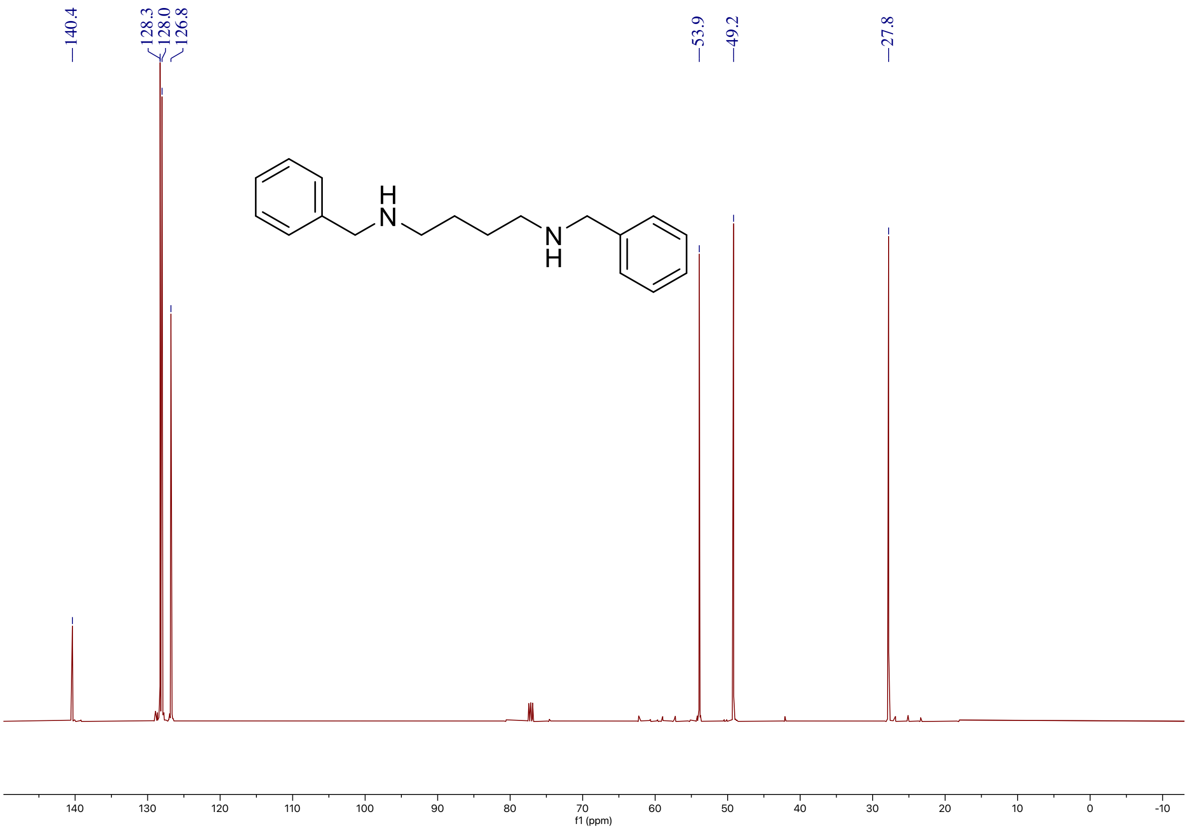

Figure S32. [13]C NMR (151 MHz) spectrum of **2m** at 25 °C in $CDCl_3$.

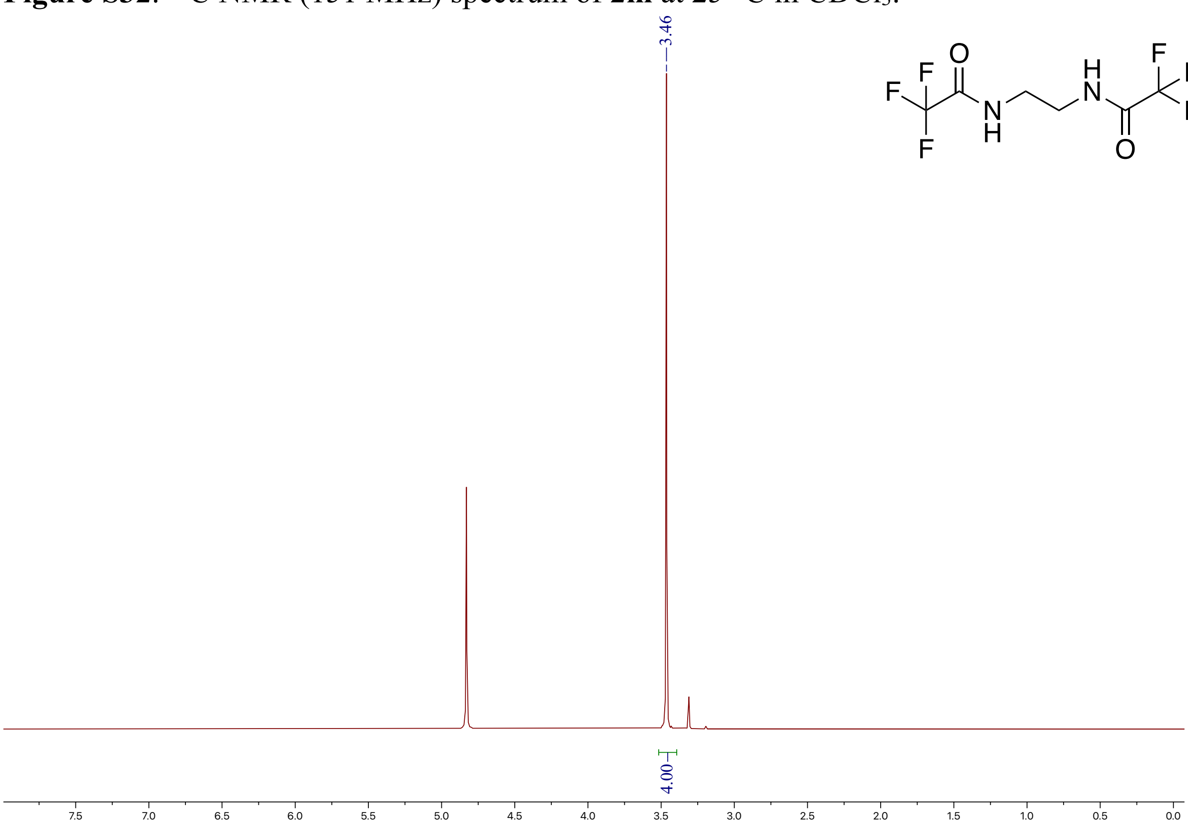

Figure S33. [1]H NMR (600 MHz) spectrum of **2n** at 25 °C in CD_3OD.

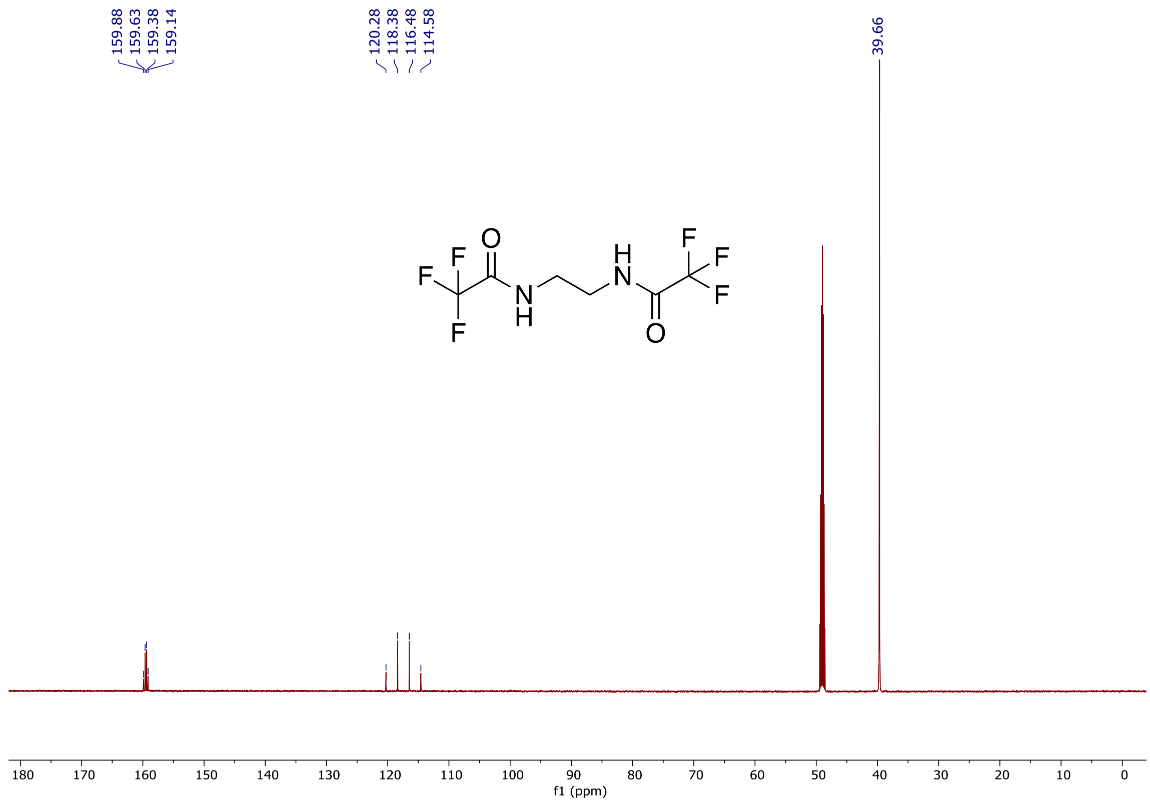

Figure S34. [13]C NMR (151 MHz) spectrum of **2n** at 25 °C in CD_3OD.

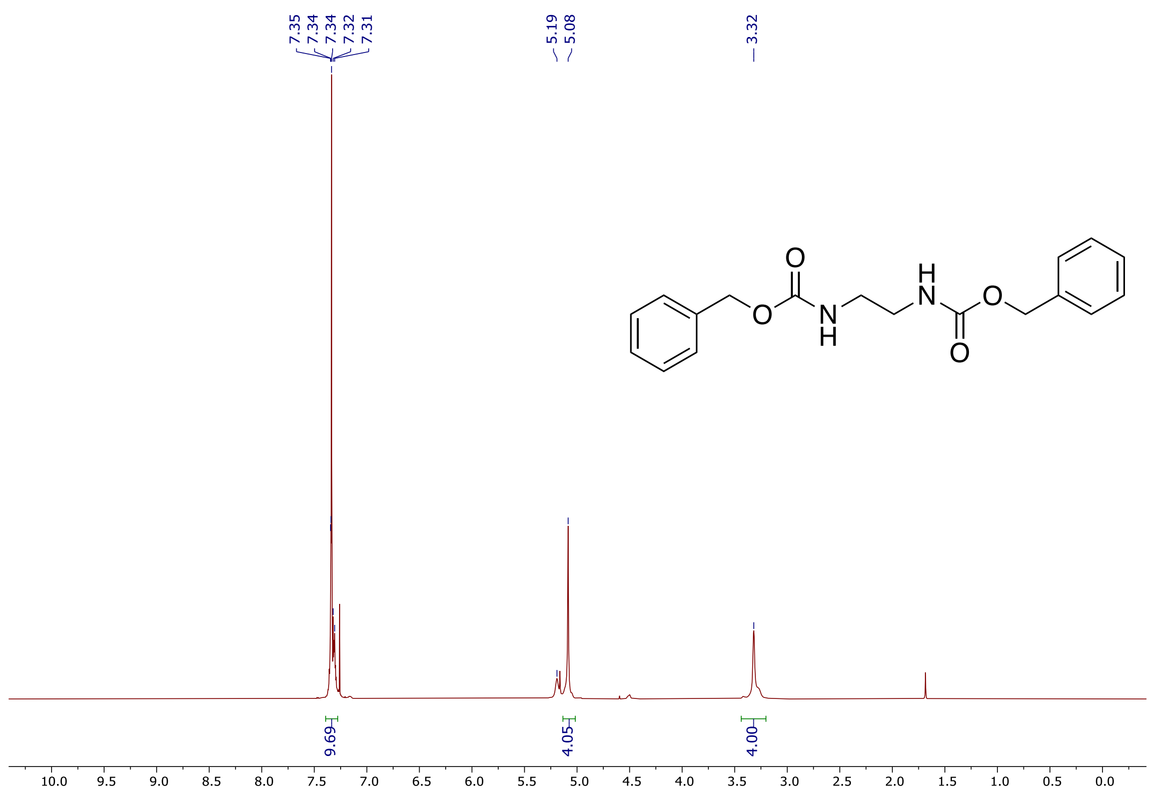

Figure S35. [1]H NMR (600 MHz) spectrum of **2o** at 25 °C in $CDCl_3$.

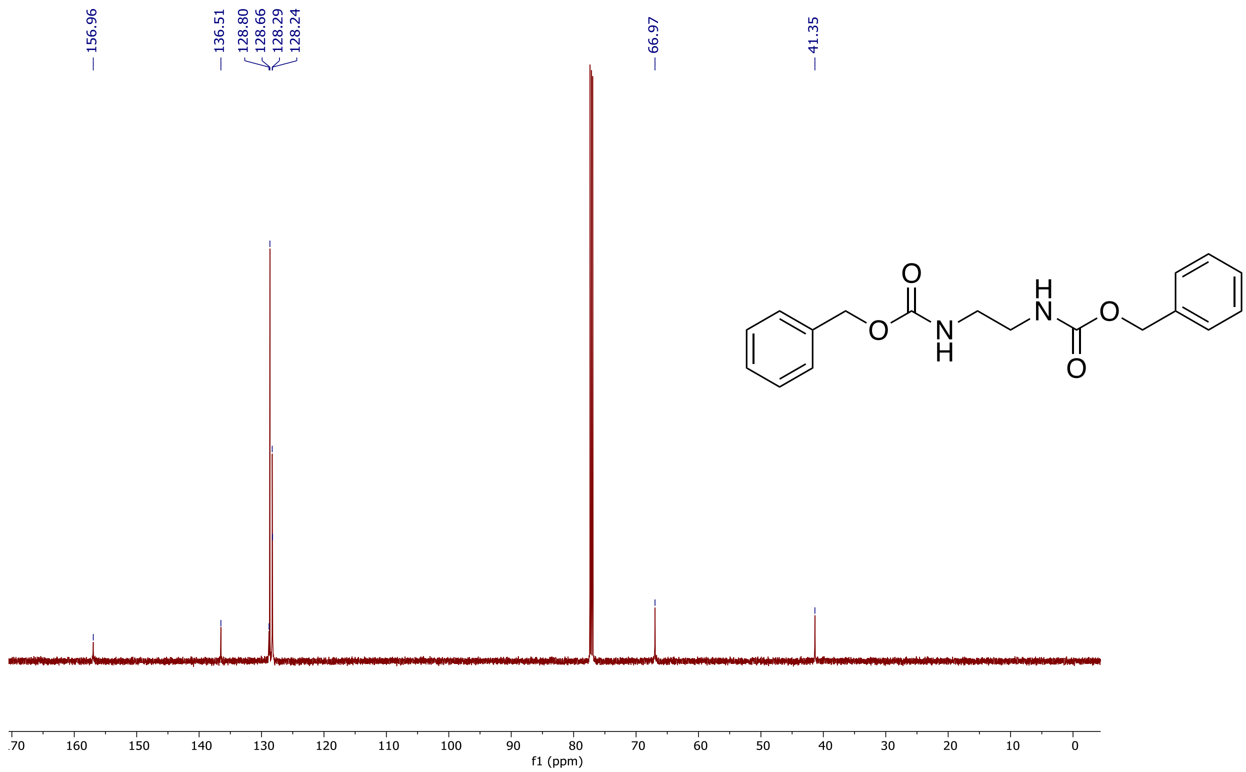

Figure S36. ^{13}C NMR (151 MHz) spectrum of **2o** at 25 °C in $CDCl_3$.

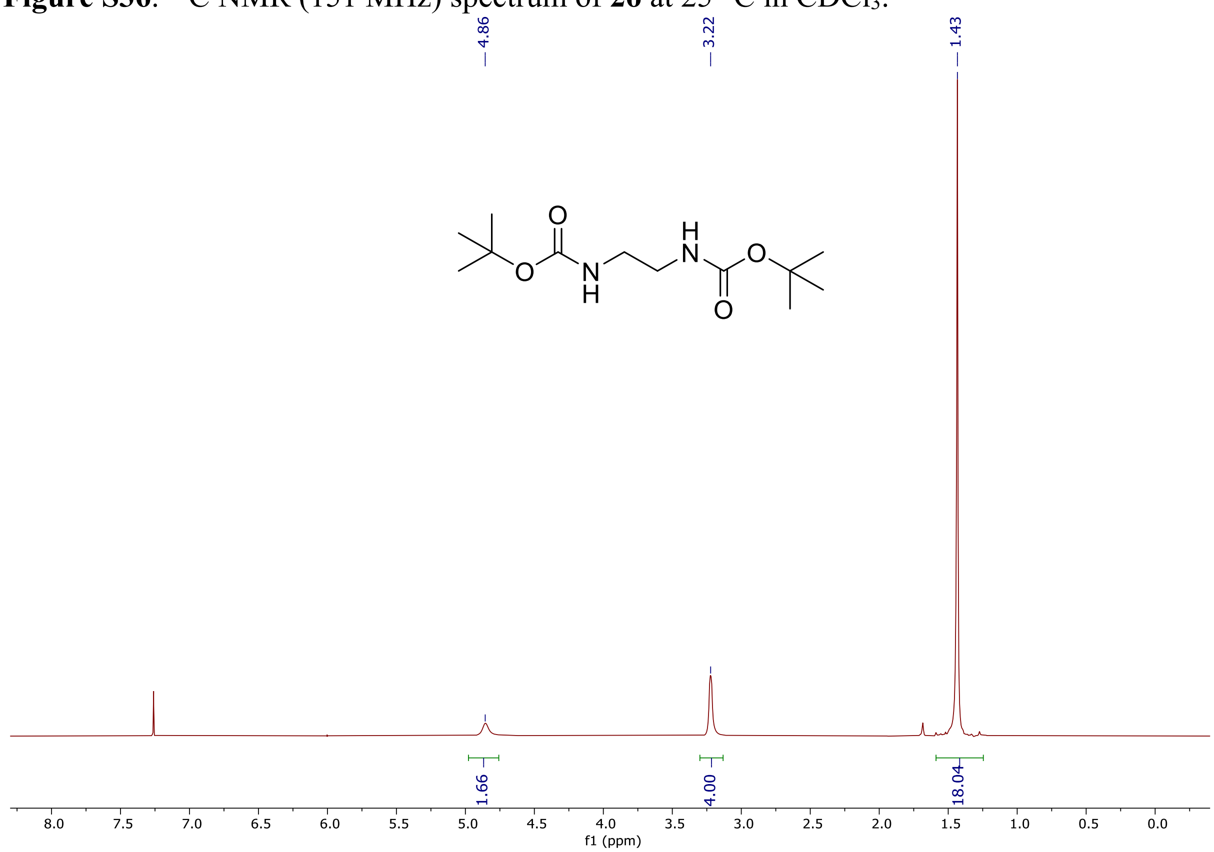

Figure S37. ^{1}H NMR (600 MHz) spectrum of **2p** at 25 °C in $CDCl_3$.

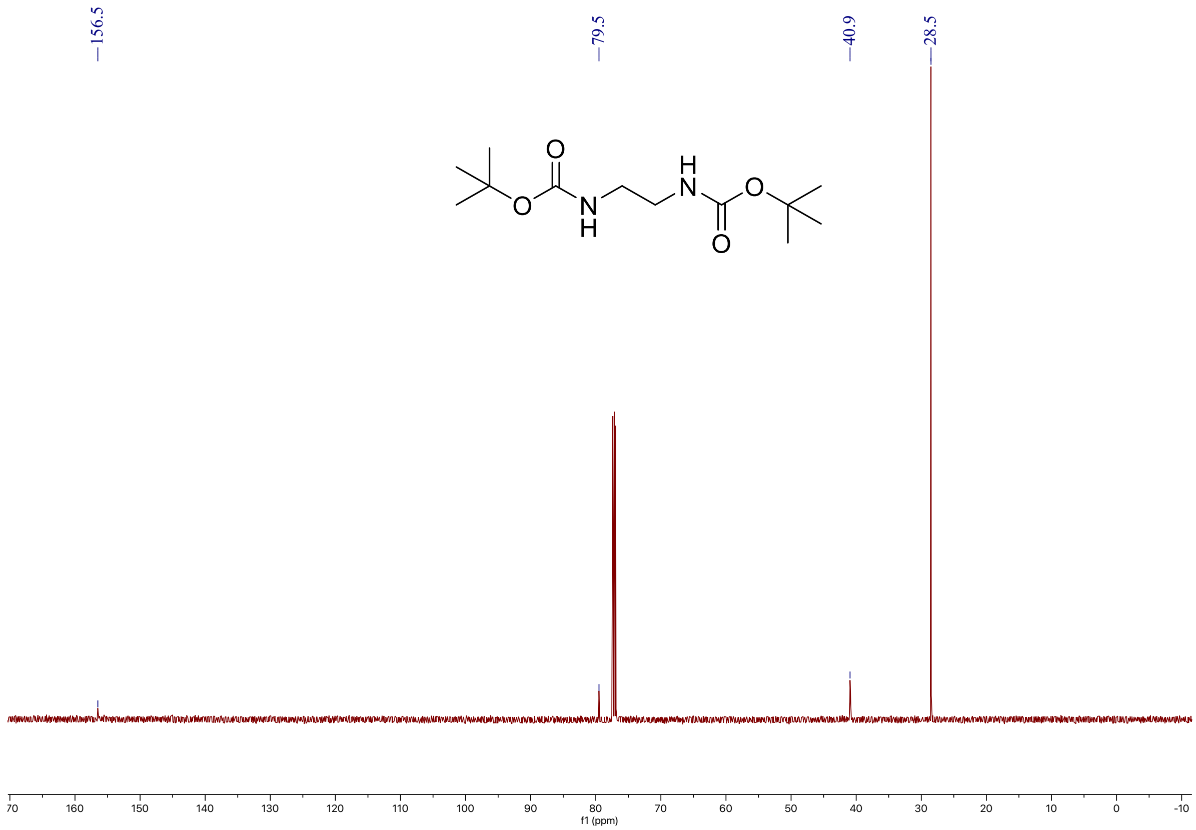

Figure S38. ^{13}C NMR (151 MHz) spectrum of **2p** at 25 °C in $CDCl_3$.

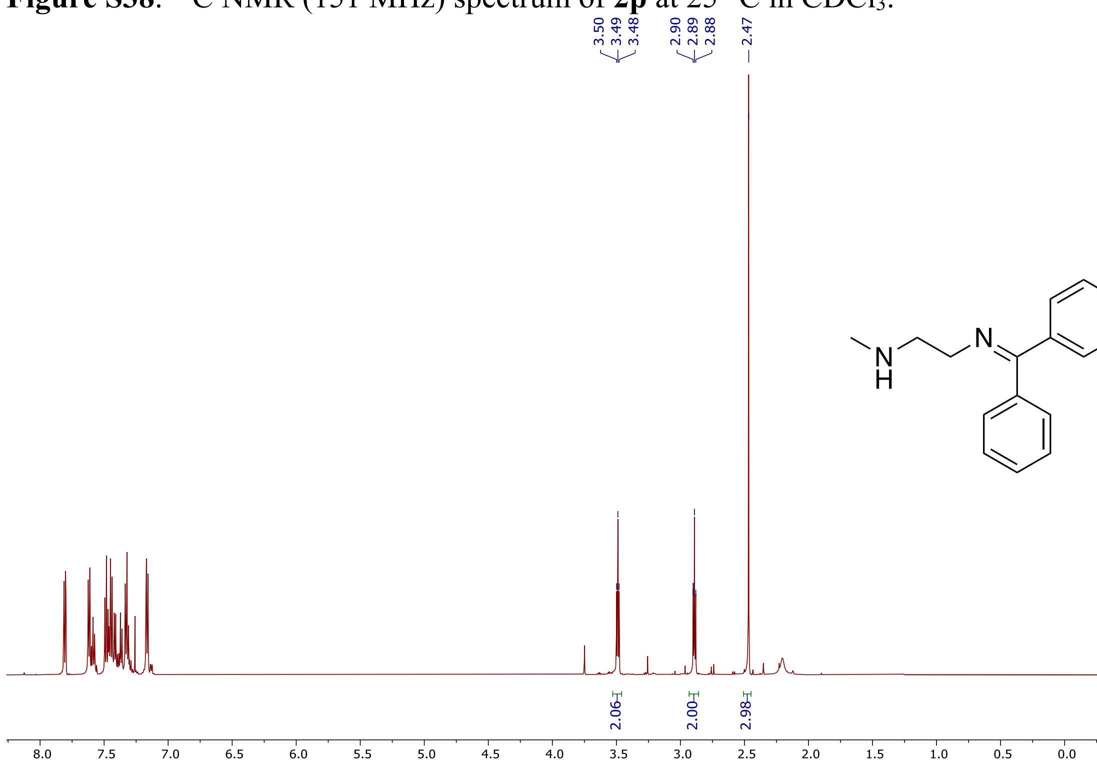

Figure S39. ^{1}H NMR (600 MHz) spectrum of **20a** at 25 °C in $CDCl_3$.

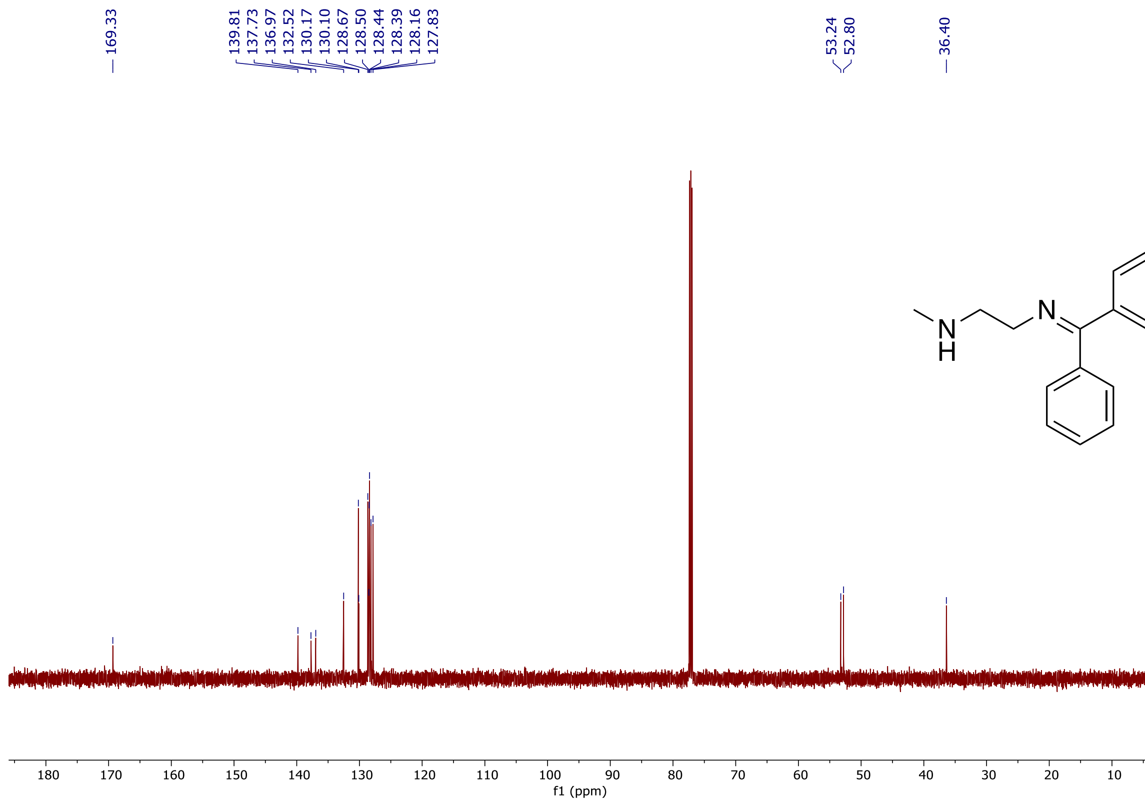

Figure S40. [13]C NMR (151 MHz) spectrum of **20a** at 25 °C in $CDCl_3$.

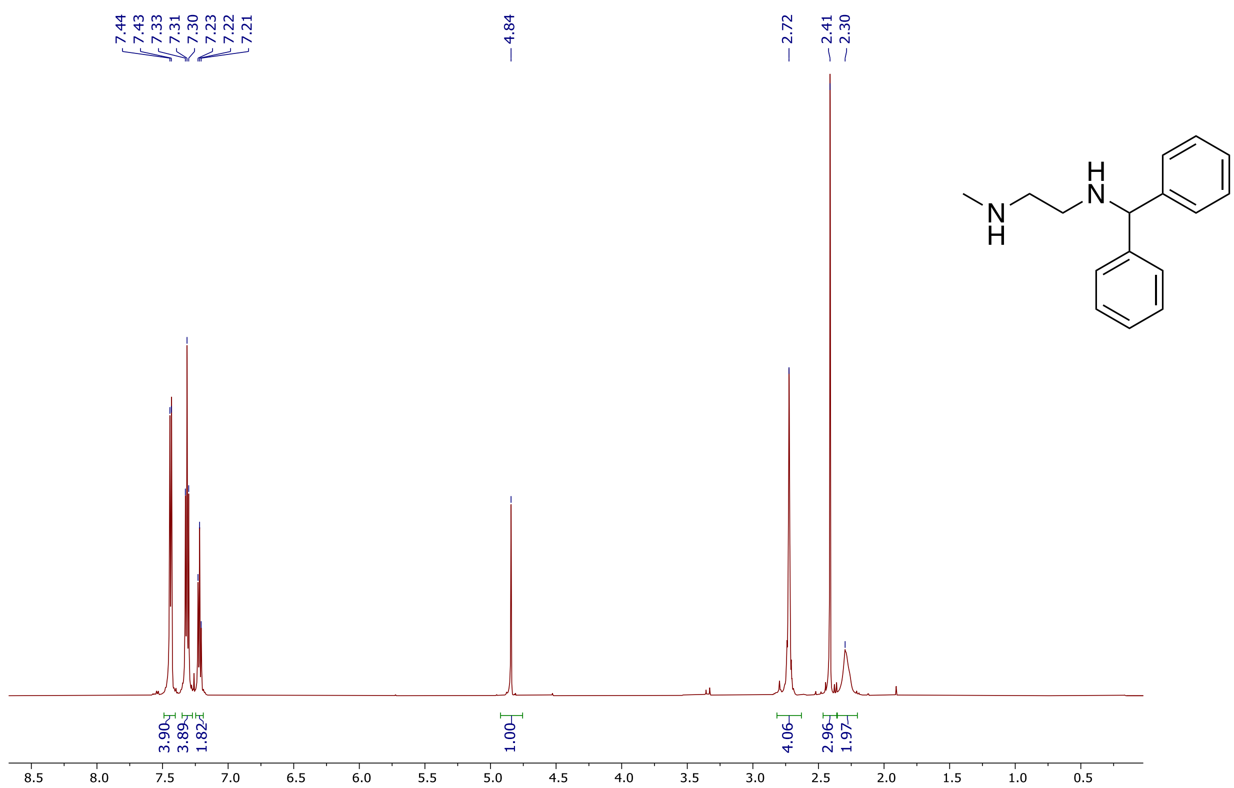

Figure S41. [1]H NMR (600 MHz) spectrum of **2q** at 25 °C in $CDCl_3$.

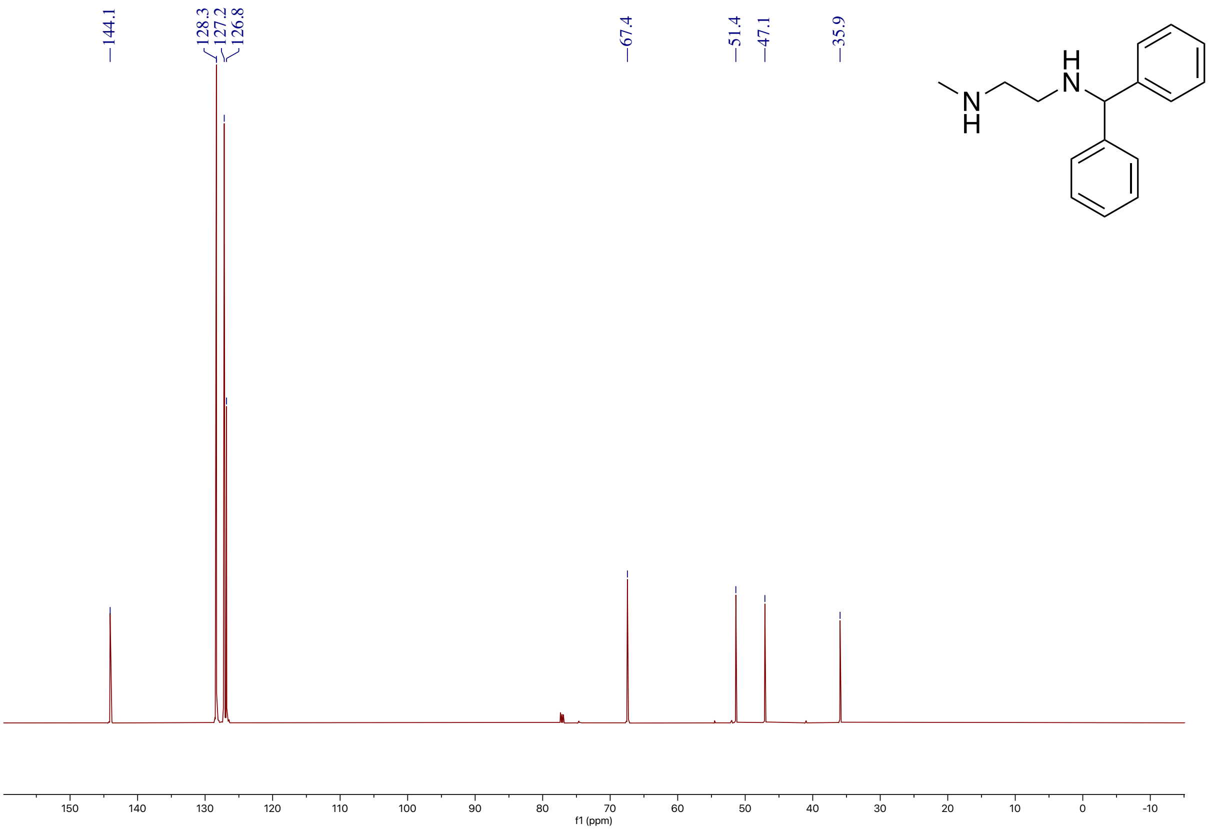

Figure S42. ^{13}C NMR (151 MHz) spectrum of **2q** at 25 °C in $CDCl_3$.

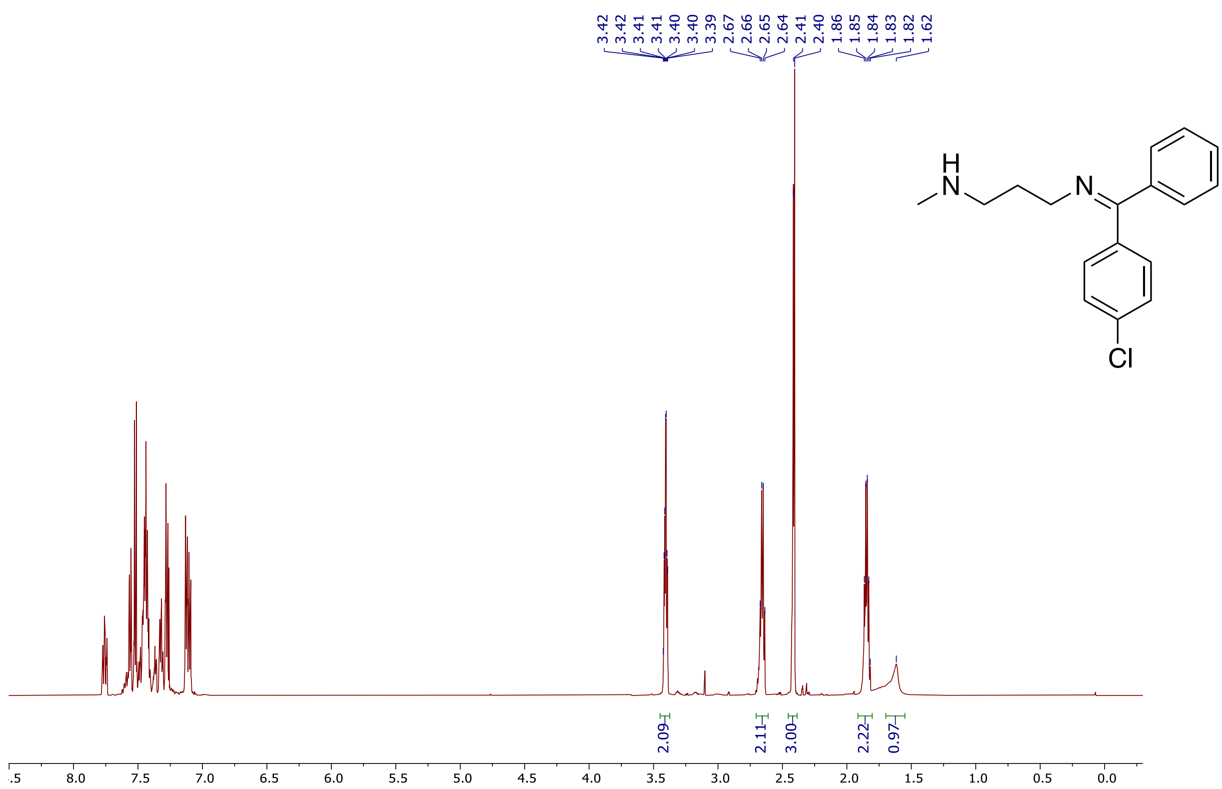

Figure S43. ^{1}H NMR (600 MHz) spectrum of **20i** at 25 °C in $CDCl_3$.

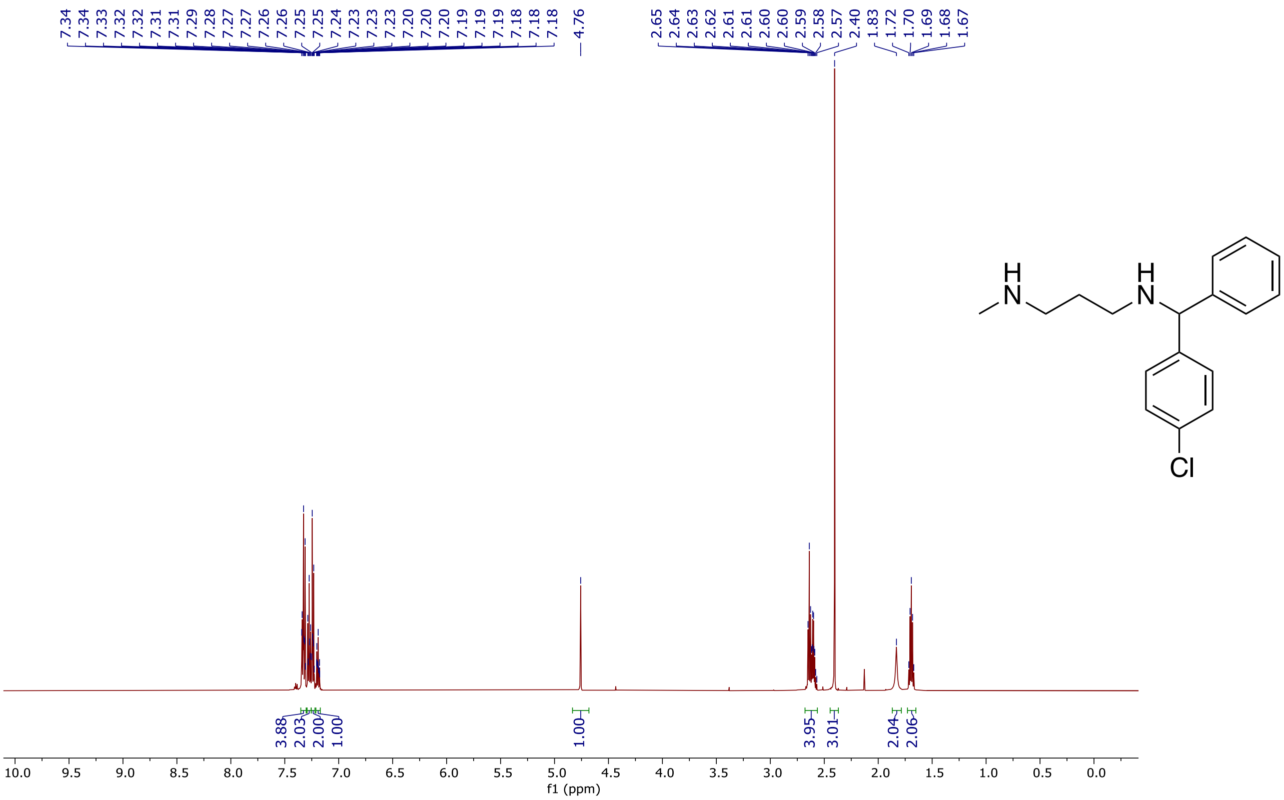

Figure S44. ^{1}H NMR (600 MHz) spectrum of **2r** at 25 °C in $CDCl_3$.

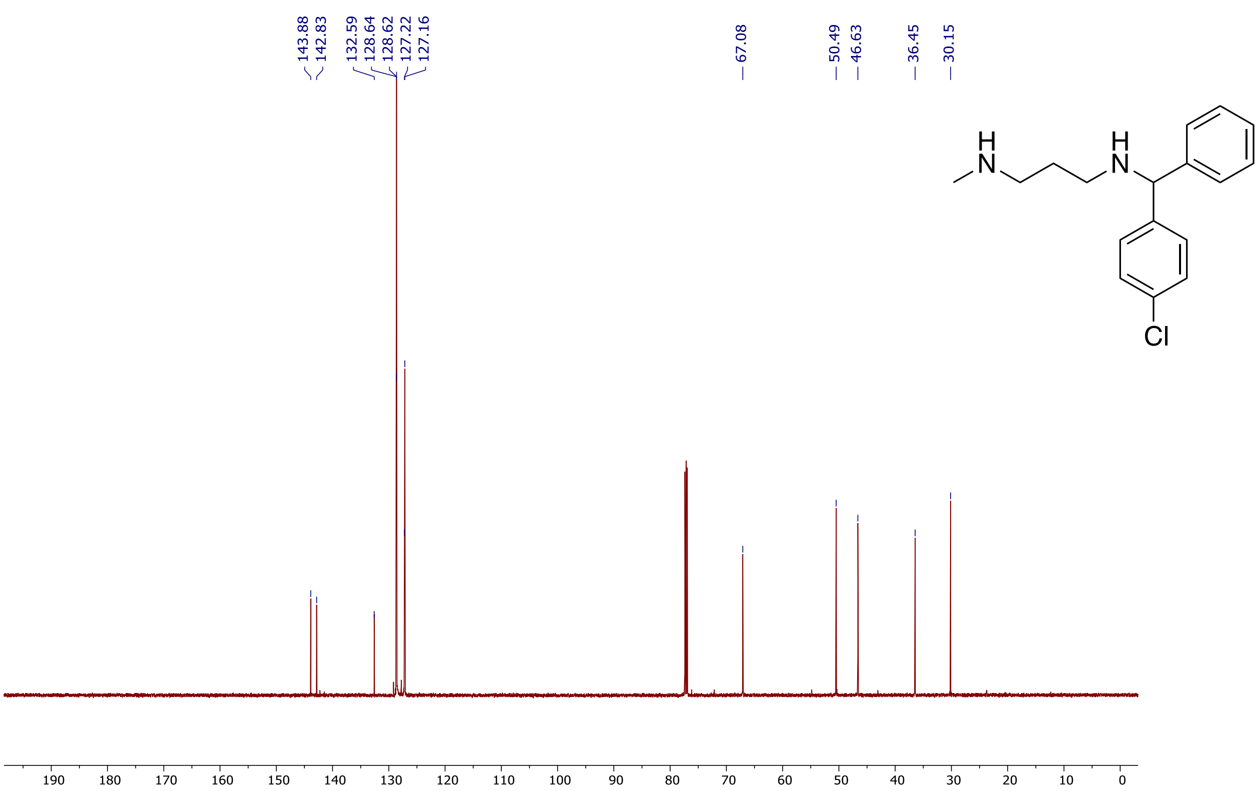

Figure S45. ^{13}C NMR (151 MHz) spectrum of **2r** at 25 °C in $CDCl_3$.

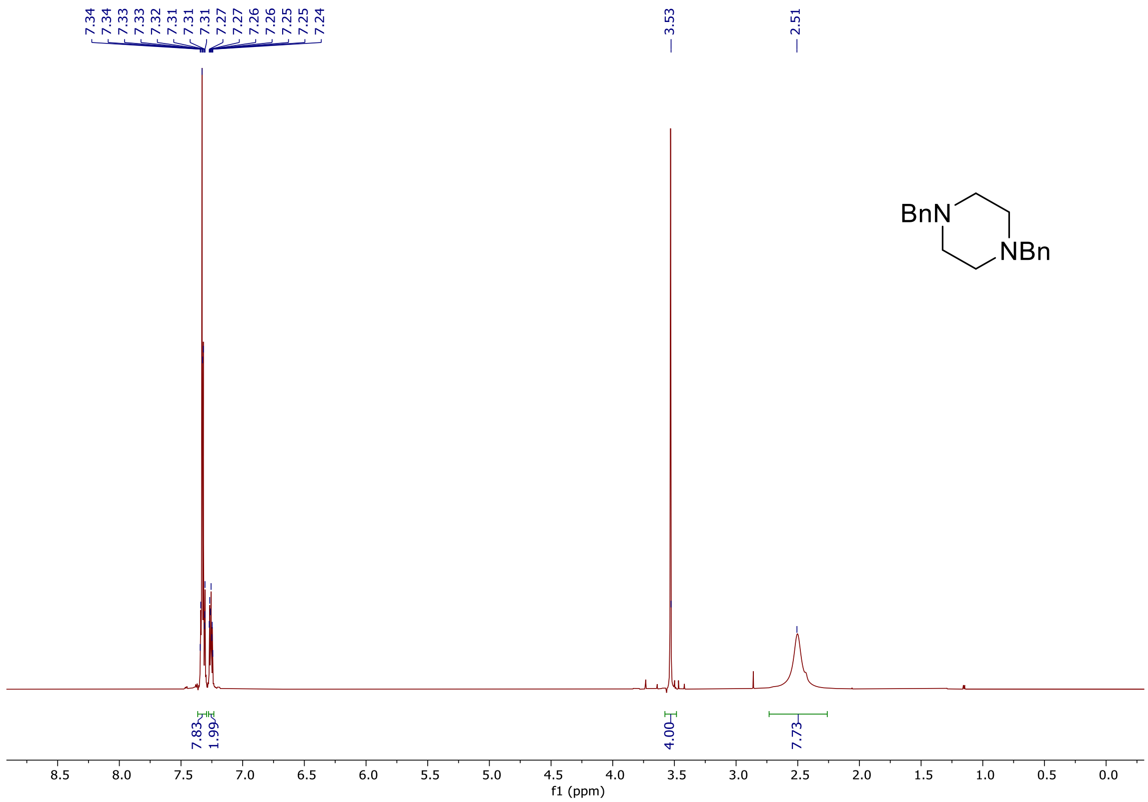

Figure S46. ^{1}H NMR (600 MHz) spectrum of **6a** at 25 °C in $CDCl_3$.

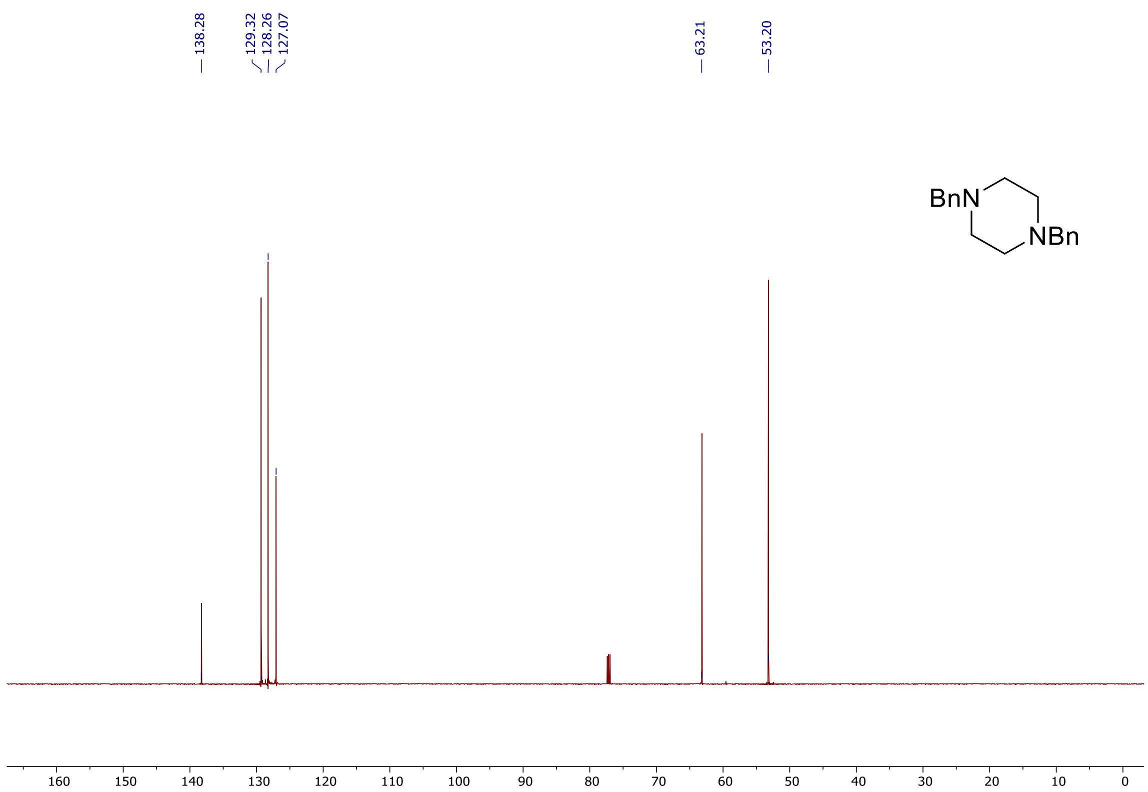

Figure S47. ^{13}C NMR (151 MHz) spectrum of **6a** at 25 °C in $CDCl_3$.

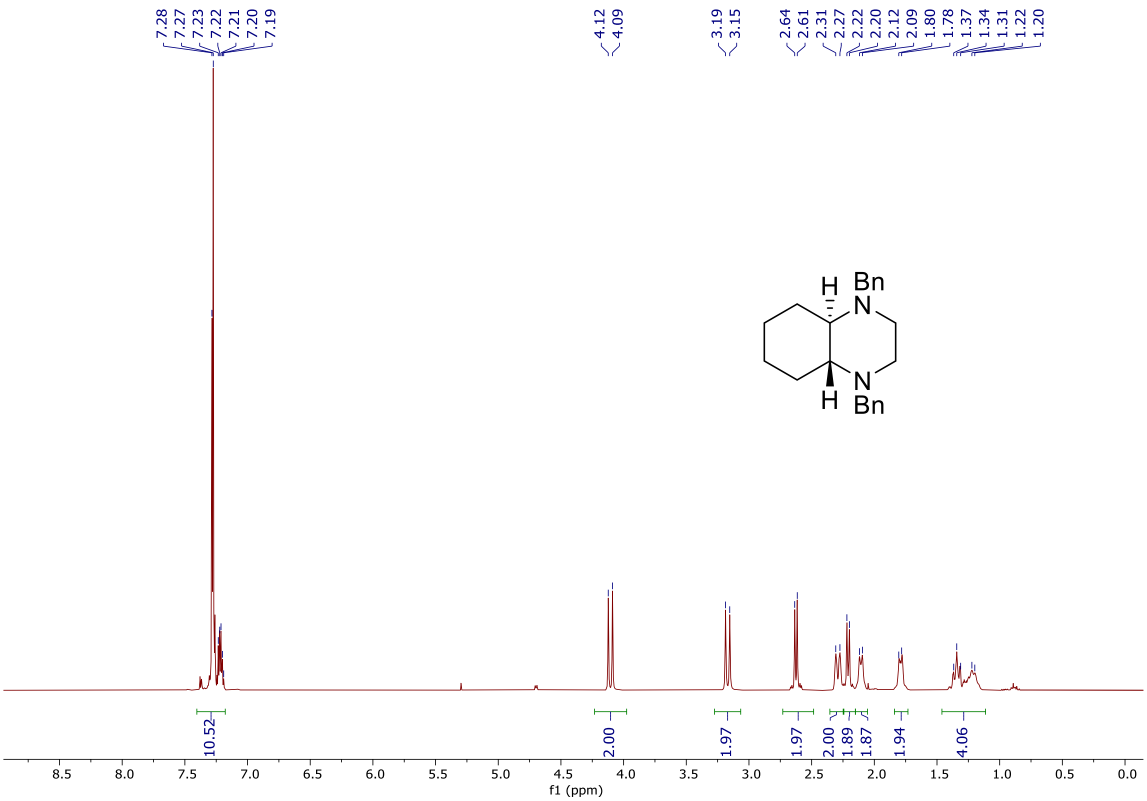

Figure S48. ^{1}H NMR (400 MHz) spectrum of **6b** at 25 °C in $CDCl_3$.

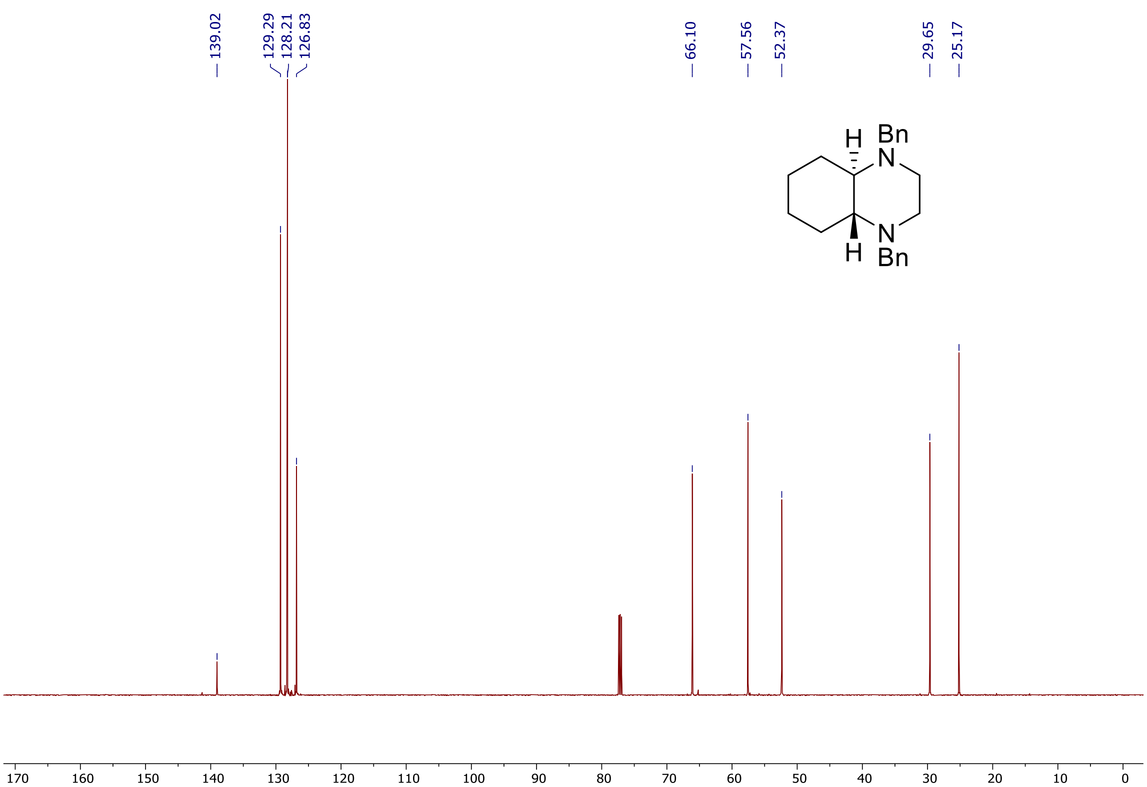

Figure S49. ^{13}C NMR (151 MHz) spectrum of **6b** at 25 °C in $CDCl_3$.

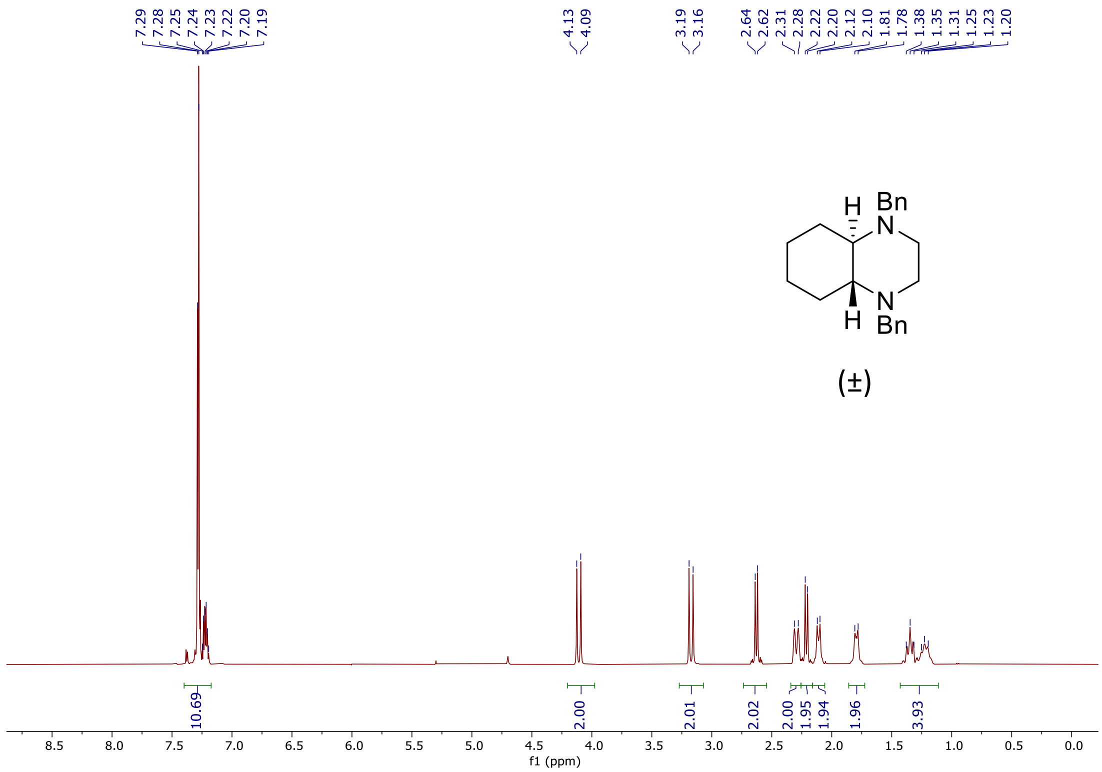

Figure S50. ¹H NMR (400 MHz) spectrum of (±)-(4a*R*,8a*R*)-1,4-dibenzyldecahydroquinoxaline at 25 °C in $CDCl_3$.

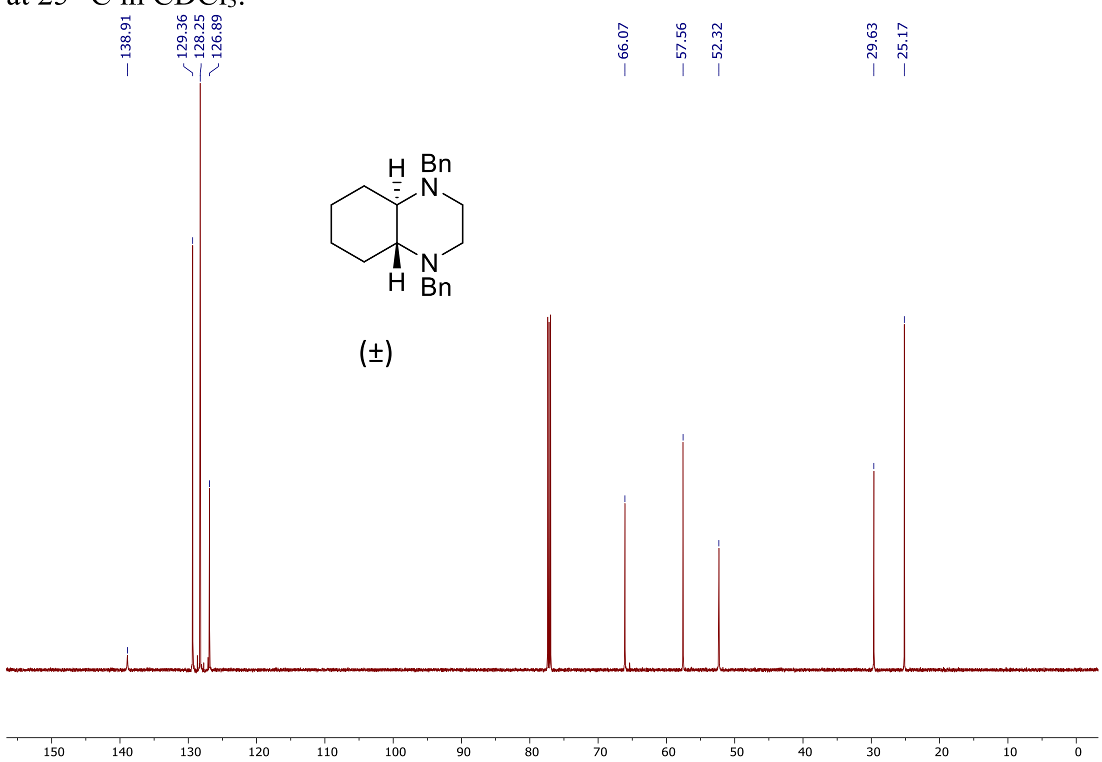

Figure S51. ¹³C NMR (151 MHz) spectrum of (±)-(4aR,8aR)-1,4-dibenzyldecahydroquinoxaline at 25 °C in $CDCl_3$.

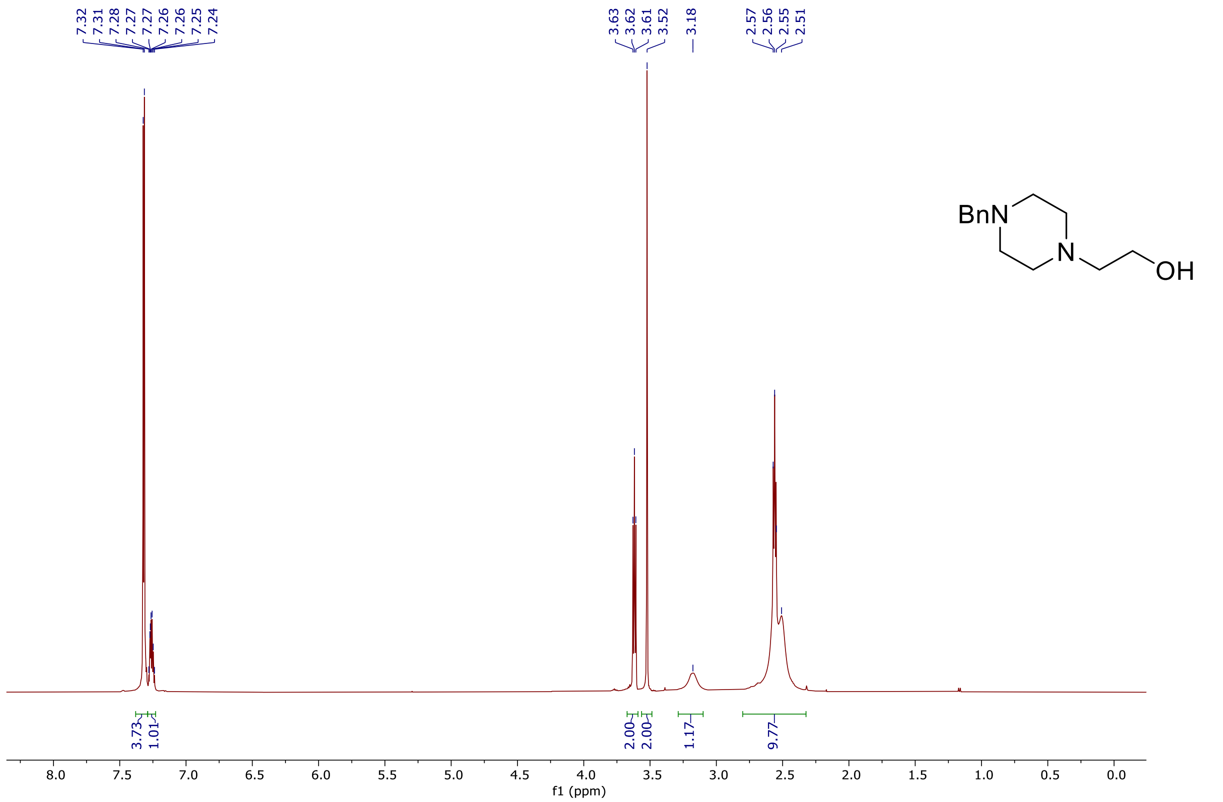

Figure S52. ^{1}H NMR (500 MHz) spectrum of **6c** at 25 °C in $CDCl_3$.

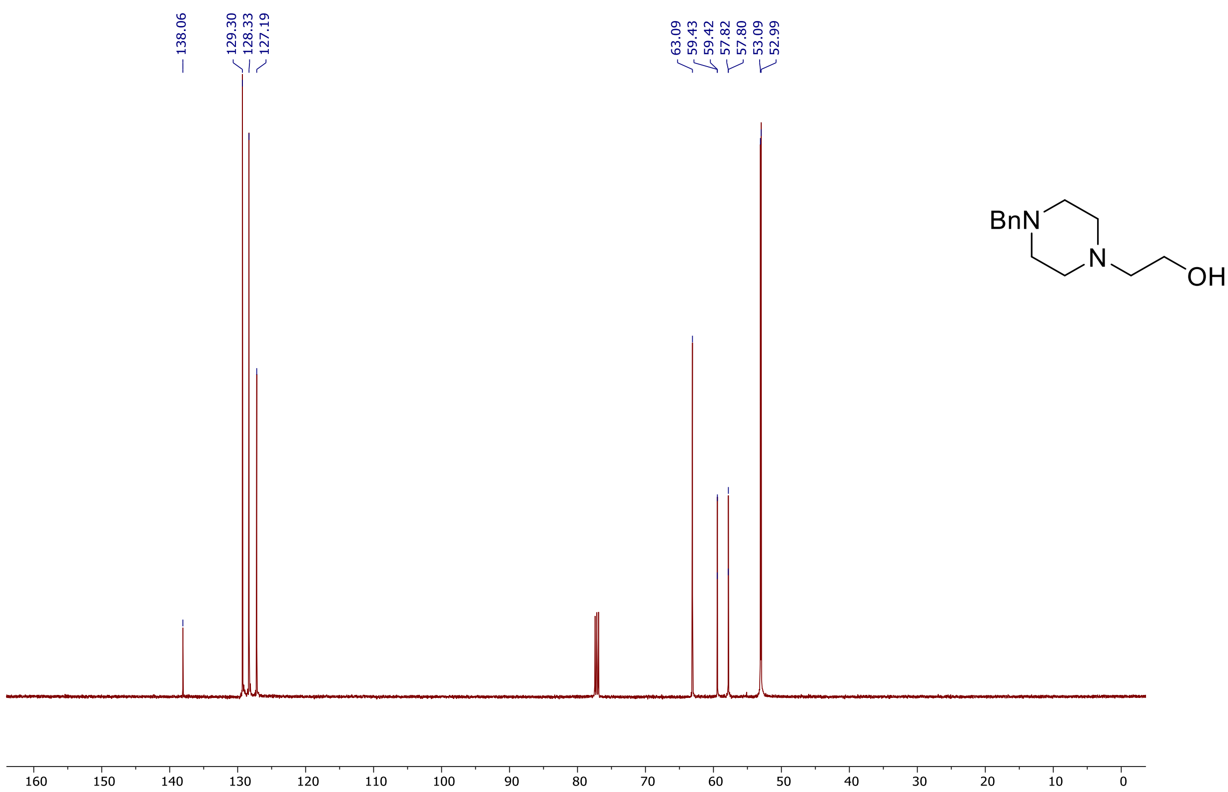

Figure S53. ^{13}C NMR (126 MHz) spectrum of **6c** at 25 °C in $CDCl_3$.

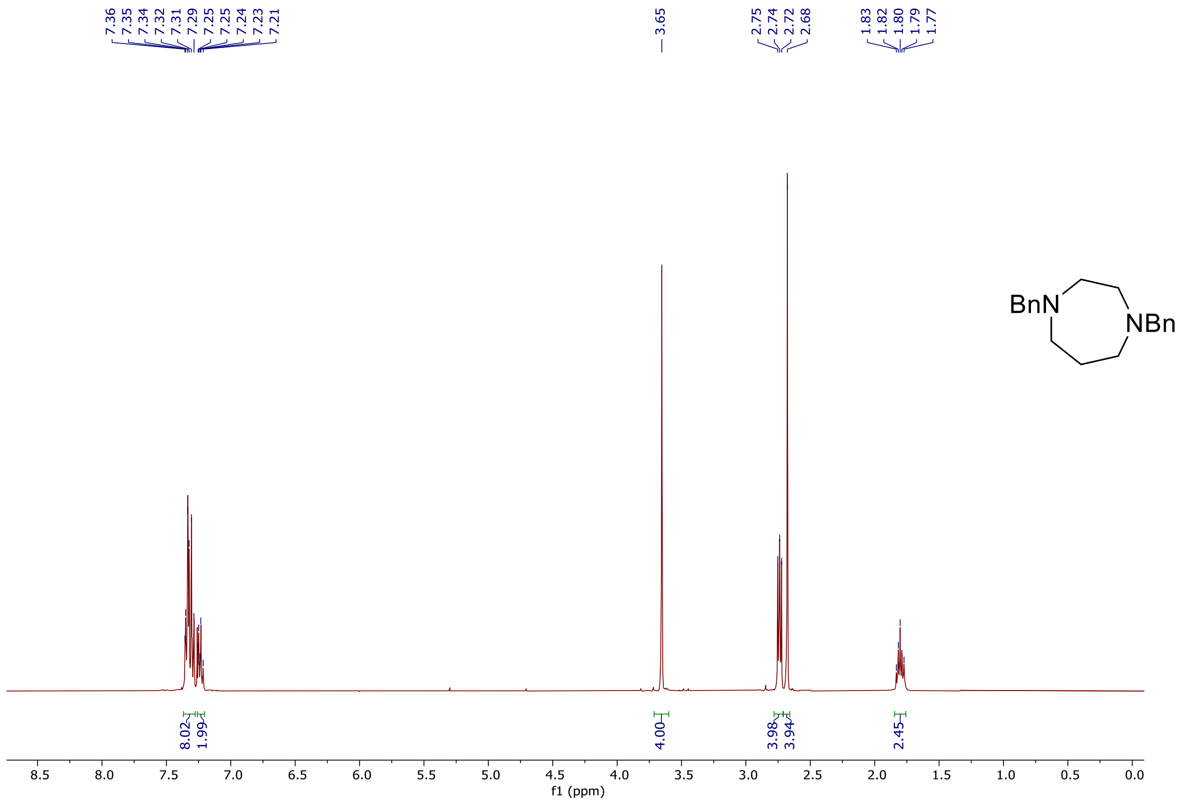

Figure S54. ¹H NMR (400 MHz) spectrum of **4a** at 25 °C in $CDCl_3$.

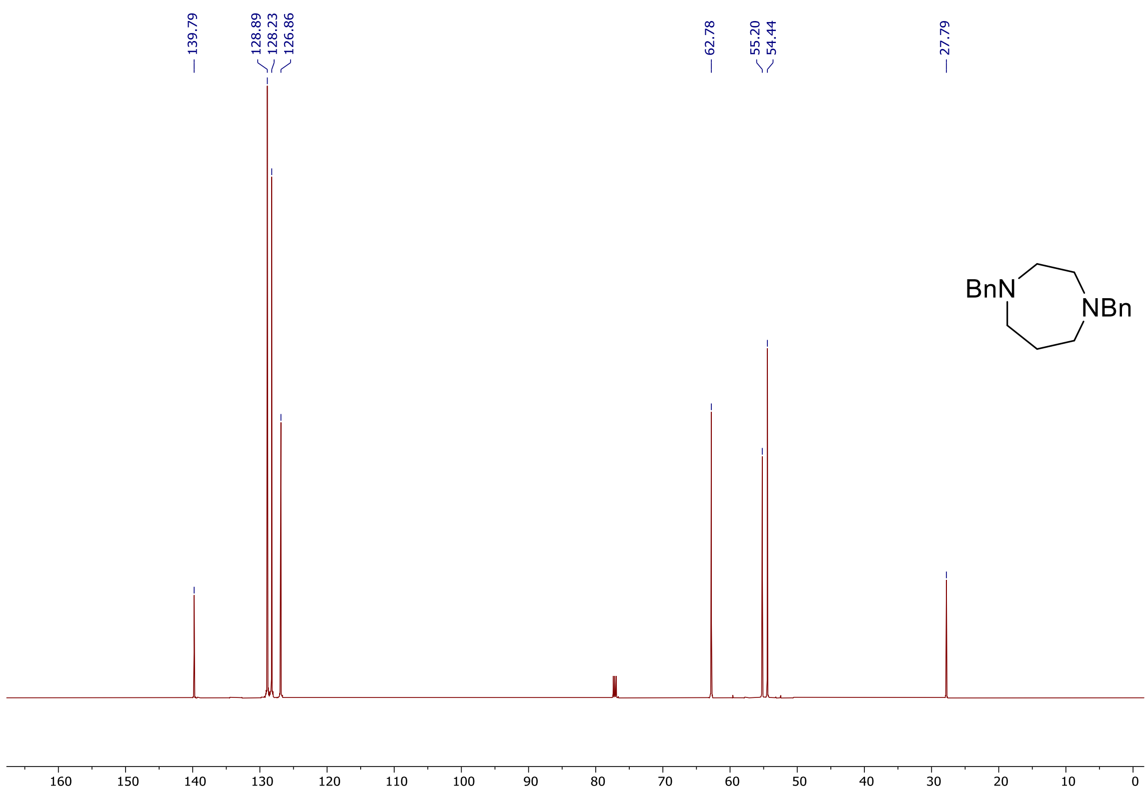

Figure S55. ¹³C NMR (151 MHz) spectrum of **4a** at 25 °C in $CDCl_3$.

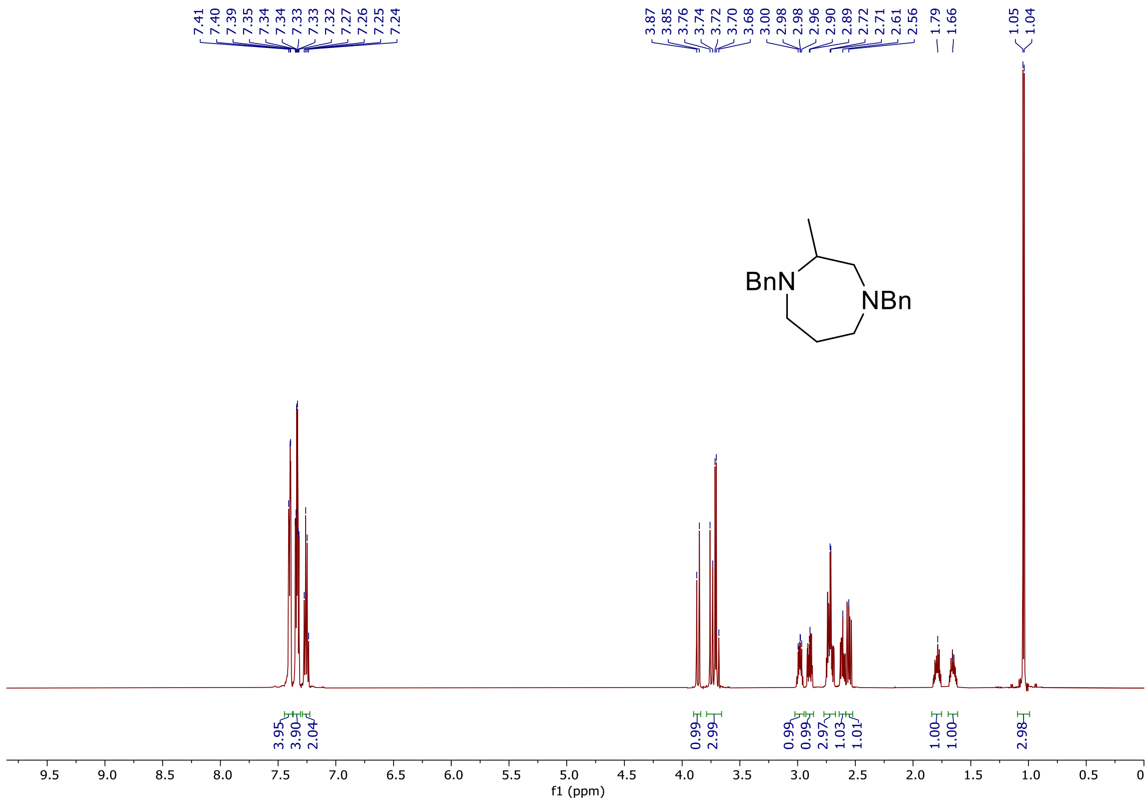

Figure S56. [1]H NMR (600 MHz) spectrum of **4b** at 25 °C in $CDCl_3$.

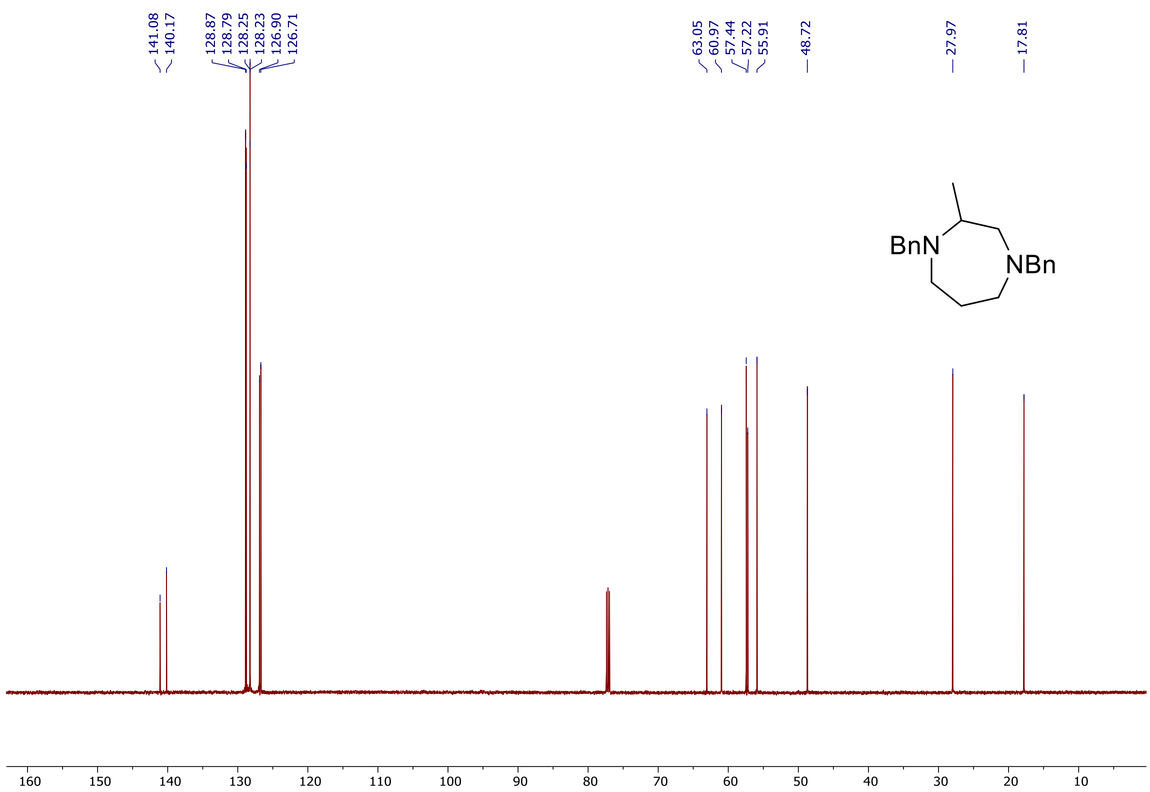

Figure S57. [13]C NMR (151 MHz) spectrum of **4b** at 25 °C in $CDCl_3$.

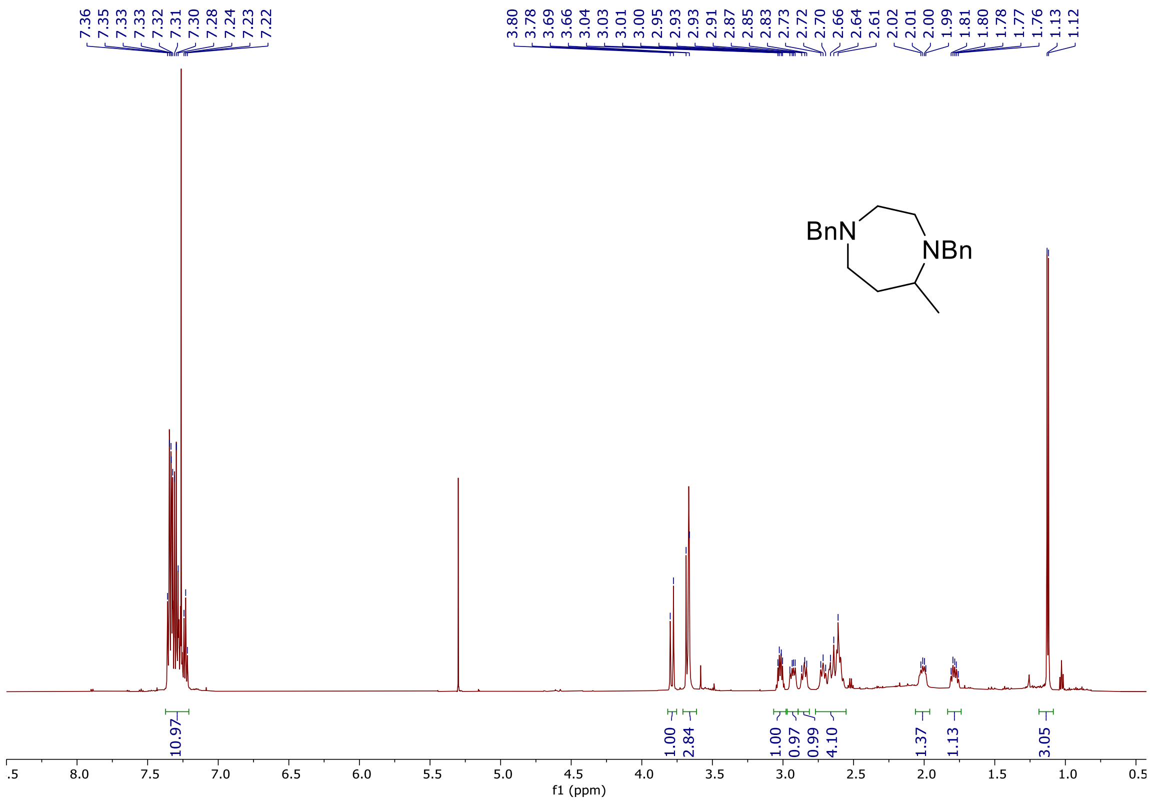

Figure S58. [1]H NMR (600 MHz) spectrum of **4c** at 25 °C in $CDCl_3$.

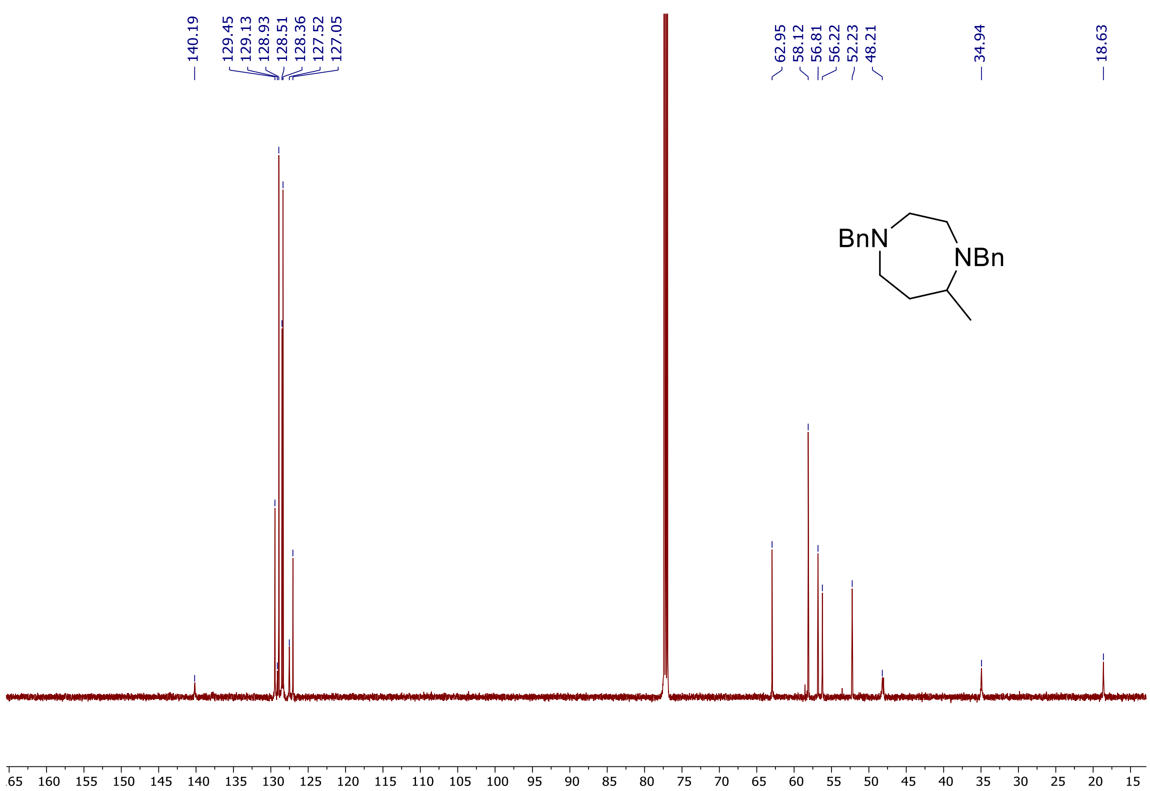

Figure S59. [13]C NMR (151 MHz) spectrum of **4c** at 25 °C in $CDCl_3$.

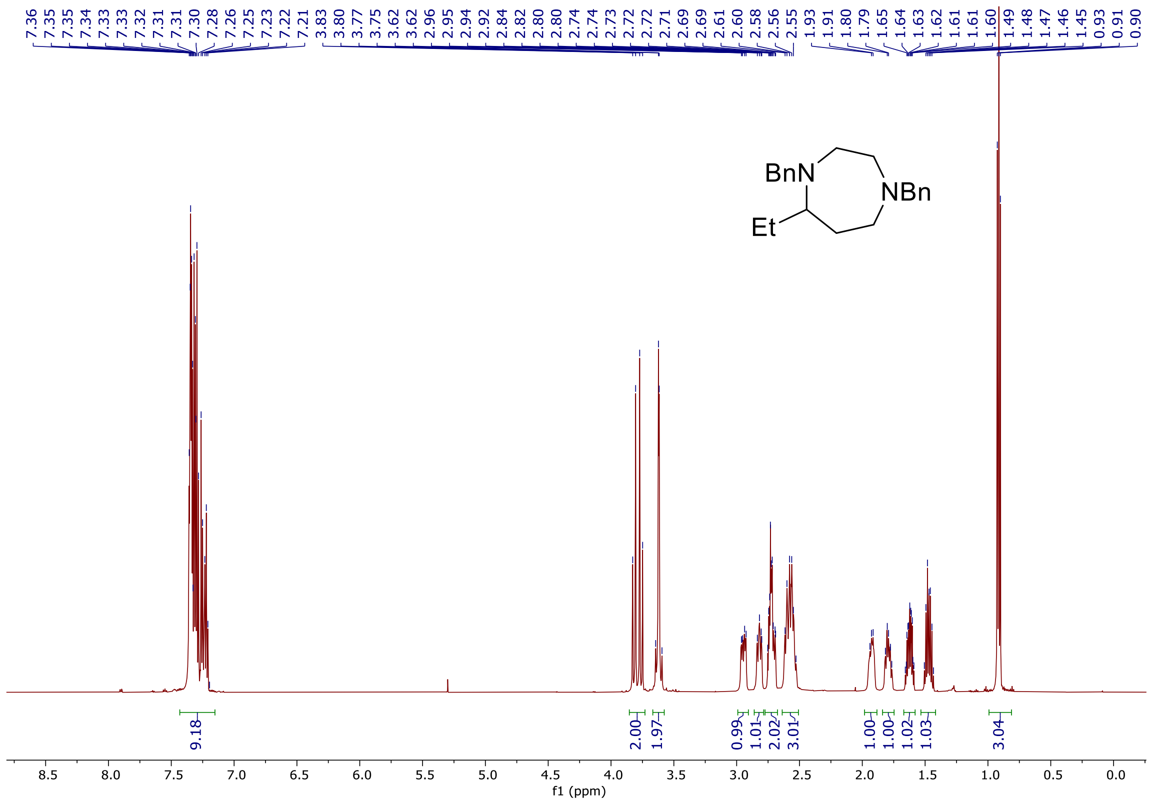

Figure S60. [1]H NMR (600 MHz) spectrum of **4d** at 25 °C in $CDCl_3$.

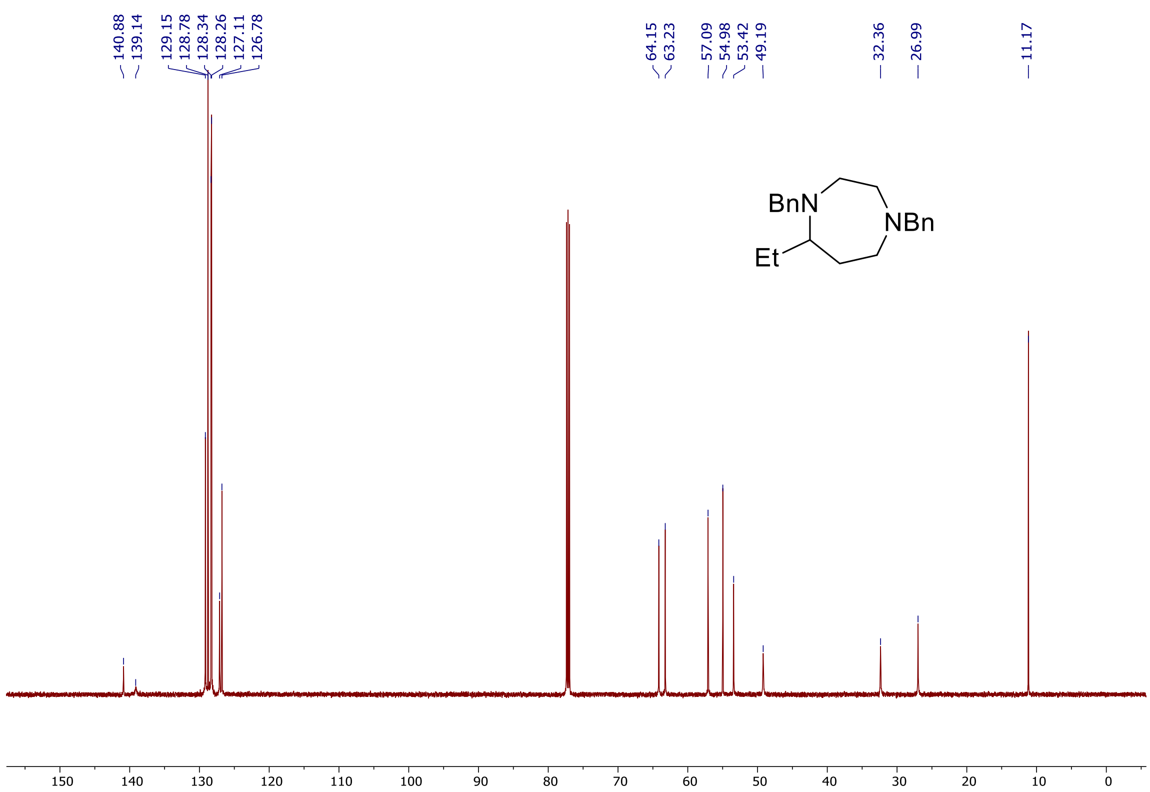

Figure S61. [13]C NMR (151 MHz) spectrum of **4d** at 25 °C in $CDCl_3$.

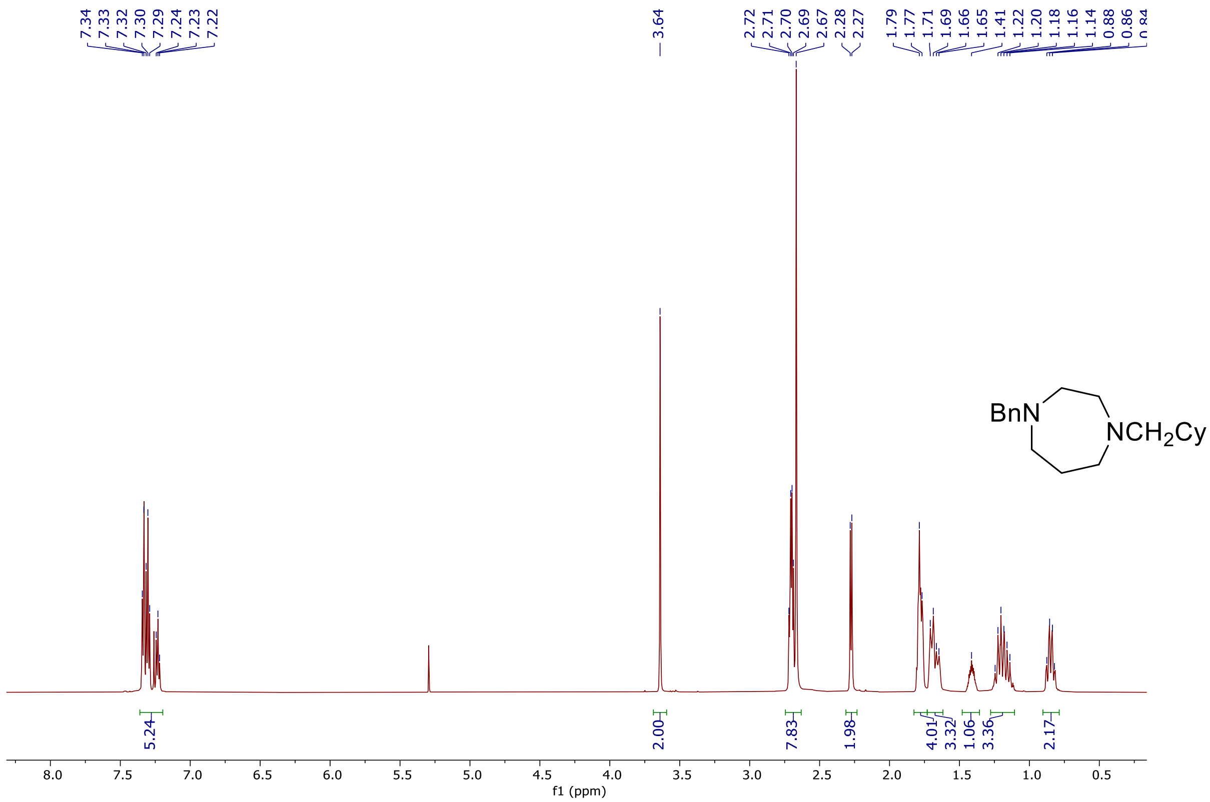

Figure S62. ^{1}H NMR (600 MHz) spectrum of **4e** at 25 °C in $CDCl_3$.

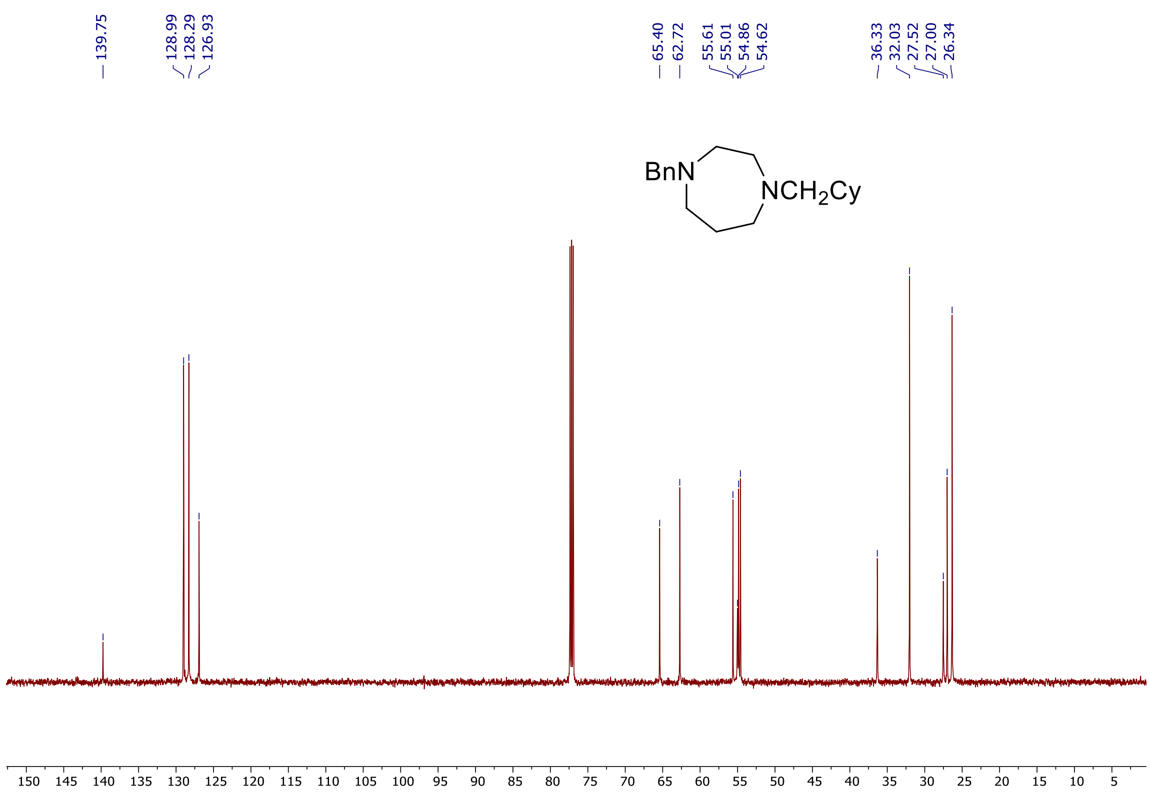

Figure S63. ^{13}C NMR (151 MHz) spectrum of **4e** at 25 °C in $CDCl_3$.

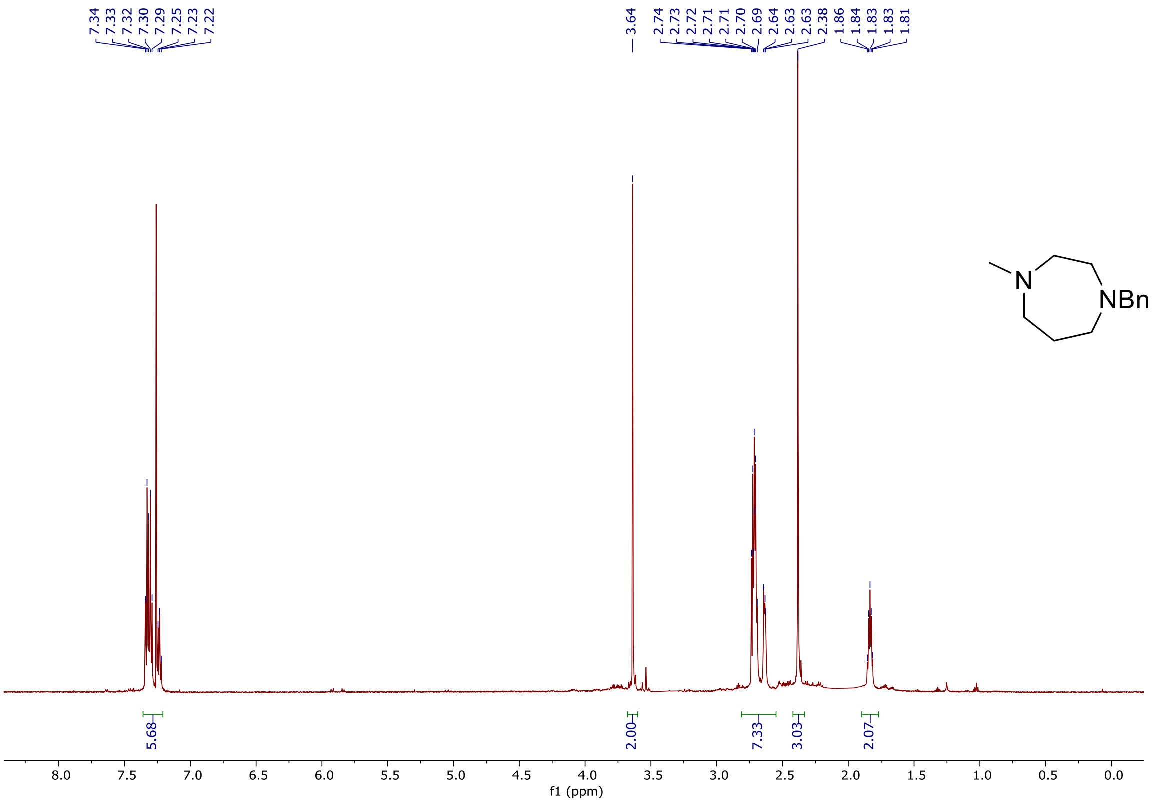

Figure S64. [1]H NMR (600 MHz) spectrum of **4f** at 25 °C in $CDCl_3$.

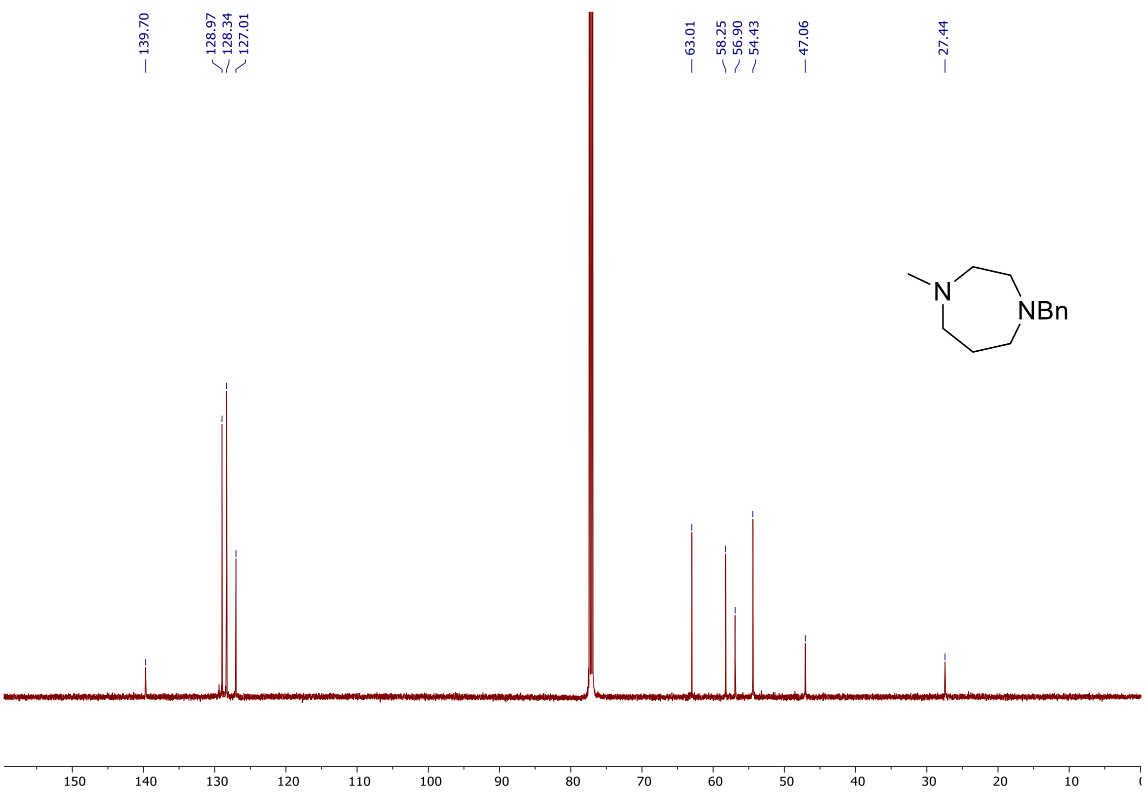

Figure S65. [13]C NMR (151 MHz) spectrum of **4f** at 25 °C in $CDCl_3$.

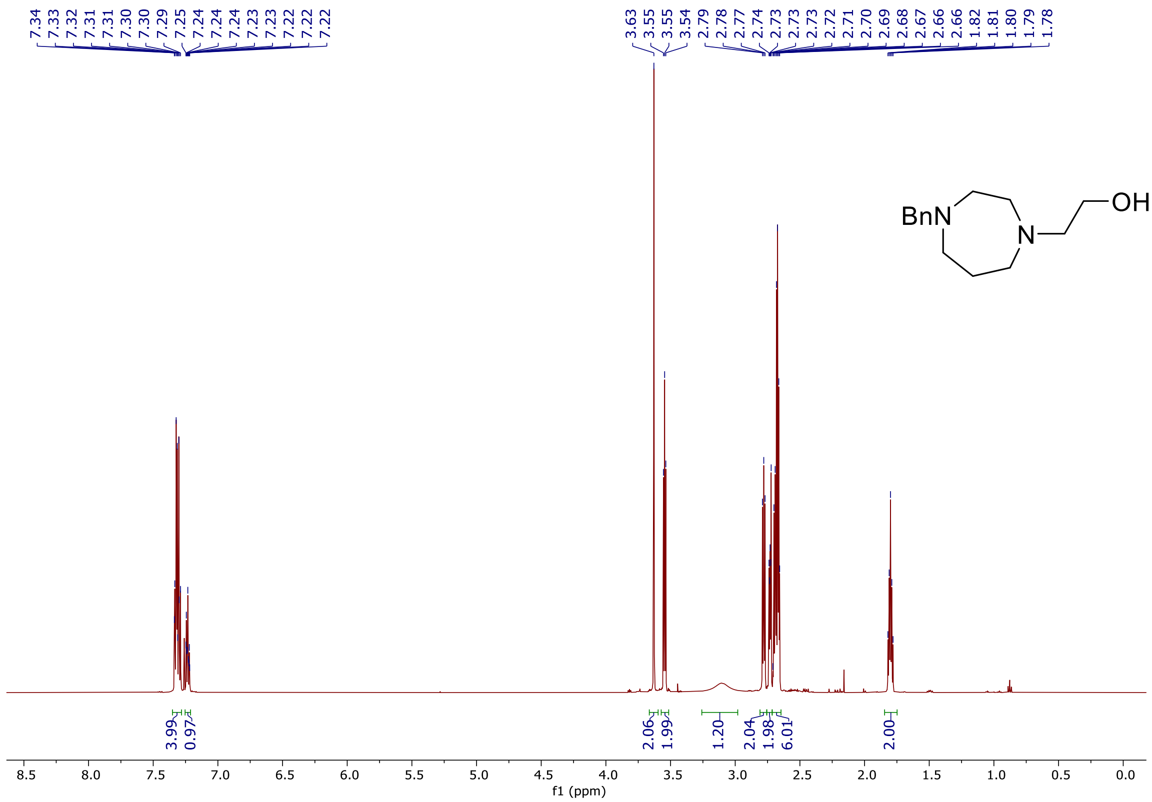

Figure S66. [1]H NMR (600 MHz) spectrum of **4i** at 25 °C in $CDCl_3$.

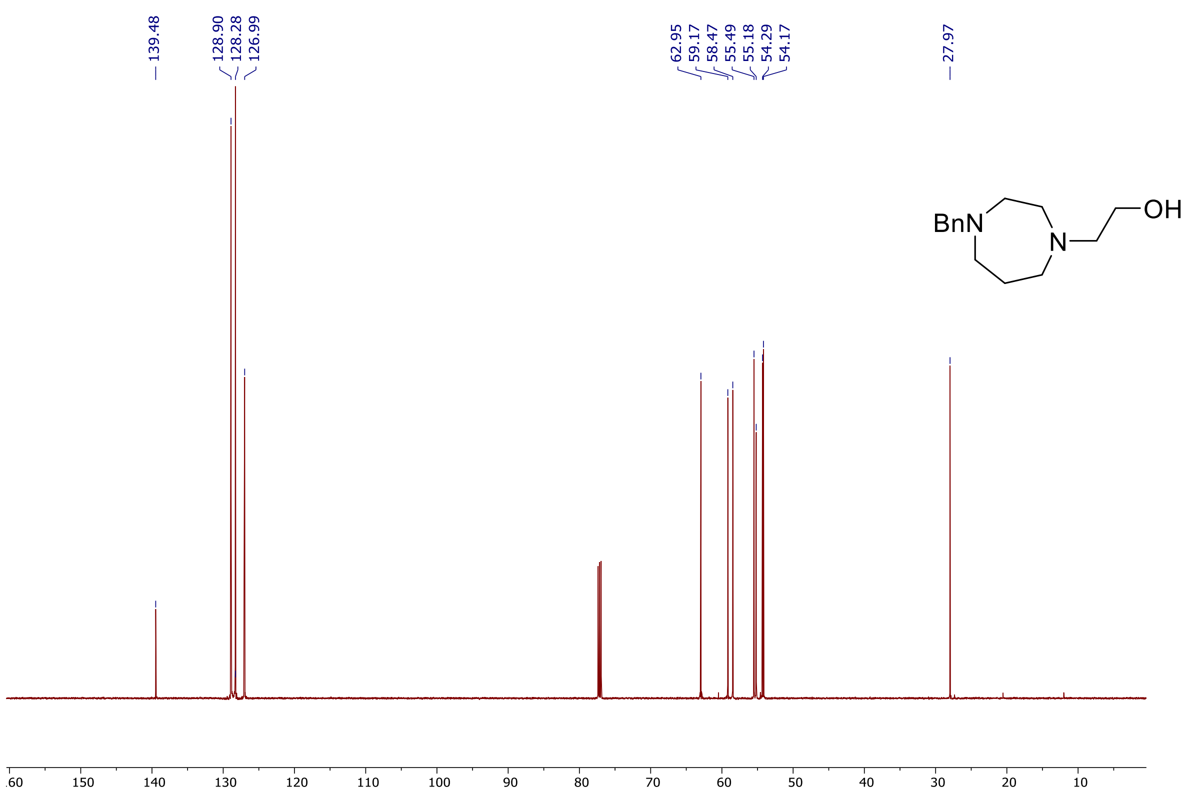

Figure S67. [13]C NMR (151 MHz) spectrum of **4i** at 25 °C in $CDCl_3$.

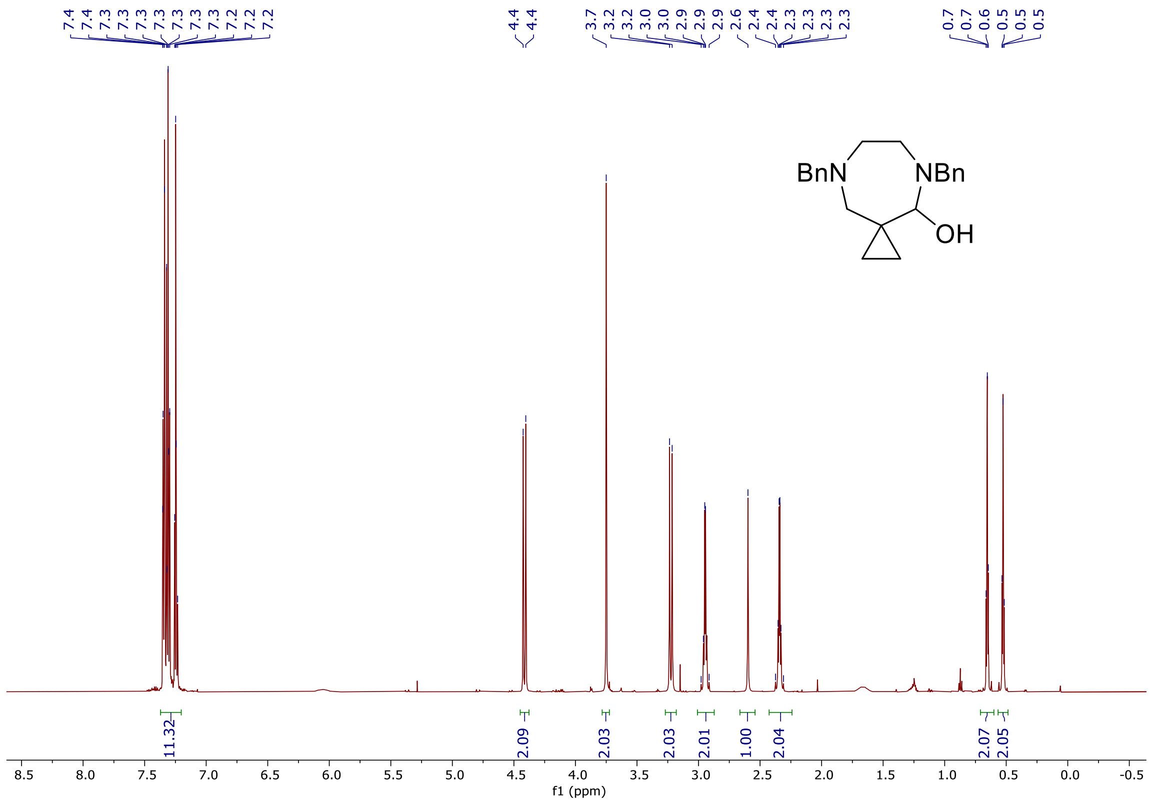

Figure S68. [1]H NMR (600 MHz) spectrum of **4j** at 25 °C in $CDCl_3$.

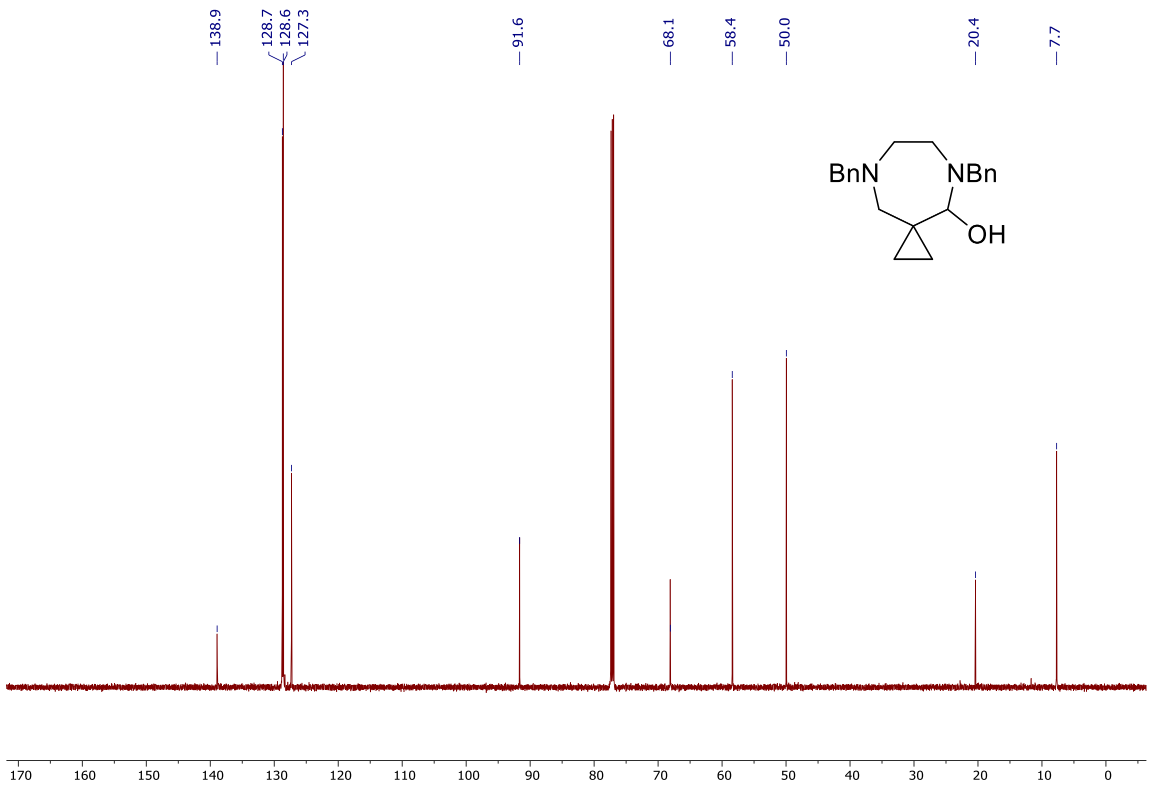

Figure S69. [13]C NMR (151 MHz) spectrum of **4j** at 25 °C in $CDCl_3$.

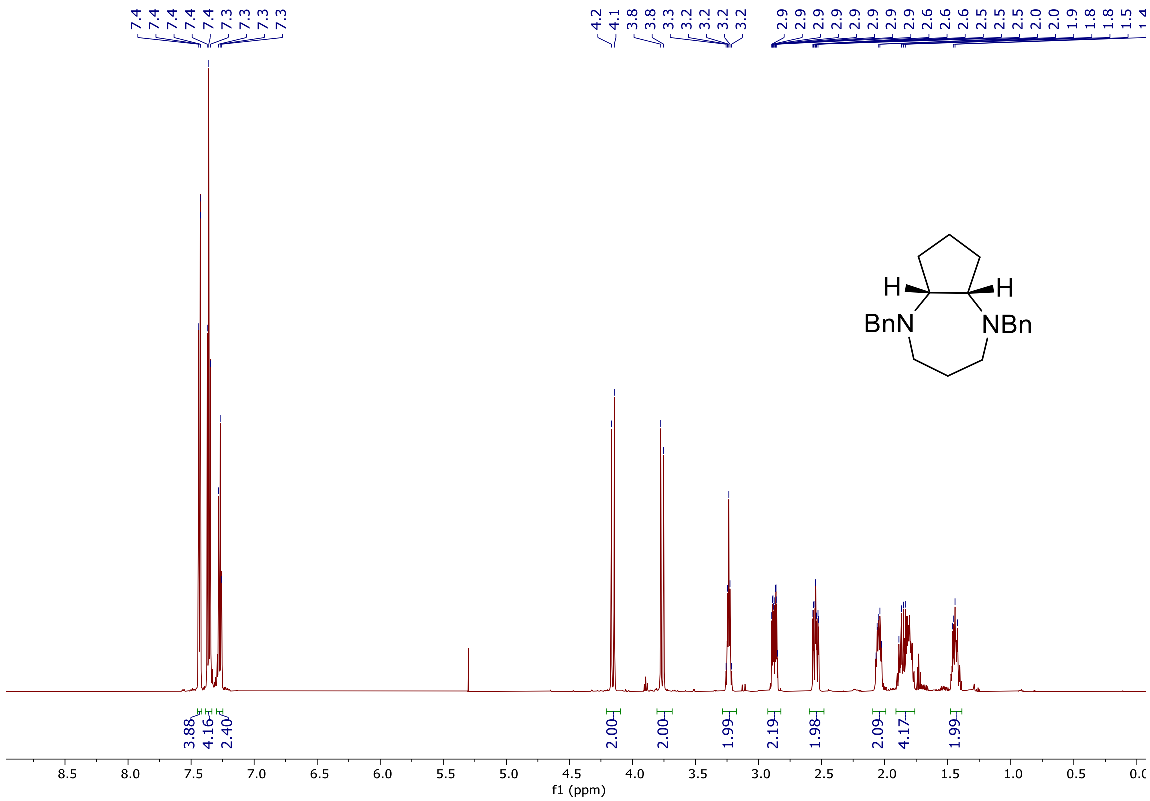

Figure S70. ^{1}H NMR (600 MHz) spectrum of **4k** at 25 °C in $CDCl_3$.

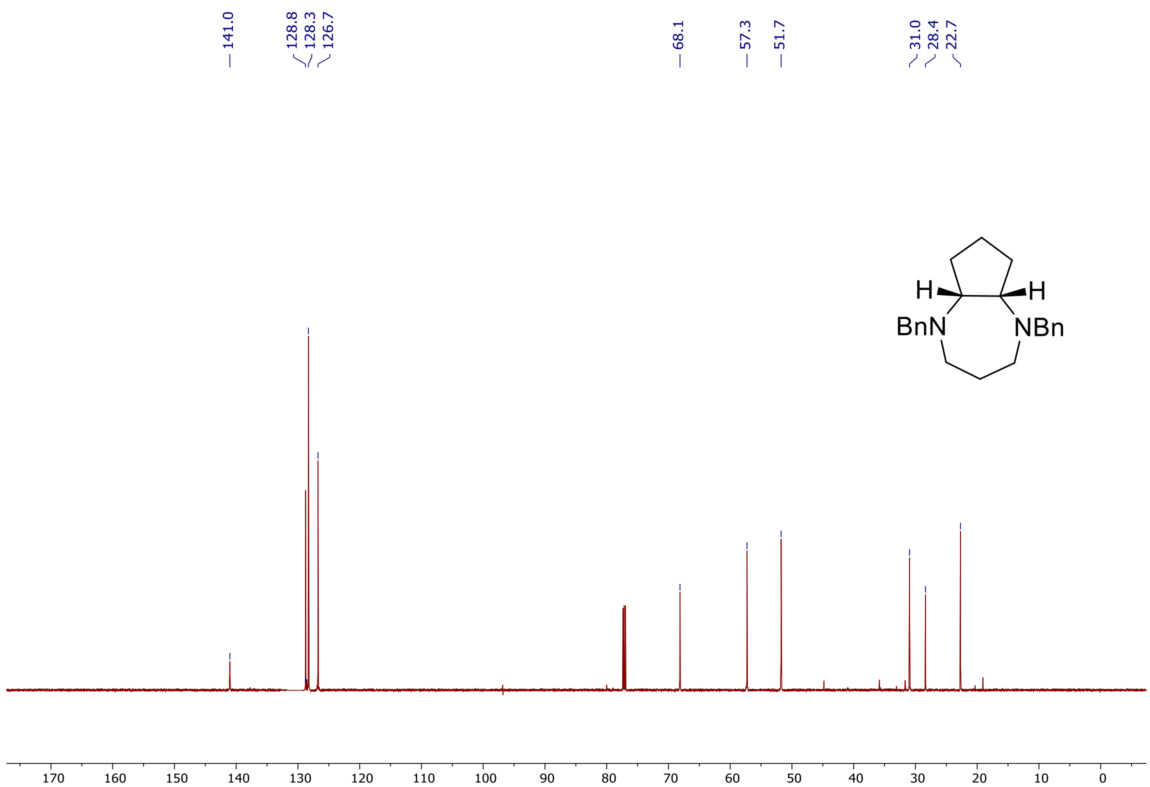

Figure S71. ^{13}C NMR (151 MHz) spectrum of **4k** at 25 °C in $CDCl_3$.

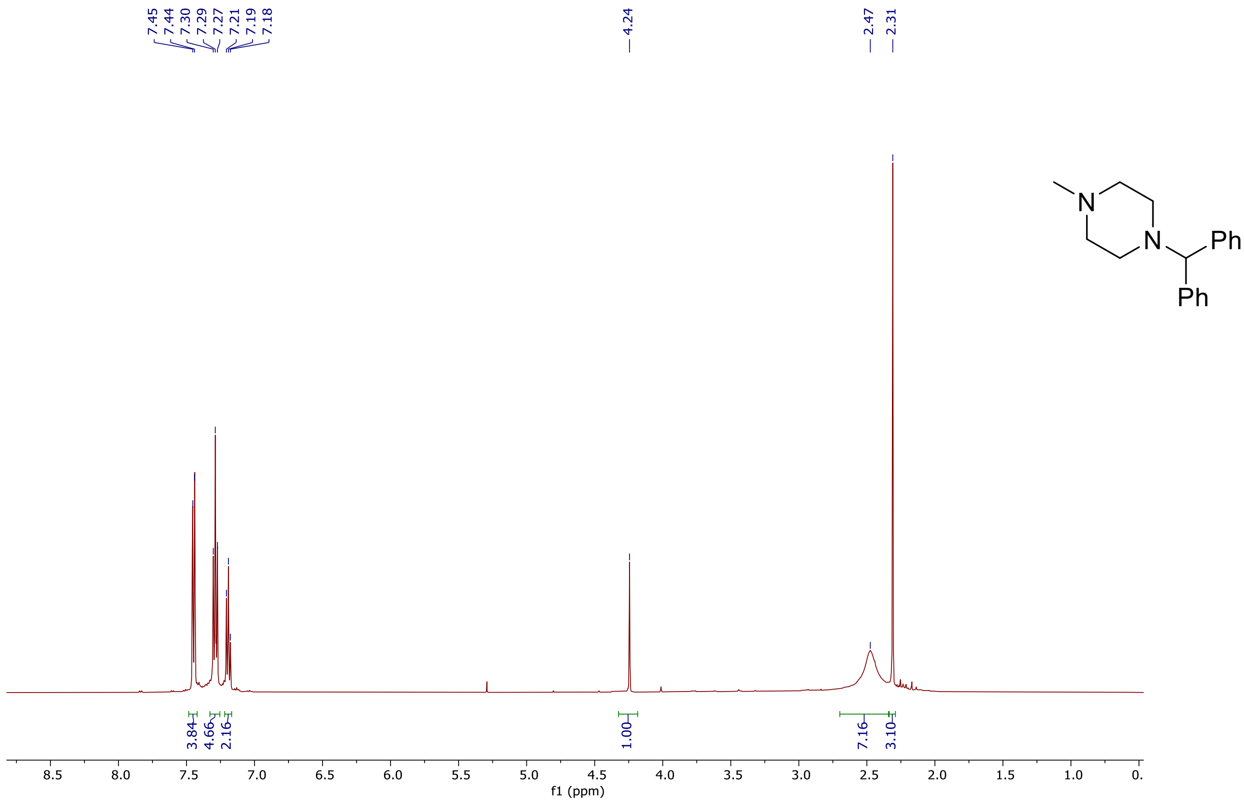

Figure S72. [1]H NMR (500 MHz) spectrum of **4l** at 25 °C in $CDCl_3$.

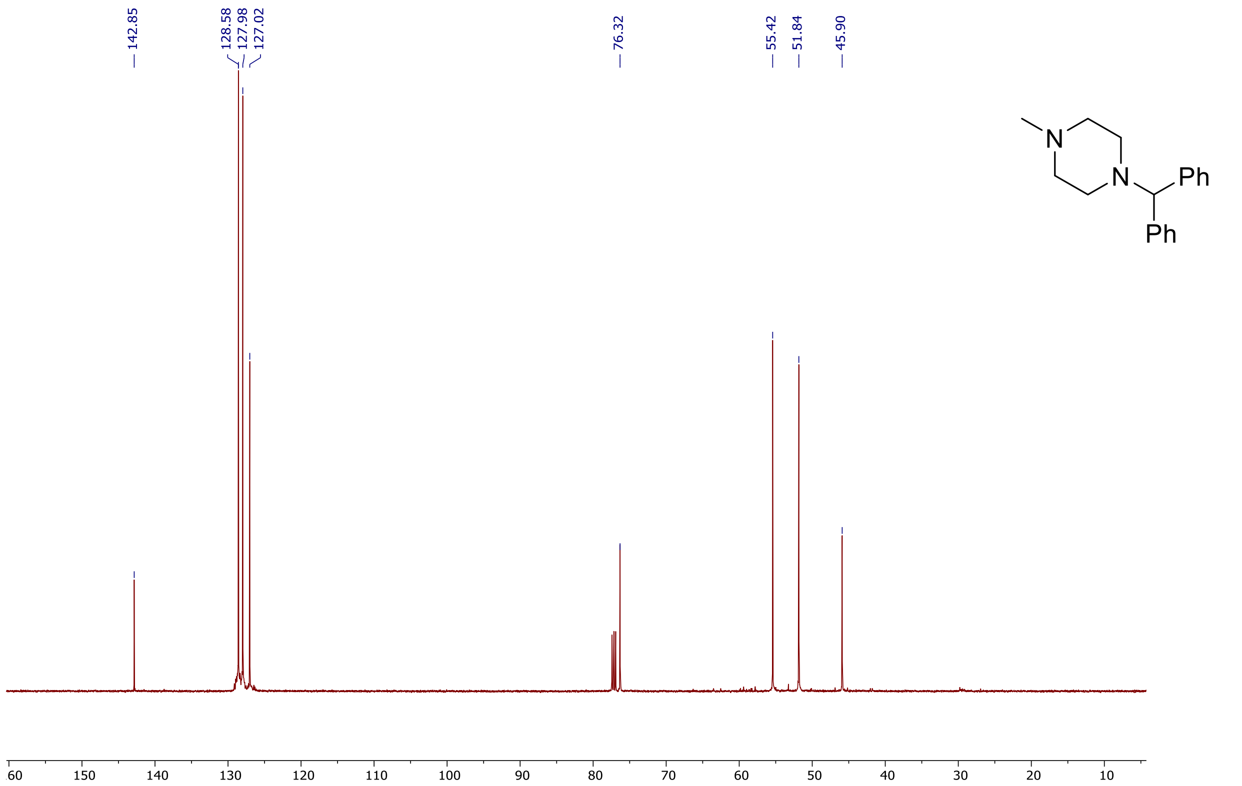

Figure S73. [13]C NMR (126 MHz) spectrum of **4l** at 25 °C in $CDCl_3$.

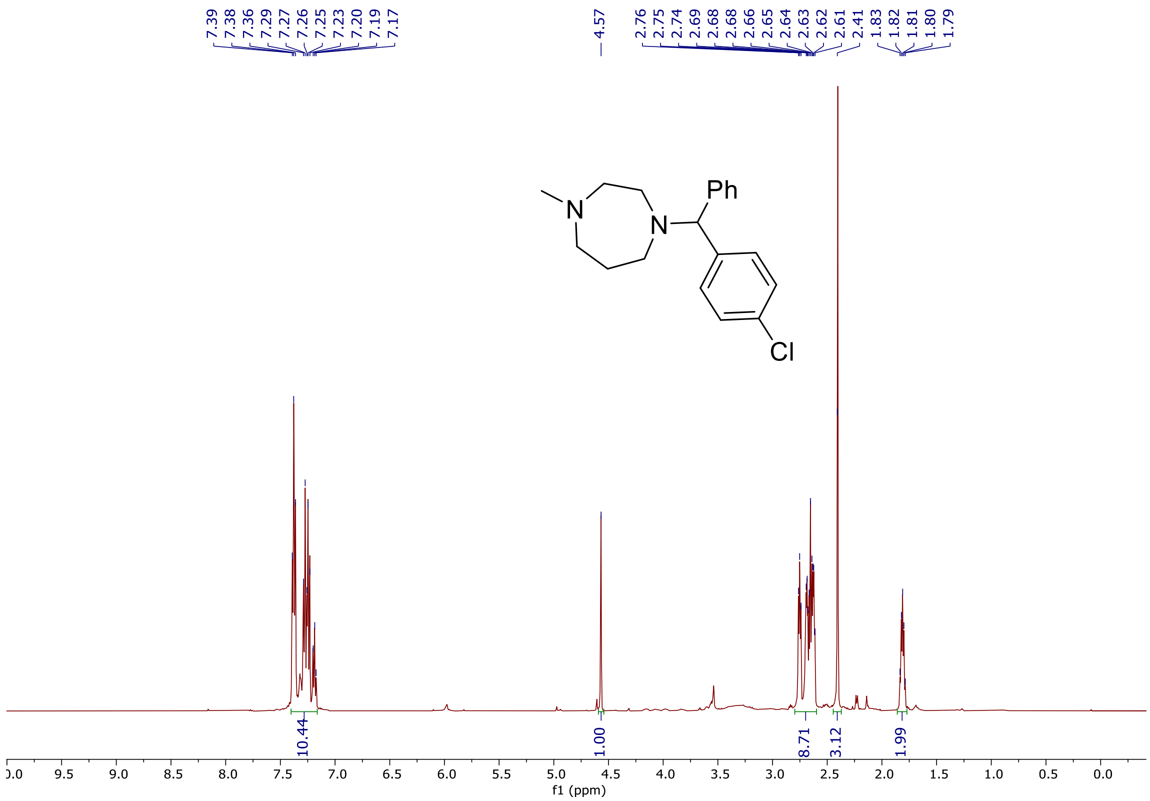

Figure S74. ^{1}H NMR (500 MHz) spectrum of **4m** at 25 °C in $CDCl_3$.

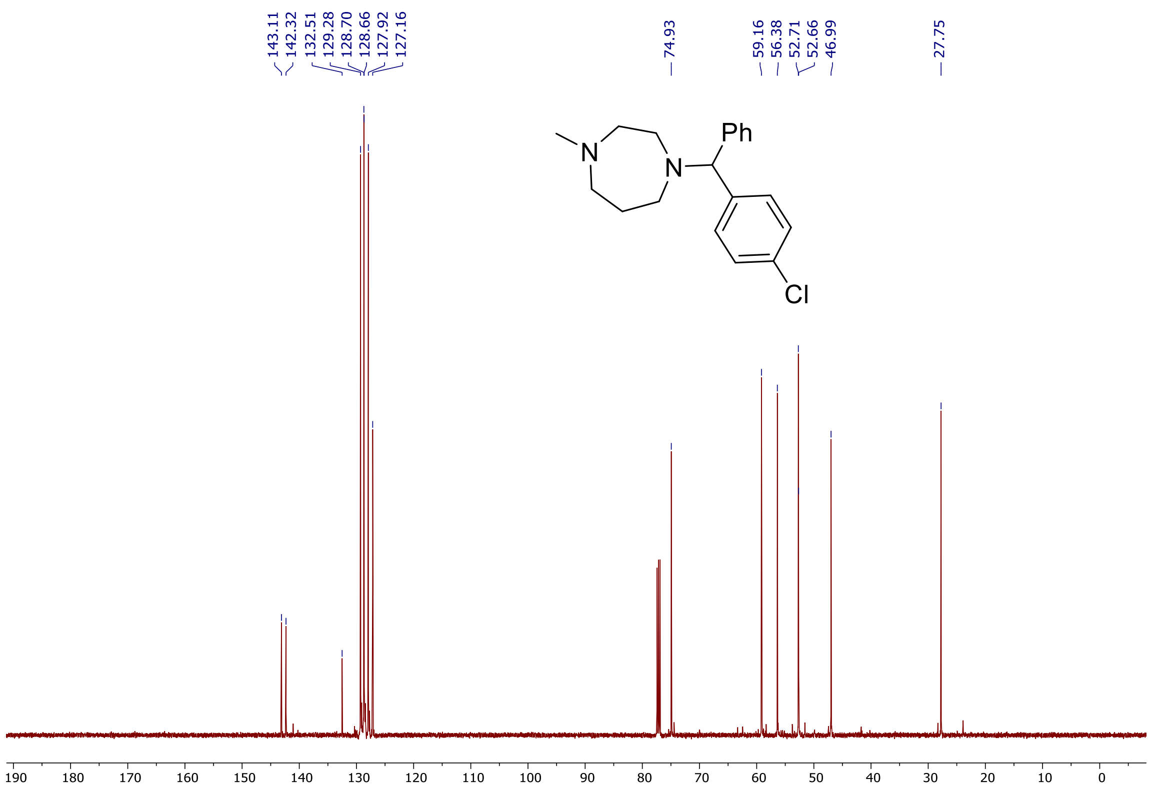

Figure S75. ^{13}C NMR (126 MHz) spectrum of **4m** at 25 °C in $CDCl_3$.

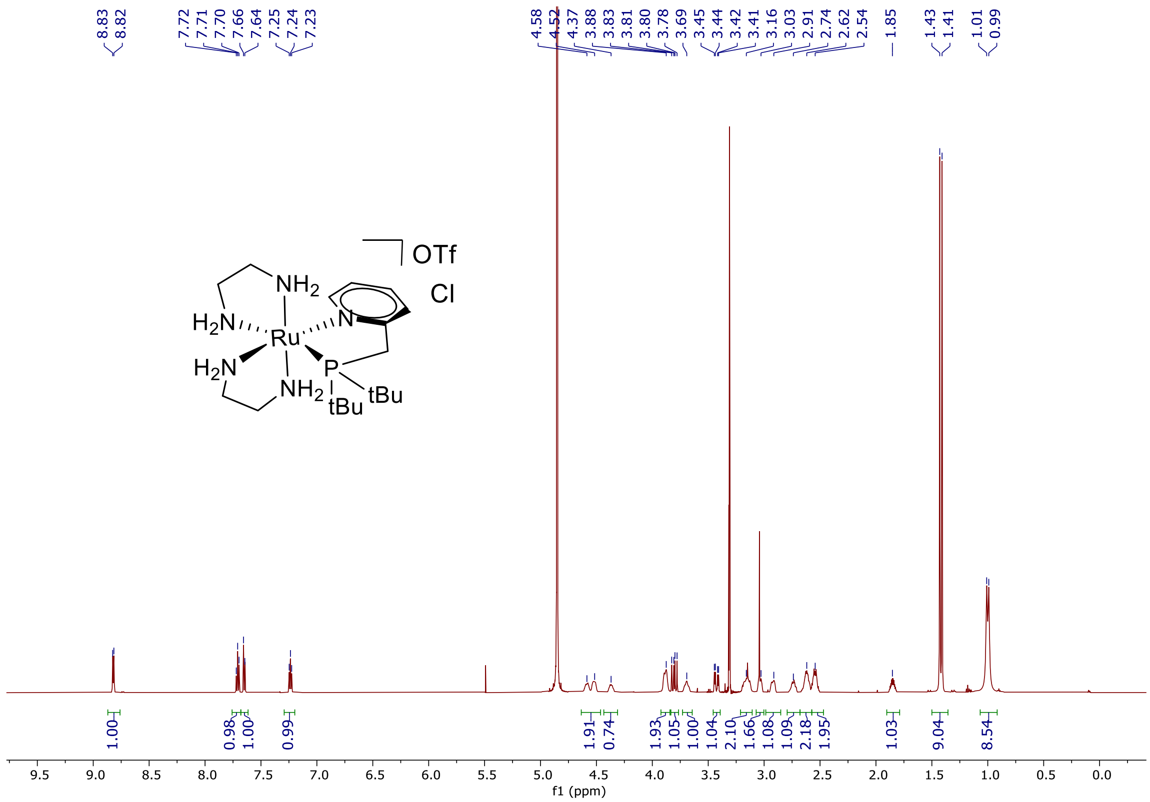

Figure S76. [1]H NMR (600 MHz) spectrum of complex **13** at 25 °C in MeOD.

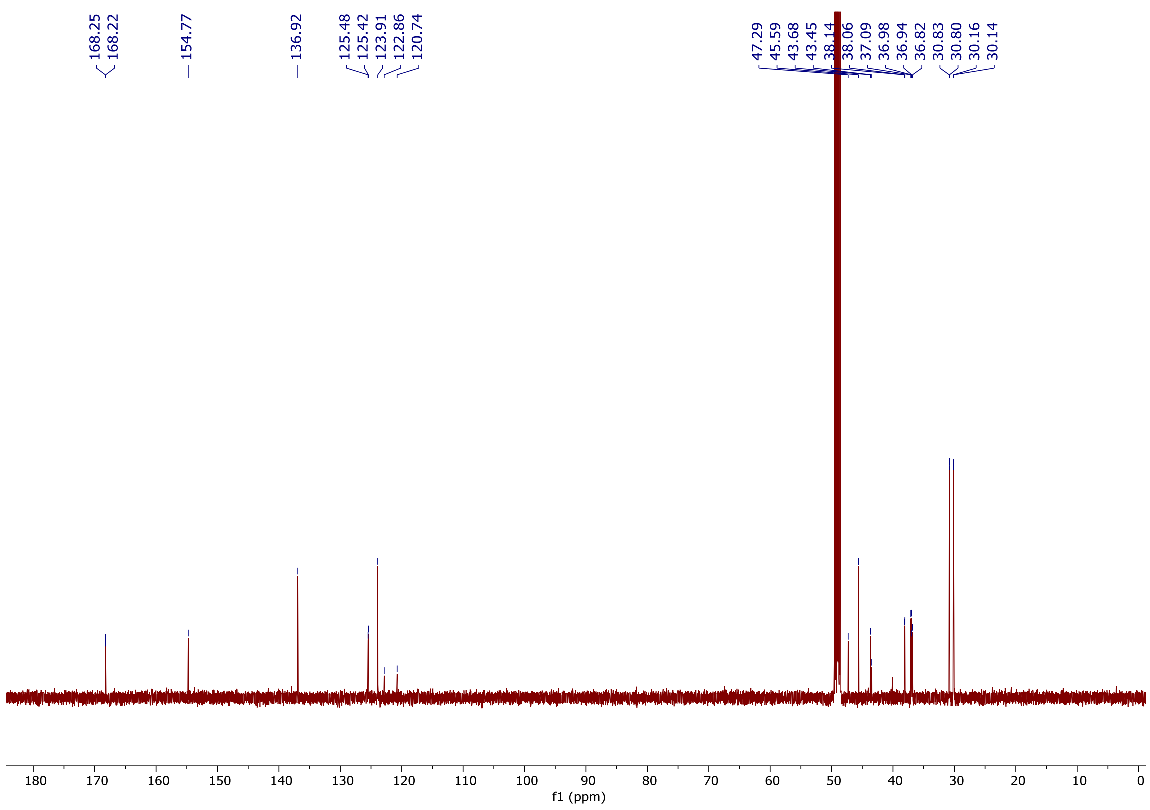

Figure S77. [13]C NMR (151 MHz) spectrum of complex **13** at 25 °C in MeOD.

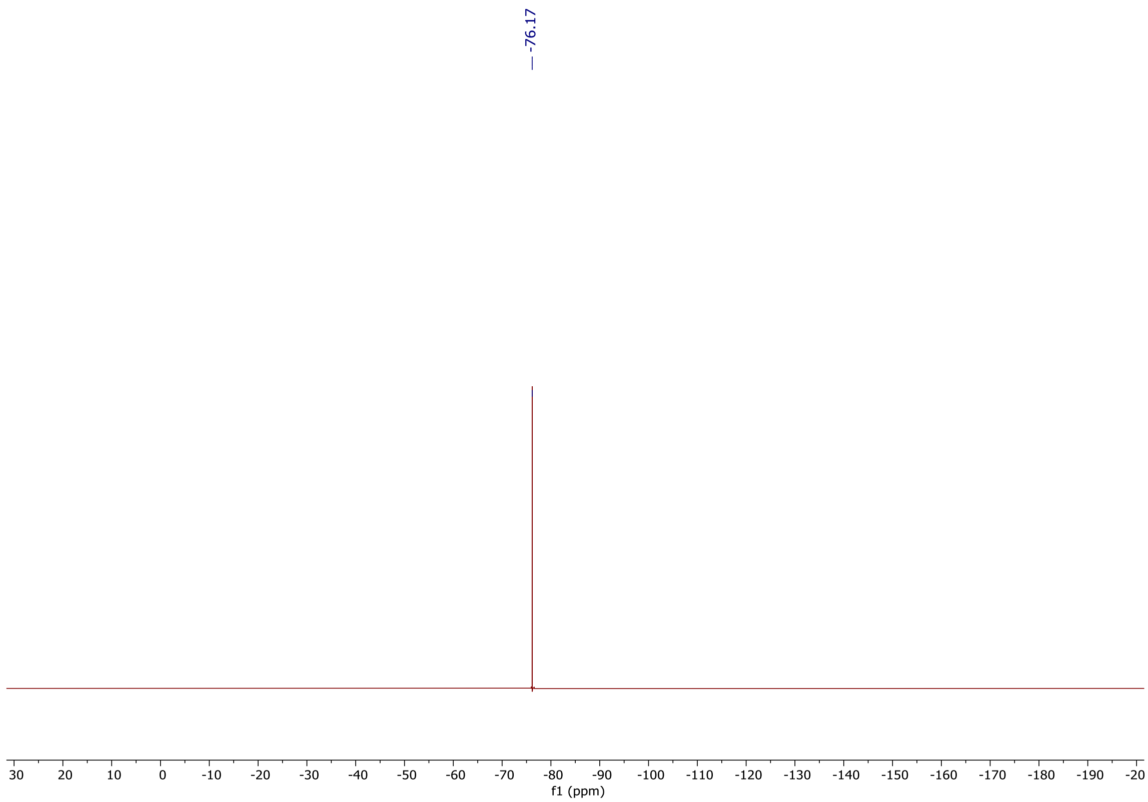

Figure S78. ^{19}F NMR (564 MHz) spectrum of complex **13** at 25 °C in MeOD.

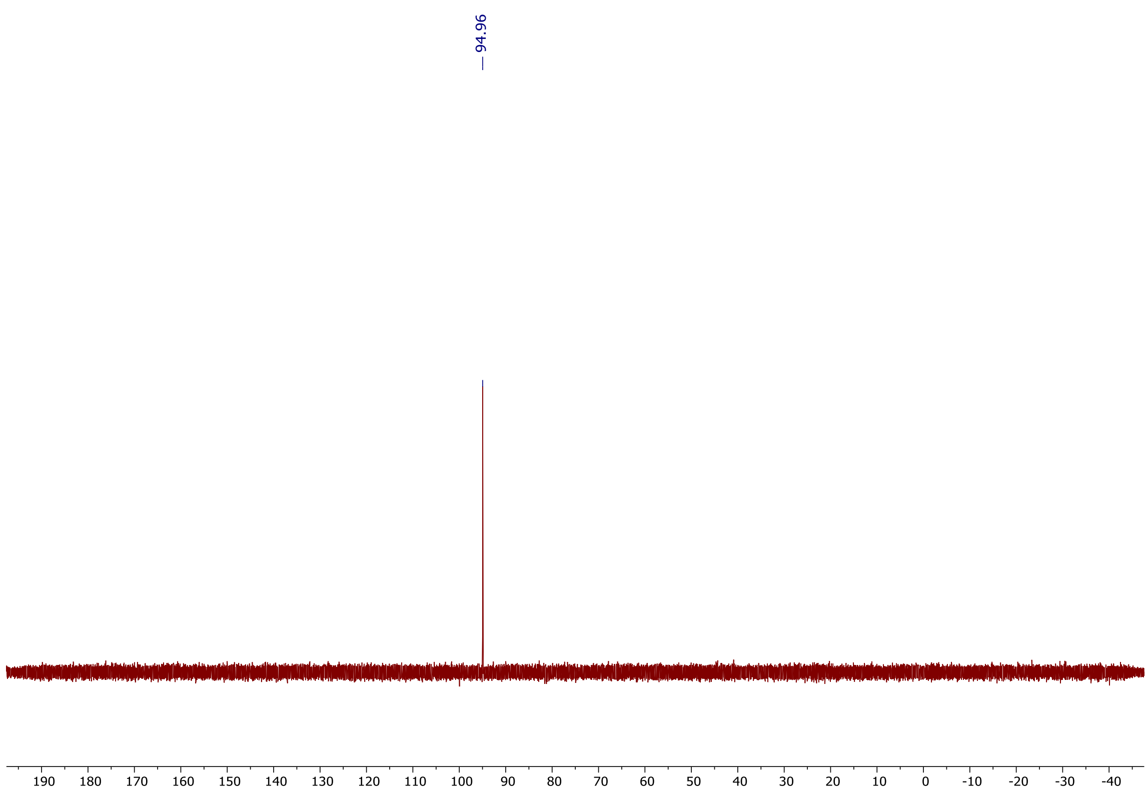

Figure S79. ^{31}P NMR (243 MHz) spectrum of complex **13** at 25 °C in MeOD.

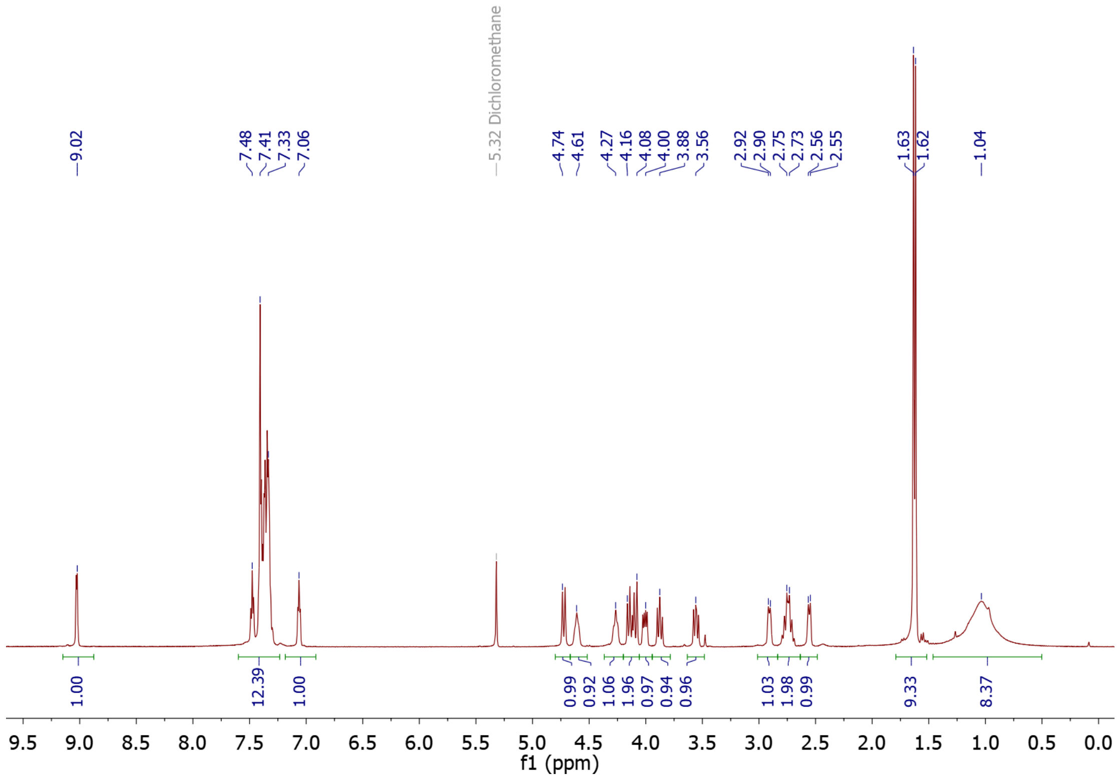

Figure S80. [1]H NMR spectrum of complex **13a** in CD_2Cl_2 at 25 °C.

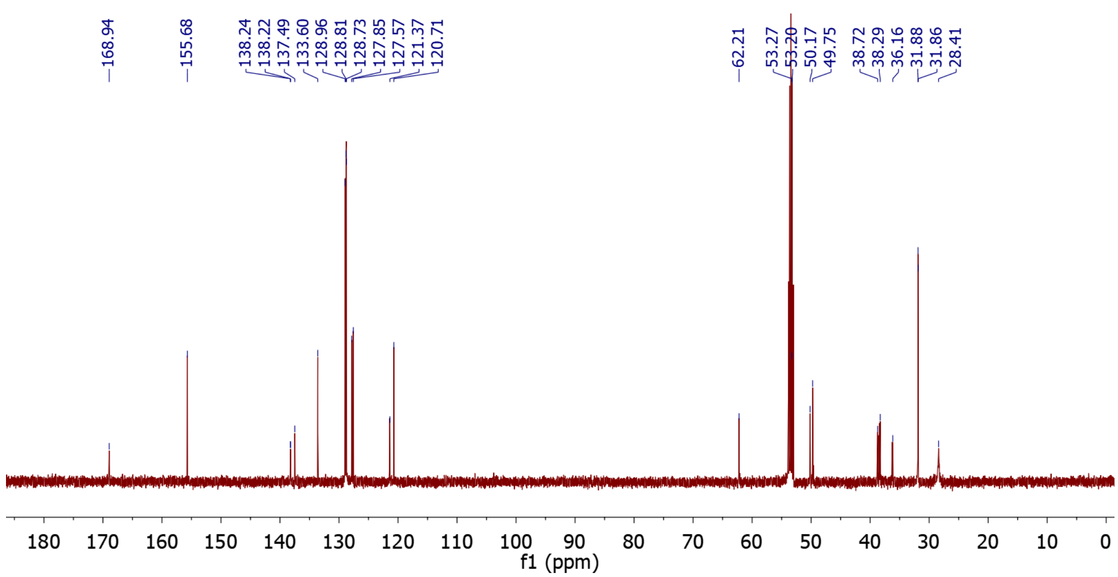

Figure S81. [13]C{[1]H} NMR spectrum of complex **13a** in CD_2Cl_2 at 25 °C.

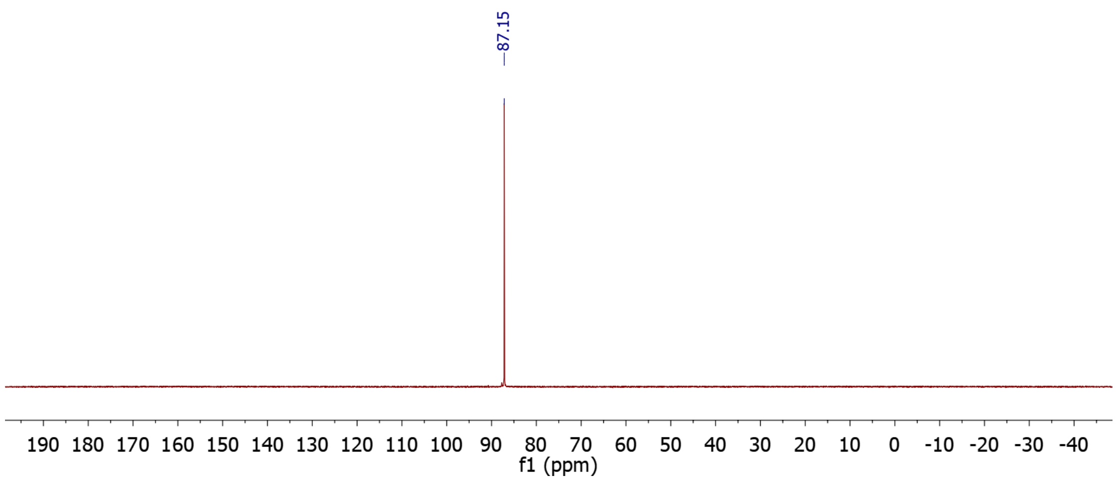

Figure S82. $^{31}P\{^{1}H\}$ NMR spectrum of complex **13a** in CD_2Cl_2 at 25 ºC.

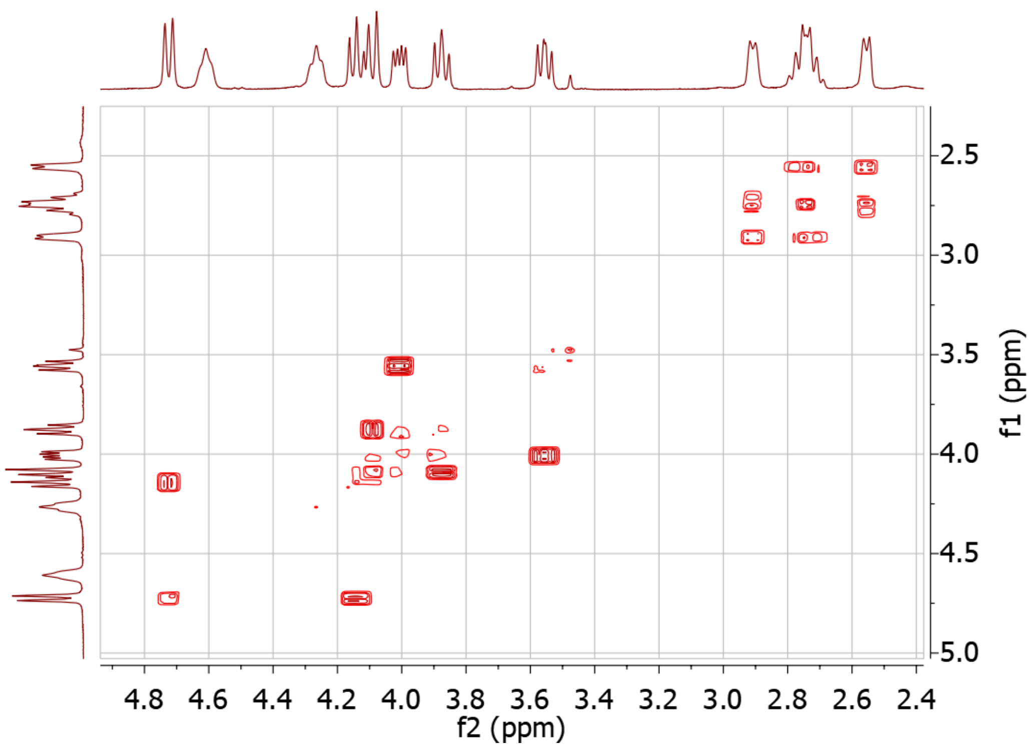

Figure S83. COSY NMR spectrum of complex **13a** in CD_2Cl_2 at 25 ºC.

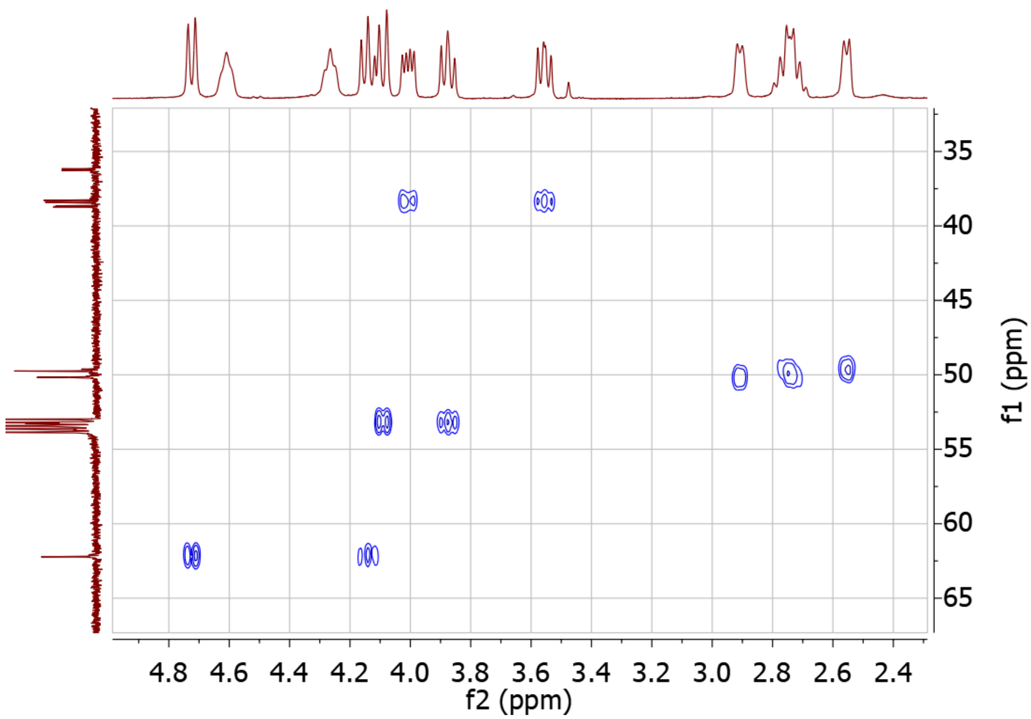

Figure S84. ^{1}H–^{13}C HSQC NMR spectrum of complex **13a** in CD_2Cl_2 at 25 ^{o}C.

XIII. Crystal Description

*Compound **4k***

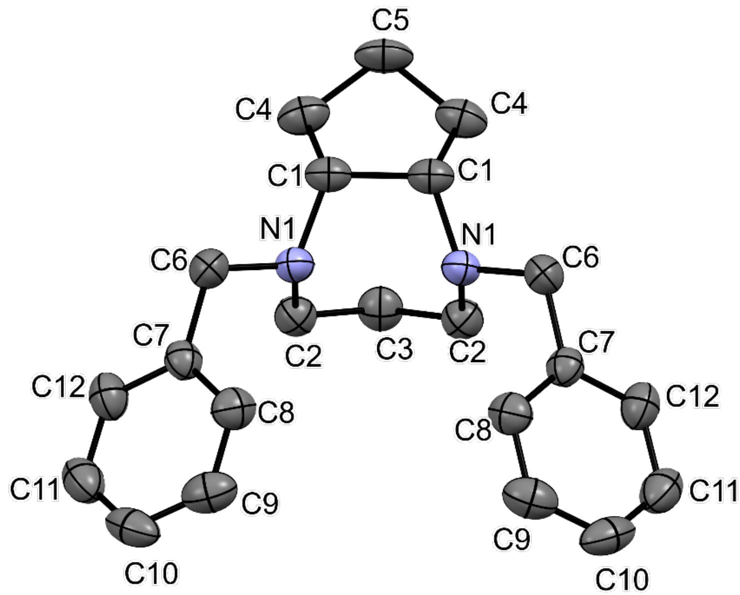

Figure S85. Molecular structure of **4k** shown with 50% ellipsoids (hydrogen atoms are omitted for clarity).

Identification code	AT 367 PF6_auto
Empirical formula	$C_{22}H_{28}F_6N_2P$
Formula weight	465.445
Temperature/K	100.0(2)
Crystal system	monoclinic
Space group	Cm
a/Å	10.2912(8)
b/Å	13.4966(12)
c/Å	7.8306(6)
α/°	90
β/°	97.280(8)
γ/°	90
Volume/Å^3	1078.87(15)
Z	2
ρ_{calc}g/cm^3	1.433
μ/mm^{-1}	1.707
F(000)	488.5
Crystal size/mm^3	0.144 × 0.05 × 0.025
Radiation	Cu Kα (λ = 1.54184)
2Θ range for data collection/°	10.86 to 153.78
Index ranges	$-12 \leq h \leq 12$, $-13 \leq k \leq 16$, $-5 \leq l \leq 9$
Reflections collected	3750

Independent reflections	1351 [R_{int} = 0.0503, R_{sigma} = 0.0378]
Data/restraints/parameters	1351/2/151
Goodness-of-fit on F^2	1.048
Final R indexes [I>=2σ (I)]	R_1 = 0.0527, wR_2 = 0.1435
Final R indexes [all data]	R_1 = 0.0584, wR_2 = 0.1487
Largest diff. peak/hole / e Å^{-3}	0.33/-0.20
Flack parameter	0.04(4)
CCDC#	2217365

*<u>Complex **13**</u>*

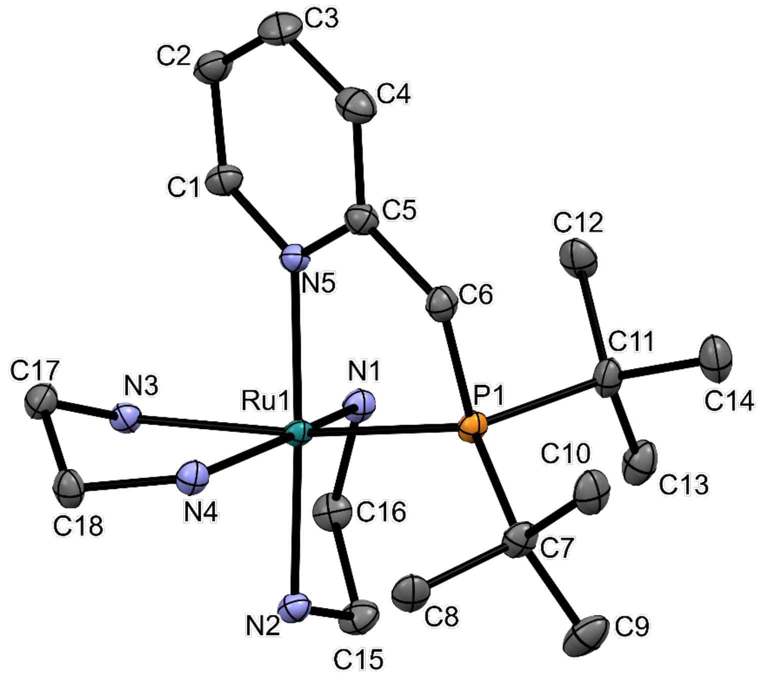

Figure S86. Molecular structure of **13** shown with 50% ellipsoids (hydrogen atoms are omitted for clarity).

Identification code	final
Empirical formula	$C_{20}H_{42}Cl_3F_3N_5O_3PRuS$
Formula weight	728.03
Temperature/K	100.0(2)
Crystal system	triclinic
Space group	P-1
a/Å	8.4163(2)
b/Å	10.8725(2)
c/Å	17.9439(4)
α/°	92.663(2)
β/°	90.426(2)

γ/°	105.701(2)
Volume/Å^3	1578.66(6)
Z	2
ρ_{calc}g/cm^3	1.532
μ/mm^{-1}	0.915
F(000)	748.0
Crystal size/mm^3	0.081 × 0.063 × 0.039
Radiation	Mo Kα (λ = 0.71073)
2Θ range for data collection/°	5.028 to 66.778
Index ranges	$-12 \le h \le 11$, $-15 \le k \le 16$, $-26 \le l \le 27$
Reflections collected	48619
Independent reflections	10744 [R_{int} = 0.0735, R_{sigma} = 0.0728]
Data/restraints/parameters	10744/6/340
Goodness-of-fit on F^2	1.048
Final R indexes [I>=2σ (I)]	R_1 = 0.0489, wR_2 = 0.1153
Final R indexes [all data]	R_1 = 0.0740, wR_2 = 0.1240
Largest diff. peak/hole / e Å^{-3}	1.79/-1.23
CSD#	2217364

Complex ***13a***

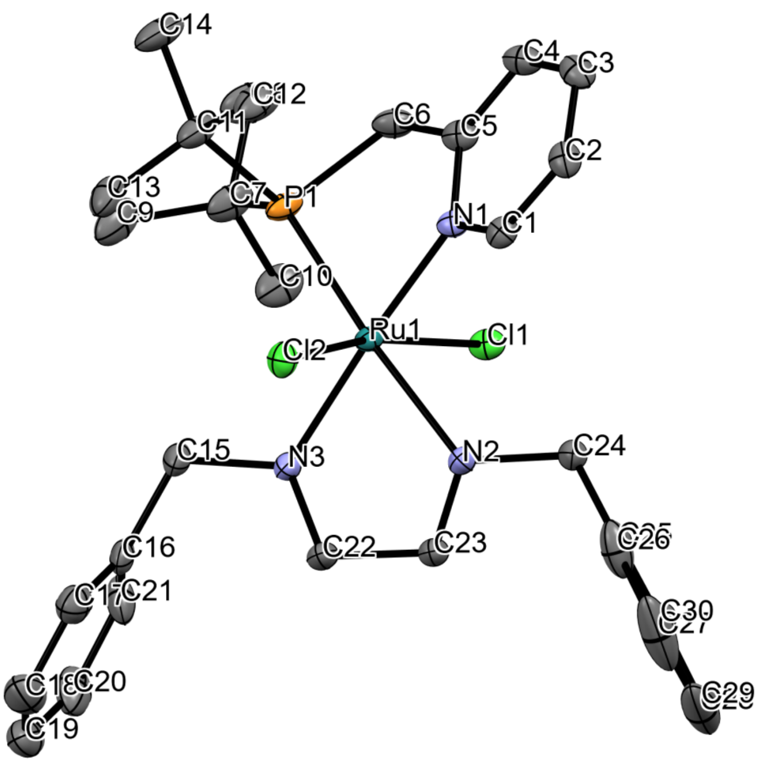

Figure S87. Molecular structure of **13a** shown with 50% ellipsoids (hydrogen atoms are omitted for clarity).

Identification code	RuCl2(PN)(NN)
Empirical formula	$C_{30}H_{44}Cl_2N_3PRu$
Formula weight	649.62
Temperature/K	102(4)
Crystal system	monoclinic
Space group	$P2_1/c$
a/Å	24.02190(10)
b/Å	13.01150(10)
c/Å	49.0389(3)
α/°	90
β/°	93.6090(10)
γ/°	90
Volume/Å^3	15297.25(16)
Z	20
ρ_{calc}g/cm^3	1.410
μ/mm^{-1}	6.420
F(000)	6760.0
Crystal size/mm^3	0.19 × 0.12 × 0.06
Radiation	Cu Kα (λ = 1.54184)
2Θ range for data collection/°	5.32 to 155.07
Index ranges	$-30 \leq h \leq 27$, $-16 \leq k \leq 15$, $-62 \leq l \leq 58$
Reflections collected	280003
Independent reflections	31959 [R_{int} = 0.0570, R_{sigma} = 0.0273]
Data/restraints/parameters	31959/0/1697
Goodness-of-fit on F^2	1.035
Final R indexes [I>=2σ (I)]	R_1 = 0.0315, wR_2 = 0.0857
Final R indexes [all data]	R_1 = 0.0390, wR_2 = 0.0897
Largest diff. peak/hole / e Å^{-3}	0.68/-0.82
CSD#	2241666

XIV. References

1. Beddie, C.; Wei, P.; Douglas, S. Titanium Pyridyl-Phosphinimide Complexes–Synthesis, Structure and Ethylene Polymerization Catalysis. *Can. J. Chem.* **2006**, *84* (5), 755-761.
2. Celaje, J. J. A.; Zhang, X.; Zhang, F.; Kam, L.; Herron, J. R. A Base and Solvent-Free Ruthenium-Catalyzed Alkylation of Amines. *ACS Catal.* **2017**, *7* (2), 1136-1142.
3. Szewczyk, M.; Stanek, F.; Bezlada, A.; Mlynarski, J. Zinc Acetate-Catalyzed Enantioselective Hydrosilylation of Ketones. *Adv. Synth. Catal.* **2015**, *357*, 3727-3731.
4. Jiang, X.; Lo, P.; Tsang, Y.; Yeung, S.; Fong, W.; Ng, D. Phthalocyanine–Polyamine Conjugates as pH-Controlled Photosensitizers for Photodynamic Therapy. *Chem. Eur. J.* **2010**, *16* (16), 4777-4783.
5. Cortes, S.; Kohn, H. Selective Reductions of 3-Substituted Hydantoins to 4-Hydroxy -2-imidazolidinones and Vicinal Diamines. *J. Org. Chem.* **1983**, *48* (13), 2246-2254.

6. Polat, D.; Brzezinski, D.; Beauchemin, A. Formation of Complex Hydrazine Derivatives via Aza-Lossen Rearrangement. *Org. Lett.* **2019**, *21* (12), 4849-4852.
7. Ralambomanana, D.; Razafimahefa-Ramilison, D.; Rakotohova, A.; Maugein, J.; Pélinski, L. Synthesis and Antitubercular Activity of Ferrocenyl Diaminoalcohols and Diamines. *Bioorg. Med. Chem.* **2008**, *16* (21), 9546-9553.
8. Rais, E.; Flörke, U.; Wilhelm, R. Synthesis and Investigation of New Cyclic Haloamidinium Salts. *Z. Naturforsch. B.* **2016**, *71* (6), 667-676.
9. Roush, W.; Grover, P. *N,N'*-Bis(2,2,2-trifluoroethyl)-*N,N'*-Ethylenetartramide: An Improved Chiral Auxiliary for the Asymmetric Allylboration Reaction. *J. Org. Chem.* **1995**, *60* (12), 3806-3813.
10. King, D.; Firestone, R.; Dubowchik, G. Preparation of Branched Peptide Linkers. WO 9819705 A1, 1998. Provided by SciFinder, 1998:323158 (accessed 2021-09-06).
11. Upadhyaya, D.; Barge, A.; Stefania, R.; Cravotto, G. Efficient, Solventless *N*-Boc Protection of Amines Carried out at Room Temperature Using Sulfamic Acid as Recyclable Catalyst. *Tetrahedron Lett.* **2007**, *48* (47), 8318-8322.
12. Shirini, F.; Jolodar, O.; Seddighi, M.; Borujeni, H. Preparation, Characterization and Application of Succinimidinium Hydrogensulfate ([H-Suc]HSO_4) as an Efficient Ionic Liquid Catalyst for the *N*-Boc Protection of Amines. *RSC Adv*. **2015**, 5, 19790-19798.
13. Chamberlain, A. E. R.; Paterson, K. J.; Armstrong, R. J.; Twin, H. C.; Donohoe, T. J. A Hydrogen Borrowing Annulation Strategy for the Stereocontrolled Synthesis of Saturated Aza-Heterocycles. *Chem. Commun.*, **2020**, *56* (24), 3563-3566.
14. Reddy, B. P.; Reddy, K. R.; Krupadanam, G. L. D.; Reddy, A. P.; Reddy, K. B. C-3 Novel Triterpenone with C-28 Urea Derivatives as HIV Inhibitors. WO/2017/064628 A1, April 20, 2017.
15. Möhrle, H.; Azodi, K. Reactions of Acetylenecarboxylic Acid Esters with Piperazine Derivatives. *Journal of Natural Research B***,** **2006**, *61* (8), 1021-1034.
16. Matsunaga, Y.; Fujisawa, K.; Amir, N.; Miyashita, Y.; Okamoto, K. Structural and Physiochemical Characterization of Zinc(II) and Cadmium(II) Complexes with 1,4-Dimethyl-1homopiperazine. *Appl. Organometal. Chem.*, **2005**, *19*, 778-789.
17. Bilke, J L.; O′Brien, P. On the Two-Ligand Catalytic Asymmetric Deprotonation of *N*-Boc Pyrrolidine: Probing the Effect of the Stoichiometric Ligand. *J. Org. Chem.* **2008**, *73* (16), 6452-6454.
18. Borys, A. M.; Gil-Negrete, J. M.; Hevia, E. Atom-Efficient Transition-Metal-Free Arylation of N,O-Acetals Using Diarylzinc Reagents through Zn/Zn Cooperativity. *Chem. Commun.*, **2021**, *57* (71), 8905-8908.
19. Nordstrøm, L. U.; Madsen, R. Iridium Catalysed Synthesis of Piperazines from Diols. *Chemical Communications* **2007**, (47), 5034-5036.
20. Jumde, V. R.; Cini, E.; Porcheddu, A.; Taddei, M. A Metal-Catalyzed Tandem 1,4-Benzodiazepine Synthesis Based on Two Hydrogen-Transfer Reactions. *European Journal of Organic Chemistry* **2015**, *2015* (5), 1068-1074.
21. Vellakkaran, M.; Singh, K.; Banerjee, D. An Efficient and Selective Nickel-Catalyzed Direct N-Alkylation of Anilines with Alcohols. *ACS Catal.* **2017**, *7*, 8152-8158.